THESIS : NUCLEONIC COMPONENT OF THE COSMIC RADIATION

By G. Davis.

Abstract

This thesis is concerned with a study of the nucleonic component of the cosmic radiation, using the nuclear emulsion technique. It is the nucleonic component which produces the characteristic nuclear disintegrations, or stars, in emulsions.

In Part I, the spatial distribution of stars in nuclear emulsions is considered. Early workers in the field had reported rather more stars at close separations from each other than would be expected on a random distribution of stars. Possible mechanisms which lead to an excess of close star-pairs are examined and it is shown that the expected excess using these mechanisms is rather less than that reported experimentally by earlier observers. The results used by Li (1950) are re-examined and it is concluded that there is insufficient evidence for an excess of the order of that claimed by Li. There seems little doubt that extreme care has to be taken in the scanning of the emulsions, as inefficient scanning can cause anomalous effects of the same order as that reported by Li.

Part II is concerned with the angular distribution

of the ionising and non-ionising components of the star-producing radiation. This has been investigated, using lead cones of various angles to attenuate the radiation. Assuming collimated interactions in the absorber, the angular distribution of the total star-producing radiation can be represented by a $\cos^{3\pm\frac{1}{2}} \theta$ steradian^{-1} zenith angle distribution law, while the charged component follows a $\cos^{5\pm1} \theta$ law. The results show an increase in the proportion of low energy stars under the absorber, and there are indications of a continuous decrease in attenuation mean free path with increase in star size.

If it is assumed that star-producing particles are produced in secondary interactions in the lead absorber, then this can considerably modify the exponent m in the zenith angle distribution law. This problem is discussed in Part III, and it is shown that taking the extreme conditions of isotropic production of secondaries, and a collision mean free path of 150 g cm^{-2} lead, the exponent m decreases from 3 to 2.2.

In Part IV a nucleon cascade model is developed for interactions in lead. Under certain conditions the cascade can lead to a variation of attenuation length with energy, the attenuation length tending to the interaction length at high energies. A method is shown for expressing a nucleon energy distribution in terms of a corresponding star-size distribution. Using this method it is

shown that the differential energy distribution of the star-producing component at the Jungfraujoch can be represented by an $E^{-2.1\pm0.2}$ law, instead of the previously reported $E^{-2.5}$ law.

Thesis entitled

NUCLEONIC COMPONENT OF THE COSMIC RADIATION

by

G. Davis

Presented to the

University of London

for the degree of

Doctor of Philosophy

and to the

Imperial College of Science and Technology

for the

Diploma of the Imperial College

Supervisors: Sir George Thomson, F.R.S. (Former)
Dr. E.P. George (Present)

CONTENTS

		Page
SUMMARY		iv
ACKNOWLEDGEMENTS		vi
GENERAL INTRODUCTION		viii
PART I.	THE ANOMALOUS DOUBLE-STAR EFFECT	
§ 1.	Introduction	1
§ 2.	Number of Stars expected on a Random Distrubition	4
§ 3.	Effects leading to a Non-Random Distribution of Stars	13
§ 4.	Analysis of 1,094 Stars in Nuclear Emulsions exposed under Lead Absorbers	27
§ 5.	The Statistical Problem of the Double-Star Effect	37
	Discussion and Conclusion	44
PART II.	THE LEAD CONE EXPERIMENT	
	Introduction	46
§ 1.	Experimental Details	47
§ 2.	Scanning of the Emulsions	50
§ 3.	Results	52
§ 4.	Analysis of the Results	55
§ 5.	The Angular Distribution	59
§ 6.	Absolute Rate of Star Production at the Jungfraujoch	64
§ 7.	Attenuation of the Star-Producing Radiation	65
PART III.	THE GEOMETRICAL PROPERTIES OF THE NUCLEAR INTERACTIONS IN THE LEAD CONES	
§ 1.	Introduction	73
§ 2.	One-Stage Cascade assuming Collimated Secondaries	75
§ 3.	Isotropic Emission of Secondaries	78

		Page
§ 4.	Calculation of Secondary Contribution assuming Isotropic Emission, under a 90° Cone	80
§ 5.	Isotropic Emission of Secondaries in a General Cone of Semi-Angle	87
§ 6.	Isotropic Emission of Secondaries, 40° Cone	89
§ 7.	Effect of the Isotropic Production of Secondaries on the Lead Cone Absorption Curves	96
PART IV.	A ONE-DIMENSIONAL NUCLEON CASCADE MODEL IN LEAD, LEADING TO AN ENERGY VARIATION OF THE ATTENUATION	
§ 1.	Introduction	101
§ 2.	The Cascade Model in Lead, neglecting Ionisation	105
§ 3.	Choice of Values of the Constants of the Theory	115
§ 4.	Results for the Cascade, neglecting Ionisation	119
§ 5.	Effect of Ionisation Loss on the Nucleon Cascade	121
§ 6.	Size Distribution of Stars caused by Nucleons formed in the Cascade	130
§ 7.	Comparison of the Results of the Theory with Experiment	136
§ 8.	Discussion of Cascade Theory	137
SUMMARY OF CONCLUSIONS		140
REFERENCES		143
PUBLICATIONS		146

SUMMARY

This thesis is concerned with a study of the nucleonic component of the cosmic radiation, using the nuclear emulsion technique. It is the nucleonic component which produces the characteristic nuclear disintegrations, or stars, in emulsions.

In Part I, the spatial distribution of stars in nuclear emulsions is considered. Early workers in the field had reported rather more stars at close separations from each other than would be expected on a random distribution of stars. Possible mechanisms which lead to an excess of close star-pairs are examined and it is shown that the expected excess using these mechanisms is rather less than that reported experimentally by earlier observers. The results used by Li (1950) are re-examined and it is concluded that there is insufficient evidence for an excess of the order of that claimed by Li. There seems little doubt that extreme care has to be taken in the scanning of the emulsions, as inefficient scanning can cause anomalous effects of the same order as that reported by Li.

Part II is concerned with the angular distribution of the ionising and non-ionising components of the star-producing radiation. This has been investigated using lead cones of various angles to attenuate the radiation. Assuming collimated interactions in the absorber, the

angular distribution of the total star-producing radiation can be represented by a $\cos^{3\pm\frac{1}{2}}\theta$ steradian^{-1} zenith angle distribution law, while the charged component follows a $\cos^{5\pm1}\theta$ law. The results show an increase in the proportion of low energy stars under the absorber, and there are indications of a continuous decrease in attenuation mean free path with increase in star size.

If it is assumed that star-producing particles are produced in secondary interactions in the lead absorber, then this can considerably modify the exponent m in the zenith angle distribution law. This problem is discussed in Part III, and it is shown that taking the extreme conditions of isotropic production of secondaries, and a collision mean free path of 150 g cm^{-2} lead, the exponent m decreases from 3 to 2.2.

In Part IV a nucleon cascade model is developed for interactions in lead. Under certain conditions the cascade can lead to a variation of attenuation length with energy, the attenuation length tending to the interaction length at high energies. A method is shown for expressing a nucleon energy distribution in terms of a corresponding star-size distribution. Using this method it is shown that the differential energy distribution of the star-producing component at the Jungfraujoch can be represented by an $E^{-2.1\pm0.2}$ law, instead of the previously reported $E^{-2.5}$ law.

ACKNOWLEDGEMENTS

Throughout the course of this work I have had much assistance from my colleagues in the Department, particularly Dr. A.J. Herz, Dr. P.E. Hodgson and Mr. S. Lattimore who introduced me to the photographic plate technique and were always at hand with useful advice (and criticism).

Mr. N.C. Barford and Mr. S. Lattimore played the major role of designing the lead cones, which were manufactured under the supervision of Messrs. Davis and Shand of the departmental workshop. In addition, Mr. Barford, Dr. D.H. Perkins and Dr. J.B. Harding performed the onerous task of erecting the lead cones at the Jungfraujoch. Thanks are due to Professor von Muralt, Dr. R. Stampfli and Herrn H. Wiedekehr for providing the facilities at the Jungfraujoch Scientific Station.

Dr. A.J. Herz and Miss M. Edgar performed the not inconsiderable task of developing the nuclear emulsions. The success of the lead cone experiment was only made possible by the careful scanning of the plates, and I am particularly indebted to Mrs. S. Lattimore (formerly Mrs. Groundwater), Miss I. Bell, Miss L. Grumer and Miss M. Edgar.

I should like to thank Professor Sir George Thomson, who was my supervisor during the greater period of this work, and Dr. E.P. George, who became my supervisor in the latter period, for their unfailing help and encouragement.

In conclusion, I must express my gratitude to the Department of Scientific and Industrial Research for a maintenance grant during the latter period of the work.

GENERAL INTRODUCTION

Since the original discovery made by C.T.R. Wilson in 1900 of a slight residual ionisation in the atmosphere, it has been found that this ionisation is mainly caused by the passage of charged particles reaching the earth from outer space. Later workers have accumulated a great wealth of evidence as to the nature of these cosmic rays.

Information about the primary radiation incident on the top of the earth's atmosphere has been obtained by various workers (survey by Peters 1952), using apparatus taken to high altitudes in balloons and rockets. The results of these experiments show that the primary radiation consists of ionised atomic nuclei with a mass spectrum similar to that of stellar matter (Brown 1949). The latest results (Kaplon, Peters, Reynolds and Ritson 1952) show that the primary particles are approximately 90% protons, 10% alpha particles and less than 1% heavier nuclei.

Many theories of the origin of the cosmic radiation have been proposed (Fermi 1949; Chang-Yun Fan 1951; Richtmyer and Teller 1949; Alfuén 1949, 1950; Unsöld 1951; Bierman and Schlüter 1951), but the experimental evidence is inadequate to verify them.

In the first few gm cm^{-2} of the atmosphere the

primary radiation interacts with the nuclei of the air and produces secondary particles, some of which are capable of further interactions in the atmosphere. This type of process is referred to as a cascade process and has been demonstrated by observers studying high-energy interactions in cloud chambers, using stacked parallel absorbers (Gregory and Tinlot 1951).

The primary interactions are very energetic, and they produce showers of secondary nucleons, accompanied by charged and neutral mesons which are created in collisions between the nucleons taking part in the interaction. The earth's atmosphere is equivalent to about 10 interaction-path lengths of the primary protons and much more than this for the heavier nuclei, so practically none of the primary radiation reaches the earth's surface. At a depth of 100 gm cm^{-2} below the top of the atmosphere (an altitude of 50,000 feet above sea-level) most of the primary radiation has interacted and the radiation below this falls into three main groups.

The first group contains the nucleonic or N-component (Rossi 1948), which interacts strongly with matter and produces the disintegrations or stars found in nuclear emulsions. At mountain altitudes it consists of secondary neutrons and protons. The second group contains the charged mesons from the shower particles already mentioned above. This consists of mesons of various masses

(O'Ceallaigh 1951; Harding 1950; Herz, Hodgson and Tennent 1952), which decay eventually into the μ-mesons forming the penetrating component of the cosmic radiation. The third group, commonly called the soft component, consists of electromagnetic cascades initiated by the neutral π-mesons which accompany the showers of charged mesons. These neutral mesons have a very short life (Carlson, Hooper and King 1950) and decay into γ-rays which then generate showers of electrons and γ-rays in a secondary cascade process. Some contribution to the soft component also comes from knock-on electrons and bremsstrahlung.

Theories have been developed by Messel (1950, 1951, 1952) and Thomson and Hodgson (1951), which provide a satisfactory explanation of the nucleon cascade in the atmosphere. Messel has, in addition, proposed expressions which describe both the μ-meson and the soft components as a development from the nucleon cascade.

This thesis is mainly concerned with the nucleonic component, which is studied by analysing the stars produced by it in nuclear emulsions. Early workers (Leprince-Ringuet and Heidmann 1948, and Li and Perkins 1948) reported an anomaly in the spatial distribution of stars in photographic emulsions. This could not be explained by any known mechanism of star production and indicated that some unknown particles contribute to the production of stars. This effect has therefore been studied in some

detail in the first part of this thesis in order to see if the stars can be used as a measure of the nucleonic component. Many other particles can produce stars in nuclear emulsions. These include fast μ -mesons (George and Evans 1951), γ -rays and electrons (Kikuchi 1951), but their cross-sections for star production are so small that their contribution at mountain altitudes is quite negligible compared with that due to the nucleonic component. However, under absorbers, locally produced fast π -mesons can produce stars with a cross-section comparable with that of the nucleons (Camerini, Fowler, Lock and Muirhead 1950). π -mesons and μ -mesons coming to rest in the emulsion can produce small stars, the characteristic δ star, but these are easily recognisable because of the scattered track of the incoming meson.

The main problem in this thesis has been the determination of the angular distribution of the star-producing component at mountain altitudes. The angular distribution for charged particles producing stars is simply found by measuring the zenith angles of the primaries, as has been previously reported by Page (1950). No such method exists for the non-ionising particles producing stars. It was therefore decided to construct special lead absorbers having good geometry. By studying the absorption of the star-producing component under these absorbers, it is possible to deduce properties of the angular distribution.

In addition, some interesting features of the absorption under lead have appeared which show disagreement with the results of Rosser and Swift (1951).

I. THE ANOMALOUS DOUBLE-STAR EFFECT

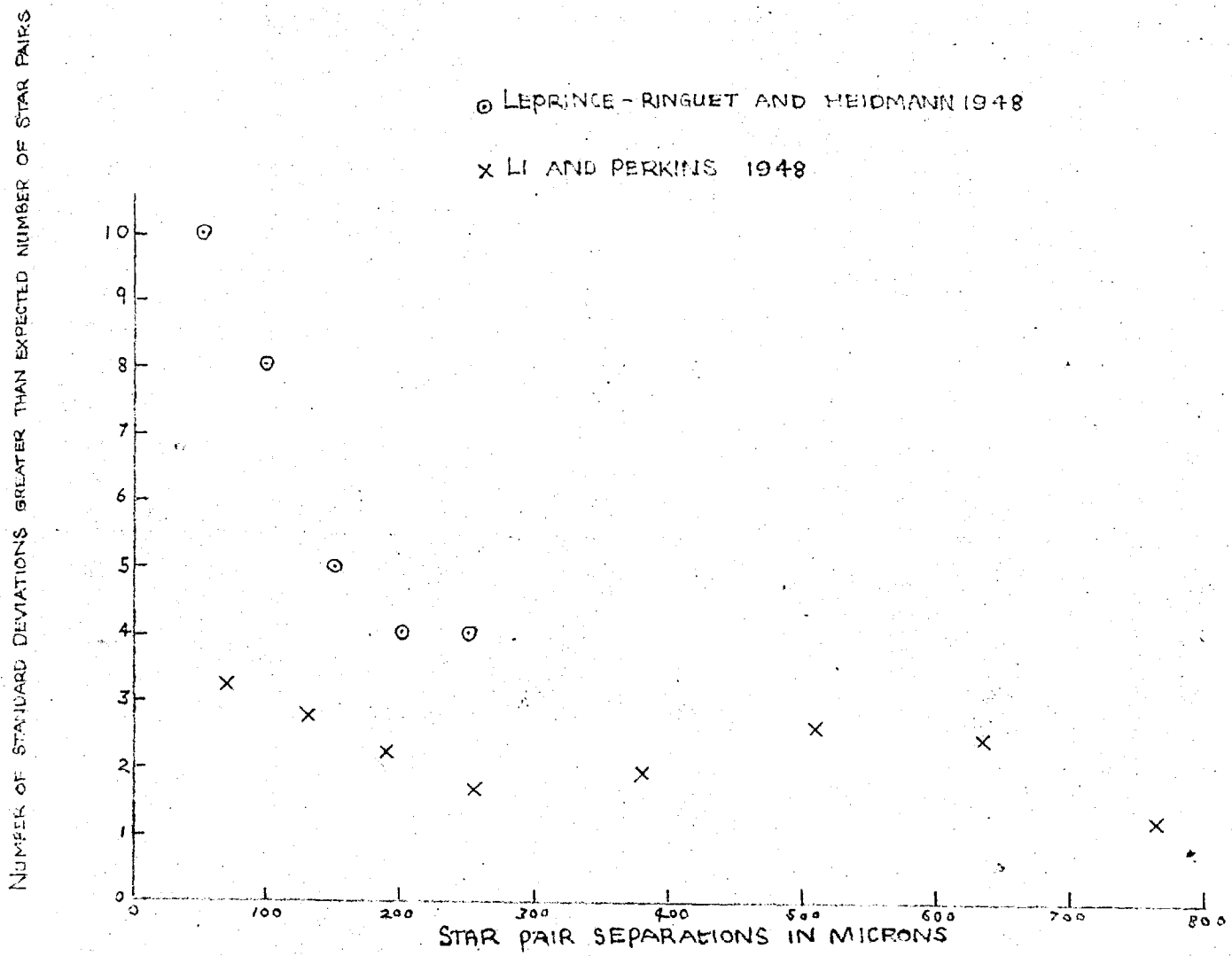
1. Introduction

The nuclear disintegrations (stars) formed in nuclear emulsion are caused by the interactions of nucleons or mesons with nuclei of the emulsion. These stars will be expected to have a random spatial distribution, unless some of them are associated with other stars, by some mechanism. If such a mechanism exists, it is very likely that an anomalous spatial distribution of stars is associated with a corresponding anomalous time distribution of stars.

Many workers have reported an anomaly in the spatial distribution of stars (Leprince-Ringuet and Heidmann 1948, Li and Perkins 1948, Li 1950, Addario and Tamburino 1950). These observers measured the projected separation between stars in the emulsion and determined the distribution of the separations of these star-pairs. They all found rather more star-pairs with small separations than would be expected on a random distribution.

Leprince-Ringuet and Heidmann analysed 2,250 stars on 640 cm^2 of 100 μ C.2 plates exposed vertically at 3600 m. elevation. They found an excess of star-pairs of some 50% of that expected on a random distribution for separations less than 250 μ. Li and Perkins, working in this laboratory, analysed 1,230 stars on 350 cm^2 of 100 μ C.2 plates exposed vertically at 3650 m. elevation. They found an

FIG I.1. EXCESS OF CLOSE STAR PAIRS OBSERVED BY LEPRINCE-RINGUET AND LI AND PERKINS



excess of 20% for separations less than 700 μ. The results found by these two groups of workers are shown in Figure I.1. These are expressed as the number of standard deviations separating the observed number of star-pairs from the expected number of star-pairs assuming random distribution. Both these groups of workers calculated the anomalous distribution due to a regenerative process of star production. They showed that the observed excess could be explained if an average of between 5 and 10 secondary particles, capable of producing further stars in the emulsion, are emitted from every star in the emulsion. However, the average number of such secondaries is certainly less than 2 for stars formed at mountain altitudes (see Section 3). The excess, therefore, is rather difficult to explain.

Li (1950) continued the analysis in 100 μ C.2 plates exposed horizontally and found an excess of close star-pairs which increased up to separations of 1500 μ. The excess was of magnitude 2% excess star-pairs per star and was again difficult to explain by any known regenerative or shower process. Li found that the excess was greatest for plates exposed under absorbing material, and in common with the two groups previously mentioned he included 2-track stars in his analysis.

Li discussed the possible errors of measurement which could cause an excess of close star-pairs. He considered

firstly an edge effect in the rectangular areas of his plates, which effectively reduces the area of each rectangle, leading to an apparent excess of star-pairs. Secondly, uneven thicknesses of up to 20% will cause a slight excess. He also discussed the effect of inefficient searching on the star-pair distribution. As a large section of his plates, the "ice" plates, was claimed to have an efficiency of more than 98%, Li considered that the effect on the star-pair distribution was negligible. He concluded that none of these experimental errors were sufficient to explain the observed excess of close star-pairs.

In view of the difficulty of accounting for this double-star effect, it was decided in this thesis to make a further analysis of the spatial distribution of stars in G.5 and C.2 emulsion (Davis 1952). As a result of this analysis it appeared that the stars in the G.5 emulsion, from plates which were searched recently in this laboratory, showed no signs of any excess of the magnitude reported by Li. The C.2 plates, searched earlier, didshow an excess of the same order as that reported by Li, but this excess completely disappeared when 2-track stars were excluded from the analysis. It seemed highly desirable to re-analyse the results used by Li in his 1950 paper, and to see the effect of excluding 2-track stars from the analysis. As a result of this repeated analysis it will be shown that the star excess, as reported by Li, and Li and Perkins,

can be explained as due to preferential inefficient searching.

The spatial distribution of stars randomly distributed in nuclear emulsions is discussed in the second section. In the third section possible processes which could lead to a non-random spatial distribution of stars are given and their maximum contribution to the anomalous star-pair distribution is determined. The expected anomalous distribution is only some 10% of that reported by Li. The fourth section contains the experimental results and the re-analysis of Li's plates, referred to in the last paragraph. In the final section the statistical problem of the anomalous double-star effect is considered. The use of a rotating plate mechanism, capable of finding an anomalous time distribution of stars, is also discussed in relation to the double-star effect.

2. Number of Double Stars expected on a Random Distribution

Nuclear emulsion plates in this laboratory are subdivided into rectangular areas, and stars are recorded by means of their cartesian co-ordinates x_j, y_j with the axes parallel to the sides of the area. The distance between two stars is thus equal to r_{hj}

$$\text{where } r_{hj}^2 = (x_h - x_j)^2 + (y_h - y_j)^2 \qquad \text{I (1)}$$

If one assumes a random distribution of stars on rectangular areas, then it can be shown (Li 1950) that the number of star-pairs having a projected distance less than or equal to r is given by Q(r) where

$$Q(r) = \sum_i \frac{N_i(N_i-1)}{2} \frac{\pi r^2}{ab} \left\{1 - \frac{4(a+b)r}{3\pi ab} + \frac{r^2}{2\pi ab}\right\} \qquad I(2)$$

with r less than a or b, a and b being the sides of the area and N_i stars lying within a typical area i.

The number of star-pairs having a projected distance between r and r+dr is equal to $Q^1(r)dr$ where

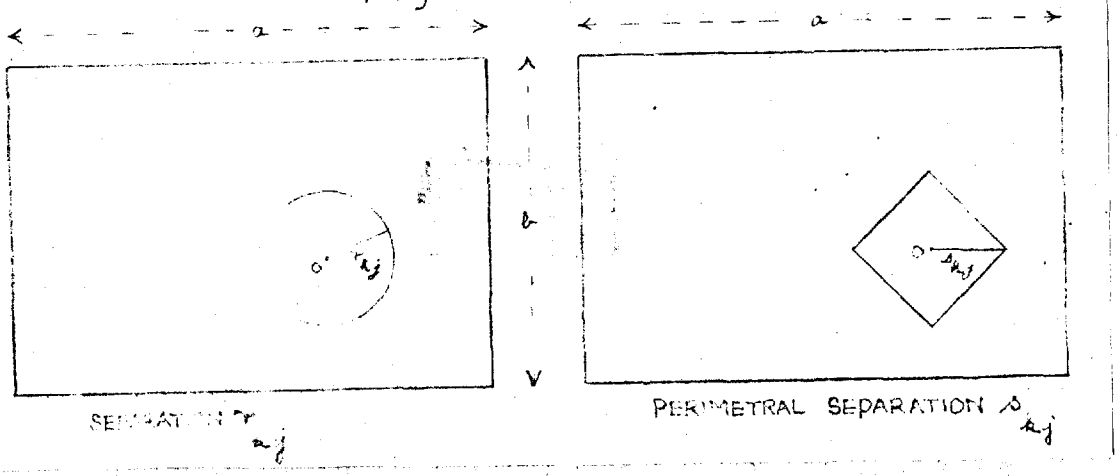
$$Q^1(r) = \sum_i N_i(N_i-1) \frac{\pi r}{ab} \left\{1 - 2\frac{(a+b)}{\pi ab} r + \frac{r^2}{\pi ab}\right\} dr \qquad I(3)$$

When calculating the observed distribution of double stars Li tabulated values of $\sum_{hj} (x_h-x_j)$ and $\sum_{hj} (y_h-y_j)$ for each area. It was then necessary to square each of these terms, add the corresponding terms in x and y, and obtain r_{hj} from equation I(1). This is a somewhat lengthy procedure, and in analysing a further 1,094 stars it was decided to define a new parameter instead of the actual separation of the star-pairs. The perimetral separation s_{hj}, between two stars h, j, is defined by

$$s_{hj} = |(x_h-x_j)| + |(y_h-y_j)| .$$

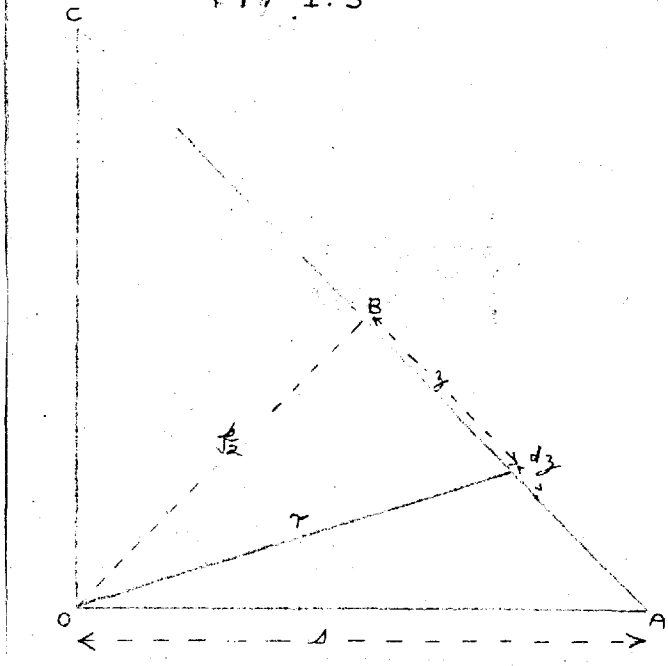
The comparison between r_{hj} and s_{hj} is shown in Figure I.2.

Fig I.2



Stars with an actual separation less than r from a star at O will lie within a circle centre O radius r. Stars having a perimetral distance less than s from a star O will lie within a square of diagonal 2s, as shown in Figure I.2.ii. Thus stars having a perimetral distance of s from other stars will have a mean distance from these stars somewhat less than s.

Fig I.3



Consider stars with a perimetral distance s from O. They will lie along the square shown in the right half of Figure I.2, one side of which AC, is shown in Figure I.3.

The average distance of these stars from O, $\bar{r}$ is given by

$$\bar{r} = \int_A^B r\,dz \Big/ \int_A^B dz$$

$$= \int_0^a \sqrt{z^2 + a^2} \Big/ a \qquad \text{where } a = \frac{1}{\sqrt{2}}\, s$$

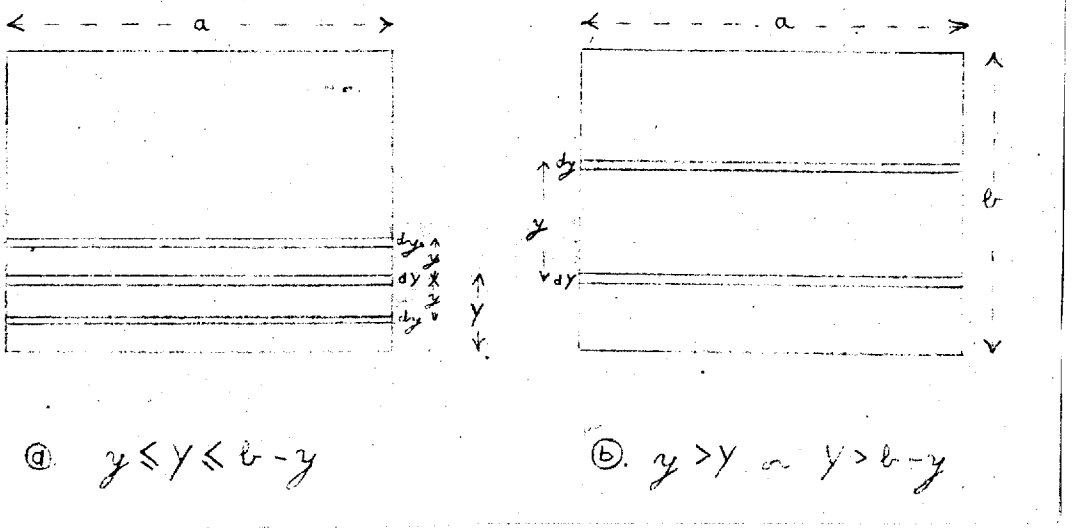
$$= \frac{1}{a}\left[\frac{a^2}{2}\log_e(s + \sqrt{a^2+s^2}) + \frac{s}{2}\sqrt{a^2+s^2}\right]$$

$$= \frac{a}{2}\left[\log_e(1 + \sqrt{2}) + \sqrt{2}\right]$$

$$\therefore \quad \bar{r} = s \times 0.87$$

The comparative simplicity of computing s_{hj} for large numbers of stars makes the perimetral analysis rather more convenient than the actual separation analysis. New relations similar to I(2) and I(3) now have to be calculated.

Fig I.4



Consider an area sides a, b, containing N stars randomly distributed. Let the cartesian axes x, y be parallel to the sides a, b respectively.

The probability of finding a star in an elemental strip dY is equal to N dY / b (Figure I.4).

The probability of finding a second star in an elemental strip dy, distant y from the element dY

is given by $N \frac{dY}{b} (N-1)\, 2 \frac{dy}{b}$ for $y < Y < b-y$

and by $N \frac{dY}{b} (N-1) \frac{dy}{b}$ for $y > Y$ and $Y > b-y$

The total probability P(y)dy of finding stars within an element y to y+dy from another star is equal to

$$\frac{N(N-1)}{b^2} dy \left[\int_y^{b-y} 2\, dY + 2 \int_0^y dY \right]$$

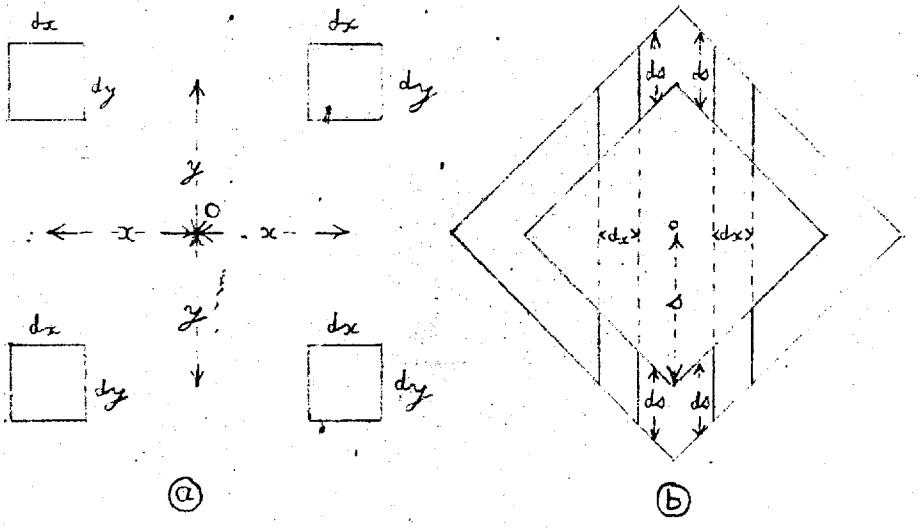
$$\therefore \quad P(y)dy = \frac{2(N)(N-1)}{b^2} (b-y)dy$$

The probability $P^1(x,y)dx\, dy$ of finding stars within an elemental area dx x dy, distance x, y from other stars is given by

$$P^1(x,y)dx\, dy = \frac{4N(N-1)}{a^2\, b^2} (a-x)(b-y)dx\, dy \qquad I(4)$$

This is independent of the direction of x and y, and thus in general $P^1(x,y)dx\, dy$ refers to four elemental areas dx dy, as shown in Figure I.5(a).

Fig I. 5



The corresponding perimetral element ds is shown in Figure I.5(b) and the element of area corresponding to dx dy can be expressed as ds dx. The probability P(s)ds of finding stars with perimetral separations between s and s+ds can be obtained by integrating I(4) over the elemental area shown in Figure I.5(b), subject to x+y = s.

$$\therefore \quad P^1(s)ds = \frac{4N(N-1)}{a^2\,b^2} \int_{x=0}^{s} (a-x)(b-s+x)dx \qquad ds$$

$$\text{and} \quad P^1(s)ds = \frac{4N(N-1)}{a^2\,b^2} \left[abs - \frac{a+b}{2} s^2 + \frac{s^3}{6} \right] ds$$

In this analysis each star-pair has been included twice, and we must therefore divide by two to obtain the actual number of star-pairs.

$$\text{Hence} \quad P^1(s)ds = \frac{2(N)(N-1)}{a\,b}\, s \left[1 - \frac{a+b}{2ab} s + \frac{s^2}{6ab} \right] ds \qquad I(5)$$

and the number of stars having perimetral separations less than or equal to s is obtained by integrating I(5)

$$P(s) = \frac{N(N-1)}{a\ b}\ s^2 \left[1 - \frac{a+b}{3ab}\ s + \frac{s^2}{12ab} \right] \qquad I(6)$$

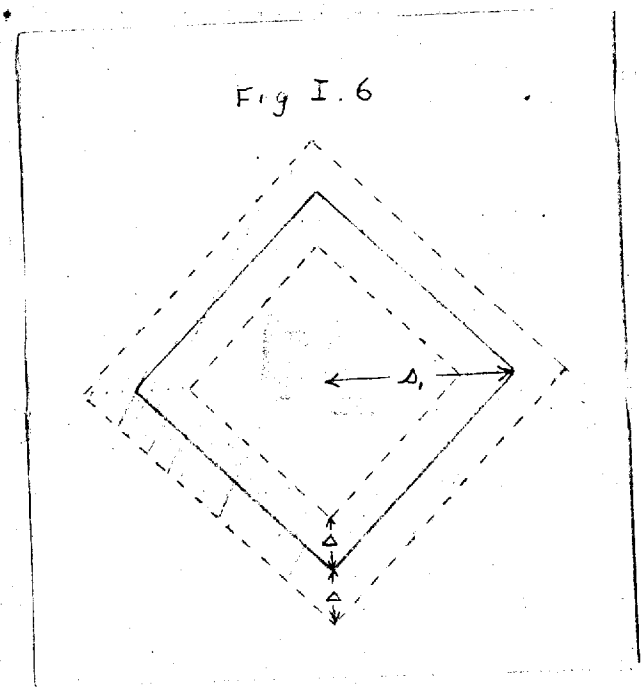
The terms inside the brackets of relations I(2), I(3), I(5) and I(6) are very similar and contain two correction terms of first and second order which allow for the edge effect of the rectangular areas. Values of these correction terms are shown in Table I.1 for the differential relations $Q^1(r)$ and $P^1(s)$ for several values of r and s, and with a = b = 2 cm. These corrections are rather important, as the reported excess is only of the order of 10^{-2} star-pairs per star.

Table I.1. Correction Terms in $Q^1(r)$, $P^1(s)$ functions.

$Q^1(r)$			$P^1(s)$		
$r(\mu)$	$-\frac{2(a+b)}{ab}\ r$	$+\frac{r^2}{ab}$	$s(\mu)$	$-\frac{a+b}{2ab}\ s$	$+\frac{s^2}{6ab}$
100	- 0.006	+ 0.000008	100	- 0.005	+ 0.000004
200	- 0.013	+ 0.000032	200	- 0.01	+ 0.000017
500	- 0.032	+ 0.000199	500	- 0.025	+ 0.000104
1000	- 0.064	+ 0.000795	1000	- 0.05	+ 0.000416
1500	- 0.096	+ 0.00179	1500	- 0.075	+ 0.000940
2000	- 0.128	+ 0.00318	2000	- 0.10	+ 0.001670
4000	- 0.254	+ 0.0127	4000	- 0.20	+ 0.006660
10000	- 0.6	+ 0.0795	10000	- 0.5	+ 0.0416

At this stage it is convenient to consider the effect on the P(s), $P^1(s)$ functions of errors of measurement in the perimetral separations s_1. It will be assumed that a measurement of s_1 is subject to an error Δ, all values lying between $s_1+\Delta$ and $s_1-\Delta$ being equally probable. Δ is independent of s. The number of stars recorded as having perimetral separations less than s will now consist of two parts:-

Figure I.6.



All stars having perimetral separations less than $s_1-\Delta$ will still be recorded as having separations less than s_1. However, stars in the shaded portions of Figure I.6, having separations between $s_1+\Delta$ and $s_1-\Delta$, have a certain probability of being recorded as being less than s_1. Some stars in the shaded region inside the

square s_1 will be recorded as lying outside s_1, and vice versa. However, the shaded portion outside the square s_1 is of greater area than the shaded portion inside square s_1. This will lead to a slight apparent increase in star-pairs above the simple random picture. For a value of s between $s_1 + \Delta$ and $s_1 - \Delta$ the probability of being recorded as less than $s_1 = \frac{1}{2} + \frac{s_1 - s}{2\Delta}$. Therefore, the measured distribution of star-pairs $P'(s_1)$ with $s \leq s_1$ is given by

$$P(s_1) = \int_0^{s_1-\Delta} P^1(s)\, ds + \int_{s_1-\Delta}^{s_1+\Delta} P^1(s) \left\{ \frac{1}{2} + \frac{s_1 - s}{2\Delta} \right\} ds$$

$$= P(s_1 - \Delta) + \int_{s_1-\Delta}^{s_1+\Delta} P^1(s) \left\{ \frac{1}{2} + \frac{s_1 - s}{2\Delta} \right\} ds$$

$$\therefore P(s_1) = \frac{2N(N-1)}{a^2 b^2} \left\{ \frac{a\, b\, s^2}{2} \left(1 + \frac{\Delta^2}{3 s_1^2}\right) - \frac{a+b}{6} s_1^3 \times \right.$$

$$\left. \left(1 + \frac{\Delta^2}{s_1^2}\right) + \frac{1}{24} s_1^4 \left\{ 1 + 2\frac{\Delta^2}{s_1^2} + \frac{1}{5}\frac{\Delta^4}{s_1^4} \right\} \right. \qquad \text{I(7)}$$

If equation I(7) is compared with equation I(6), it can be seen that the error in measurement in s has led to an apparent increase in the number of random star-pairs. The relative increase in star-pairs only becomes important for small values of s, and so only the first bracketed term in equation I(7) need be considered. However, the total number of increased star-pairs is independent of s,

and is equal to $\frac{N(N-1)}{ab} \times \frac{1}{3} \Delta^2$. For areas having an average of m stars per area and dimensions a = b = 2 cm., then the excess of star-pairs per star is equal to $\frac{1}{3} m \left(\frac{\Delta}{200}\right)^2$, where Δ is measured in 100 μ units.

However, the error Δ introduced by inaccuracies in reading the verniers of the microscope stage will probably not be greater than 100 μ. The apparent excess of star-pairs is therefore equal to $1 \times 10^{-5} m$ star-pairs per star. As m was of the order of 10 for the areas used by Li, the maximum excess caused by the reading error is 2×10^{-4}. This is smaller by a factor of 100 than the excess reported by Li for separations up to 1500 μ.

3. Effects leading to a Non-random Distribution of Stars

If the stars are not randomly distributed in nuclear emulsions, it is reasonable to assume that the mechanism responsible for this non-random distribution causes the simultaneous production of a certain fraction of the stars on the emulsion . It will be assumed that all stars are produced by nucleons or mesons either in the "shower" particle energy region or with energies corresponding to the "grey" tracks. Although γ rays have been shown to produce stars (Kikuchi 1951), the cross-sections are so small that they can be neglected in the following work.

There are two possible mechanisms by which stars could be simultaneously formed in nuclear emulsions.

(a) Firstly, there is a regenerative process. The incident particle produces a "primary" star, which then emits further particles capable of producing secondary stars in the emulsion.

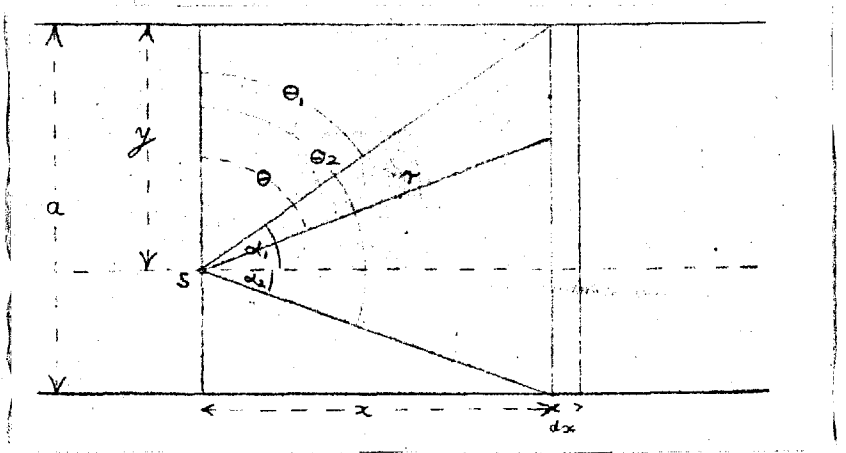
(b) Secondly, there is a possible shower process. A number of particles, produced in a nuclear interaction in material above the plates, pass simultaneously through the emulsion. Two or more of these particles can then form stars in the emulsion.

(a) Regenerative Process.

It will be assumed, in this regenerative process, that the secondary particles capable of producing further stars are emitted isotropically from the stars in the emulsion. It is well known that energetic secondary nucleons are strongly collimated about the direction of the primaries (Brown, Camerini, Fowler, Heitler, King and Powell 1949). As star-producing primaries at the Jungfraujoch have a $\cos^3\theta$ zenith angle distribution (see Part III of this thesis), the secondaries will be collimated about the vertical. However, the plates analysed by Li were exposed horizontally and this collimation of secondaries will cause them to pass downwards through the emulsion, giving little chance to form stars. The above

assumption of isotropic secondary emission will therefore give an upper limit to the number of secondary stars.

It will therefore be supposed that each primary star in the emulsion emits on the average q particles, both charged and uncharged, with energies sufficient to form secondary stars.



Consider a star S, distant y from the surface of an emulsion of thickness a. The number of secondaries producing stars with projected distance from S between x and x+dx is equal to $N_y(x)dx$

$$\text{where} \quad N_y(x)dx = \int_{\theta_1}^{\theta_2} q \frac{2\pi}{4\pi} \sin\theta \, d\theta \, e^{-\frac{r}{\lambda}} \frac{dx}{\lambda \sin\theta}$$

$$\therefore N_y(x)dx = \frac{q}{2\lambda} e^{-\frac{r}{\lambda}} dx \, (\alpha_1 + \alpha_2) \qquad \text{I(8)}$$

where r is the actual distance of the secondary star from

S, and λ is the mean free path for star-production in emulsion ($\sim$ 25 cm. for shower particles) (Camerini et al. 1950).

Although r is not constant as Θ varies, in the regions where $e^{-\frac{r}{\lambda}}$ begins to differ from unity r can be regarded as independent of Θ and equated to x, the projected distance.

Stars have equal probabilities of occurring at any depth in the emulsion and the expression I(8) has to be averaged over y. The number of secondary stars with projected distance between x and x+dx from S is then equal to

$$N^1(x)dx = \frac{q}{2\lambda}\, e^{-\frac{r}{\lambda}}\, dx\, \frac{1}{a} \int_0^a (\tan^{-1}\frac{y}{x} + \tan^{-1}\frac{a-y}{x})\, dy$$

$$\therefore\ N^1(x)dx = \frac{q}{\lambda}\, e^{-\frac{r}{\lambda}}\, dx\, \frac{1}{a} \left[a \tan^{-1}\frac{a}{x} - \frac{x}{2}\log_e\left(1 + \frac{a^2}{x^2}\right)\right] dx \qquad I(9)$$

The number of stars N(x) having a separation less than x from S is given by

$$N(x) = \frac{q}{a\lambda} \int_0^x e^{-\frac{r}{\lambda}} \left(a \tan^{-1}\frac{a}{x} - \frac{x}{2}\log_e\left[1 + \frac{a^2}{x^2}\right]\right)dx \qquad I(10)$$

if $x \ll \lambda$ (i.e. $\approx$ 1 cm.) then the $e^{-\frac{r}{\lambda}}$ term can be equated to unity. On integrating I(10) and thus neglecting absorption, it can be shown that

$$N(x) = \frac{q}{a\lambda}\left\{ax \cot^{-1}\frac{x}{a} - \frac{1}{4}x^2 \log_e\left(1 + \frac{a^2}{x^2}\right) + \frac{1}{4}a^2 \log_e\left(1 + \frac{x^2}{a^2}\right)\right\} \qquad I(11)$$

For $x > a$, equation I(11) is very nearly equal to

$$N(x) = \frac{q}{\lambda}\left\{\frac{3}{4}a + \frac{a}{2}\log_e\frac{x}{a}\right\} \qquad \text{I(12)}$$

as was formerly derived by Li and Perkins (1948).

It is possible to calculate the total number of secondary stars produced in the emulsion by integrating equation I(10) from 0 to ∞ . The absorption can no longer be ignored, but it is reasonable to replace $e^{-\frac{r}{\lambda}}$ by $e^{-\frac{x}{\lambda}}$

$$\therefore N(\infty) = \frac{q}{q\lambda}\int_0^\infty e^{-\frac{x}{\lambda}}\left[a\tan^{-1}\frac{a}{x} - \frac{x}{2}\log_e\left(1+\frac{a^2}{x^2}\right)\right]dx \qquad \text{I(13)}$$

on integrating each term on the R.H.S by parts, I(13) becomes

$$N(\infty) = \frac{q}{q\lambda}\left\{\left[-a\lambda\, e^{-\frac{x}{\lambda}}\cot^{-1}\frac{x}{a}\right]_0^\infty - \int_0^\infty \frac{\lambda}{2}e^{-\frac{x}{\lambda}}\log_e\left(\frac{x^2+a^2}{x^2}\right)dx\right\} \qquad \text{I(14)}$$

the integral on the right hand side of I(14) is a standard infinite integral (Bierens de Haan 1858) and is equal to

$$\frac{\lambda^2}{2}\left\{\log a^2 - 2\,\mathrm{Ci}\frac{a}{\lambda}\cos\frac{a}{\lambda} - 2\,\mathrm{Si}\frac{a}{\lambda}\sin\frac{a}{\lambda} + \pi\sin\frac{a}{\lambda}\right\} - \frac{\lambda^2}{2}\left\{A + \log_e\frac{1}{\lambda}\right\}$$

where $\mathrm{Ci}(\frac{a}{\lambda})$ is the cosine integral of $\frac{a}{\lambda}$ and equals

$$A + \log(\tfrac{a}{\lambda}) - \frac{1}{4}(\tfrac{a}{\lambda})^2 \quad \text{if } \frac{\lambda}{a} \gg 1$$

$\mathrm{Si}(\frac{a}{\lambda})$ is the sine integral of $\frac{a}{\lambda}$ and equals

$$\frac{a}{\lambda} - \frac{1}{18}\left(\frac{a}{\lambda}\right)^3 \quad \text{if } \frac{\lambda}{a} >> 1$$

$$A = 0.577$$

$$\therefore N(\infty) = \frac{q}{\lambda}\left\{\frac{3}{4}a - \frac{A}{2}a + \frac{a}{2}\log_e\frac{\lambda}{a}\right\} \qquad \text{I(15)}$$

for $a = 100\,\mu$ and $\lambda = 25$ cm. then $N(\infty) = 4.26\, q\, \frac{a}{\lambda}$

The mean distance $\bar{x}$ of secondary stars from the primary star is given by

$$\bar{x} = \frac{\int_0^\infty ax\, e^{-\frac{x}{\lambda}} \cot^{-1}\frac{x}{a}\, dx - \frac{1}{2}\int_0^\infty e^{-\frac{x}{\lambda}} x^2 \log\left(\frac{x^2+a^2}{x^2}\right) dx}{\int_0^\infty a\, e^{-\frac{x}{\lambda}} \cot^{-1}\frac{x}{a}\, dx - \frac{1}{2}\int_0^\infty e^{-\frac{x}{\lambda}} x \log\left(\frac{x^2+a^2}{x^2}\right) dx}$$

Both numerator and denominator have been integrated by parts and resolved into standard infinite integrals. Using the condition that $\lambda >> a$, $\bar{x}$ can be expressed as

$$\bar{x} = \lambda\frac{3}{2}a^2 \Big/ a^2\left(\frac{3}{4} - \frac{A}{2} + \frac{1}{2}\log_e\frac{\lambda}{a}\right)$$

for $a = 100\,\mu$ and $\lambda = 25$ cm.

then $\bar{x} \approx \frac{\lambda}{3} \approx 8$ cm.

It can be seen from I(11) and I(12) that the number of secondaries is a slowly increasing function for increasing x. The number of secondary stars per primary star within a distance x can be expressed as $q\,\frac{a}{\lambda}\,f(x)$. Values of f(x) are shown in Table I.2. This is calculated for $a = 100\,\mu$, $\lambda = 25$ cm.

Table I.2.

x	10 μ	50 μ	100 μ	200 μ	300 μ	400 μ	500 μ	600 μ
f(x)	0.14	0.5	0.8	1.1	1.3	1.45	1.56	1.65

700 μ	800 μ	900 μ	1000 μ	1500 μ	1 cm.	10 cm.	∞
1.73	1.8	1.85	1.9	2.05	3.05	4.0	4.26

It can be seen that the secondaries are closely grouped around the primary star. Actually one quarter of the secondaries lie within 200 μ of the primary, and one half within 1500 μ. Using the values of a and λ given above, then for separations less than or equal to 1500 μ, the number of secondary stars per primary is equal to q. 10^{-3}. This number is only doubled if separations are taken up to infinity.

Look and Yekutieli (1952), disoussing the analysis of 30,000 stars in G.5 emulsion, found 14,800 shower particles emitted, 40 of which produced secondary stars in the emulsion. This is equal to 1.3.x 10^{-3} secondary stars per primary, and can be compared with the number expected from the isotropic regenerative theory. The dimensions of the plates are of the order of 1 cm., and q is equal to $\frac{1}{2}$ for the average number of charged shower particles. If we assume that the average thickness of the emulsion is 200 μ, then the expected number of secondaries within 1 cm. is 1.1 x 10^{-3} secondaries per primary. If the average is

400 μ thickness, then the expected number is 1.8×10^{-3} secondaries per primary. The stars described by Lock and Yekutieli include most of those found by the Bristol cosmic ray group, and are mainly on 200 μ and 400 μ G.5 emulsions. Although some of these plates were exposed vertically and others horizontally, it can be seen that the isotropic regenerative theory gives very close agreement with the observed number of secondary stars.

This value of q applies only to charged shower particles and includes stars formed in emulsions flown at 80,000 ft.

In estimating a value of q for stars formed at the Jungfraujoch, the analysis of stars given by Brown et al. (1949) will be used. These showed that 1,223 shower particles were emitted from 4,923 stars, and making allowance for fast neutrons, the total number of fast particles in the shower energy region is certainly not greater than 0.5 per star. The average number of grey tracks was 0.8 per star, and multiplying by 2.25 to allow for neutrons, we find an average of 1.8 particles in the grey energy region. However, this includes protons with energies between 25 and 330 MeV, and not all of these can produce stars with more than 2 tracks. Brown et al. (1949) found that the average energy release in the nucleons corresponding to black and grey tracks can be represented by the empirical relation $E(MeV) = 37N + 4N^2$, where N is the

number of black and grey tracks. Therefore, the average energy required to produce a 2-track star is at least 90 MeV, and for a 3-track star the energy is at least 150 MeV. Tidman and Hodgson (1952) have shown that for 3-track stars the energy release is somewhat greater, 196 MeV, owing to the inefficiency of searching for small stars in the results discussed by Brown et al. Therefore, we have emitted from each star 0.5 particles of shower energy and 1.8 of grey energy, only a certain fraction of the latter being able to produce stars. It can be concluded that the maximum value of q is equal to 2. Taking this value of q, then the total number of secondary stars produced per primary is equal to 4×10^{-3} for 100 μ emulsions.

The effect of this non-random distribution of secondary stars on the observed distribution of star-pairs will be discussed after the consideration of the shower process.

(b) Shower Process

If a shower process can explain the anomalous excess of close star-pairs, it will require that the particles in the shower produce stars close together in the emulsion. Such showers will be closely collimated about the direction of the primary causing the shower and can be reasonably assumed to have a $\cos^n \theta$ zenith angle distribution, with n greater than 2. The average path length through a

horizontal emulsion of thickness a is then equal to $(n+2)\overset{a}{\downarrow}/\ (n+1)$. As n is greater than 2, the average path length of these shower particles through the emulsion is less than $\frac{4}{3}$ a.

We then have a number of shower particles traversing the emulsion, each with a probability p, of producing a star, where $p = \frac{4}{3}\ a\ /\lambda$, with λ equal to the interaction length. For a = 100 μ and λ = 25 cm. (geometric), then $p = \frac{1}{2} \times 10^{-3}$.

If we consider n incident particles, the probability of producing 1 star is equal to n p.

The probability of finding 2 stars produced by these n shower particles is equal to $^{n}C_{2}\ p^{2}$

$$= n\ p.\ (n-1)\ p\ /\ 2.$$

Hence, having found a particular star in the emulsion the probability of finding another star associated in the same shower process will be $(n-1)\ p\ /\ 2$ I(16)

The chance of finding 2 such stars, associated in the same shower as the first star, is much smaller, being proportional to $(n\ p)^{2}$.

Brown et al. (1949) analysed 4,923 stars formed at the Jungfraujoch. They found only 223 had more than 1 shower particle and 13 more 10 shower particles. As the anomalous distribution of stars on emulsions occurs over distances of the order of 1 mm., sufficiently collimated showers could only be formed in very-high-energy interactions,

producing the characteristic highly collimated bundle of shower particles. Such events are observed in less than 1% of the stars in emulsions exposed at the Jungfraujoch. For the present, the actual separation of the shower particles will be ignored in calculating the magnitude of the shower contribution to the number of associated pairs of stars. Using the results of Brown et al. it has been shown that the number of shower particles in emulsion is equal to 0.5 per star, having made allowance for neutrons. If the absorber above the emulsion consists of lead, it is certain that on the average less than 2 shower particles are emitted from interactions in the lead. Even if this is arbitrarily increased to 5, the contribution to the number of associated pairs of stars is equal to $2p = 0.1\%$, while Li reported an excess of star-pairs of magnitude 2.5% per star.

In order to obtain associated pairs of stars of the magnitude reported by Li, it would be necessary to assume that all the star-producing particles inoident on the emulsion occur in groups of 100 shower particles, each of these groups passing through the emulsion within an area of a few square mm. This is rather unlikely.

It can be seen that both these processes would cause each star in the emulsion to be associated with a certain number of stars formed at the same time. This number can be expressed as $m \times \alpha$, where m or m+1 is the average

number of particles taking part in the process and is of the order of $\frac{a}{\lambda}$ ~1/2500. However, while the regenerative process produces secondary stars close grouped about the primary star, there is no simple way of explaining how the shower process can produce associated stars with separations predominantly of the order of 1 mm. It therefore seems that only the regenerative process can have an appreciable effect on the distribution of star-pairs for separations less than 1500 μ.

Effect of the Regenerative Process on the Star-Pair Distribution

In determining an experimental excess of star-pairs in the emulsion it is assumed that all the stars in the area have a random spatial distribution. The excess is then found by subtacting the calculated random number of star-pairs from the observed number.

It has already been shown in this section that the regenerative process causes each primary star to be associated with N(x) secondary stars (given by equation I(12)) for separations less than or equal to x. As N(x) is of the order of 10^{-3}, there is little likelihood of two close secondary stars being produced by a primary star. Li assumed that the expected excess of close star-pairs, given by the regenerative process, was actually equal to N(x) star-pairs per star. However, due to the added

secondary stars, the total number of stars in the area is increased, and the expected number of star-pairs, calculated from a random distribution of all the stars is therefore also increased. The observed excess of star-pairs will therefore be somewhat less than N(x) star-pairs per star.

Consider m primary stars in an area of sides a^1, b^1. Each star will have an average of β secondary stars associated with it in the same area. β is given by N(x) in equation I(12) with x of the order of the dimensions of the area a^1, b^1. The total number of stars observed in the area is now equal to $m(1+\beta)$. These will consist of two classes, a randomly distributed class of primary stars, and the class of secondary stars which are bunched around their respective primary stars. The resulting distribution is therefore not random. However, if the star-pair separations between all these stars are measured, the resulting distribution of separations will be very nearly the same as that obtained from a random distribution of the stars, except in the particular case of a separation between a secondary and its own particular primary. The expected excess of star-pairs with separations $\leq$ r is therefore given by two factors. Firstly, we calculate the expected number of secondaries within a distance r of their primary stars, assuming the regenerative process. To find the expected excess of close pairs we must subtract from this

figure the expected number of secondary stars within a distance r of their primary stars, assuming that they would have had a random distribution.

Originally there were m primary stars in the area. The random number of star-pairs with separations $\leq$ r is given by equation I(2) and can be written as m(m-1)Cr. Due to the regenerative process there are now $m(1+\beta)$ stars in the area. The corresponding random number of star-pairs is therefore equal to $(m+m\beta)(m+m\beta-1)Cr$. The increased random number of star-pairs is therefore equal to $2m^2 \beta Cr$, neglecting terms in β^2. A fraction $\frac{1}{m}$ of this increase will have been due to separations between primary stars and their particular secondaries, and the contribution to the calculated random number of star-pairs by associated primary and secondary stars is therefore equal to $2m\beta Cr$.

The observed excess of star-pairs will then equal

$$m N(r) - 2 m \beta Cr$$

this can be written $m\beta \left(\frac{N(r)}{\beta} - 2Cr\right)$ I(17)

The term outside the brackets is the number of secondary stars in the area. The first term in the brackets is the probability that a secondary star, lying in the same area as its primary star, should be within a distance r from it. The second term is the probability that a star, lying within an area, should be within a distance r of an unassociated star.

In calculating the value of β , which gives the number of secondaries per primary in each area, it has been assumed that the star separations extend up to the dimensions of the area. This is not strictly true, and there is an uncertainty in the value of this separation not greater than a factor of 2. Owing to the logarithmic increase in the N(r) function, the uncertainty in β is then 10%.

For a value of r equal to 1500 μ and areas similar to those used by Li (1" x $\frac{1}{2}$"):-

$$\text{then } \frac{N(1500\,\mu)}{\beta} = \frac{2}{3} \quad \text{and } 2Cr = 0.02.$$

The second term in equation I(17) can therefore be neglected for values of r less than 1500 . The excess of star-pairs expected by the regenerative effect is therefore equal to N(r) star-pairs per star, as was assumed by Li. For r = 1500 μ, N(r) = 2 x 10^{-3}, and the excess is only some 10% of the experimental excess reported by Li.

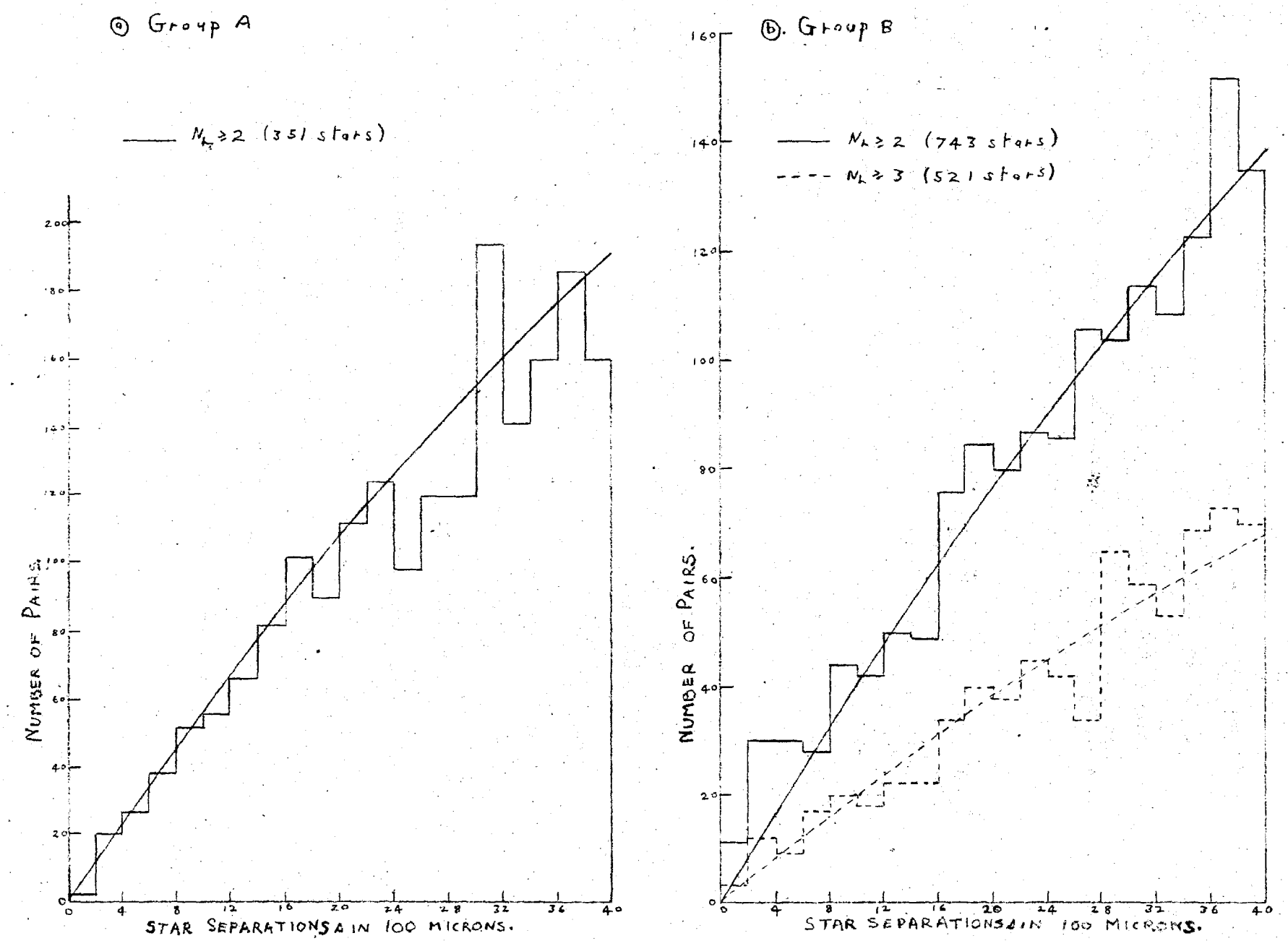
4. Analysis of 1,094 Stars in Nuclear Emulsions exposed under Lead Absorbers

The stars analysed in this work were in two groups:

A. 351 stars on 4 (2cm.)^2 areas of 400 μ G.5 plates, exposed as part of the Lead Cone experiment. This will be referred to as Group A.

B. 743 stars on 15 areas (1" x ½") of 100 μ C.2 plates, exposed by Li under lead blocks. This will be referred

Fig I.7. Distributions of Star Separations for Plates – Groups A and B.



to as Group B.

Both these groups of stars were analysed using the "perimetral" separation method discussed in Section 2. For each area the number of star-pairs having separations between s and s+ds were determined. A histogram was then tabulated with intervals ds equal to 200 μ and values of s up to 4000 μ. The experimental histogram for Group A is shown in Figure I.7(a) and can be compared with the expected distribution $P^1(s)$, given by equation I(5). The parameters a, b are now both equal to 2 cm. It can be seen that there is no sign of any excess for separations less than 1600 microns. The excess of 2% reported by Li would lead to an excess of 7 star-pairs in this region, if the anomalous "Li" effect generally applied to all stars in photographic plates. The 351 stars in this group included definite 2-track stars, that is, those which were definitely not deflections.

The second group, shown experimentally in Figure I.7(b), shows an excess of star-pairs of magnitude 3.8×10^{-2}/ star for $s \leq 1500\,\mu$. This is larger than that reported by Li. The actual excess is 28 star-pairs, over the expected number of 510 star-pairs having separations less than 1500 μ. Thus the excess is some 1.3 times the root mean square deviation of the expected number, and is certainly not inconsistent with that reported by Li. The results in this case tend to confirm the presence of an anomalous

star-pair effect. It was decided to repeat the analysis for Group B, but excluding 2-track stars. The resulting histogram, the lower dashed curve in Figure I.7(b), shows no excess over that expected on a random distribution. The anomalous star-pair effect, therefore, only applies to Group B if 2-track stars are included in the analysis. It is difficult to see any simple mechanism which could produce an excess of close 2-track stars only. Many of the 2-track stars in C.2 plates contain 1 or more "grey" tracks, invisible in C.2 plates, and will be recorded as 3- or 4-track stars in G.5 plates.

The two groups of plates were searched at different stages of this laboratory. Group B was searched in the early days and searching efficiency was a little doubtful. Group A was searched for the recent Lead Cone experiment and high efficiency here was extremely important. However, 2-track stars are difficult to find and define unambiguously, due to the difficulty of separating out deflections, possible π-μ decays etc. Their inclusion in an analysis of high statistical accuracy is rather unsuitable, unless great care is taken in searching for these stars and identifying them.

It is quite likely that the close star excess found originally for Group B could be due to a preferential inefficiency in the searching of the plates, 2-track stars having a greater probability of being found in the

neighbourhood of another star. Suppose that a 2-track star has a probability p of being found if it lies within 1500 μ of a larger star, and a probability q of being found at larger distances from another star. It is assumed that all stars with 3 or more tracks are found. If there are in a number of areas an average of m stars per area, then the random number of star-pairs within a certain separation is proportional not to m(m-1) but to m^2, as will be shown in the next section. Suppose an average of N large stars (with more than 2 tracks) and n 2-track stars lie in each area. The number of star-pairs found for separations less than 1500 μ will be proportional to $(N+np)^2$, as the total star population is effectively N+np for this separation. For the areas of Group B (1" x ½"), N is equal to 35 and so a 2-track star has a probability of approximately 0.75 of occurring within 1500 μ of a larger star. The total number of stars found in an area will therefore be $N + \frac{1}{4} n (3p+q)$ and the expected number of star-pairs lying within separations of 1500 μ will be proportional to $\left[N + \frac{1}{4} n (3p+q)\right]^2$. The observed number of star-pairs (including 2-track stars) for Group B was 538, with an expected "random" number of 510

$$\therefore \quad (N + np)^2 \Big/ \left[N + \tfrac{1}{4} n (3p+q)\right]^2 = 538/510 \qquad \text{I(18)}$$

where N = observed number of stars with more than 2 tracks/area = 35

(continued overleaf)

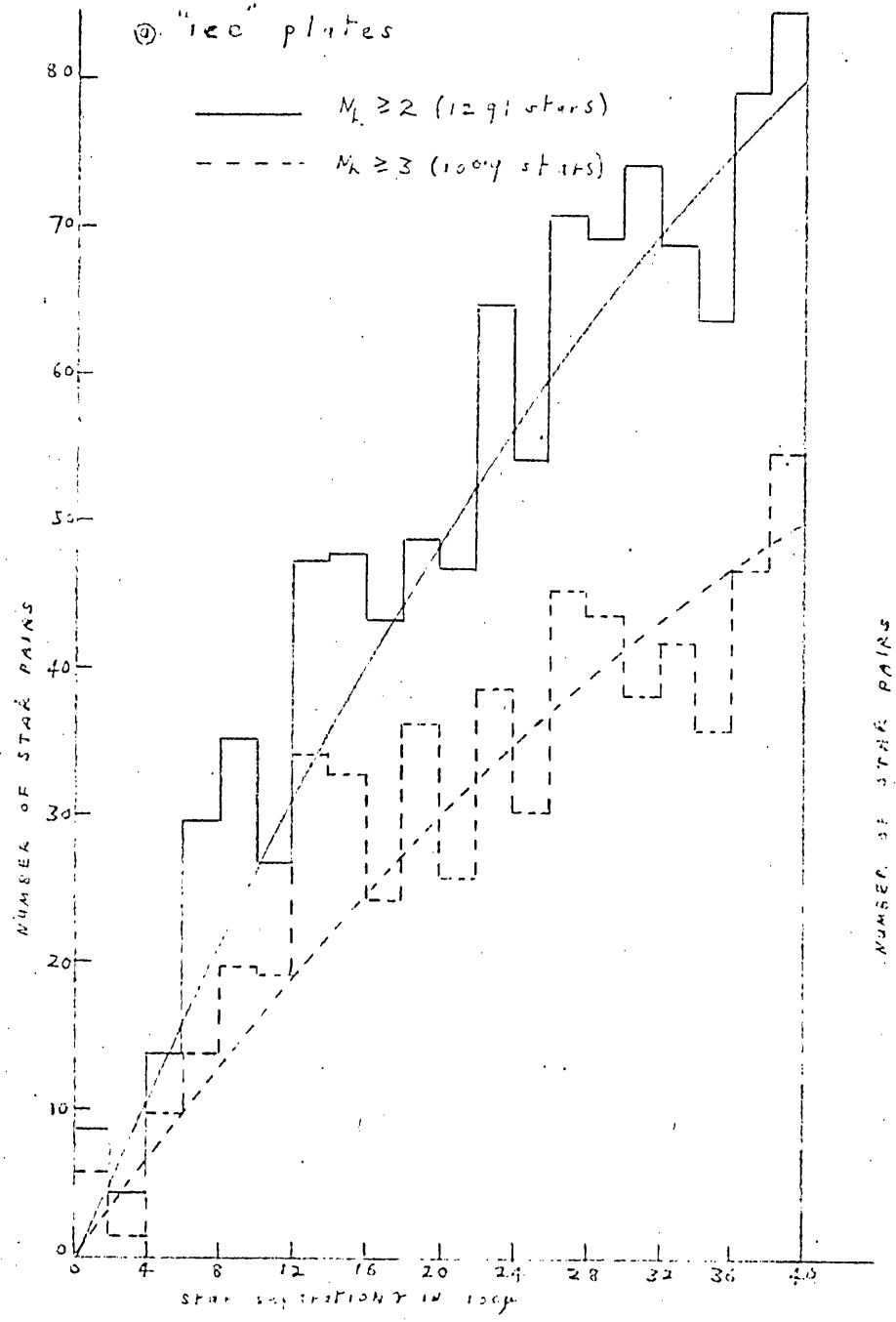
$\frac{1}{4}$ n (3p+q) = observed number of 2-track stars/area = 15

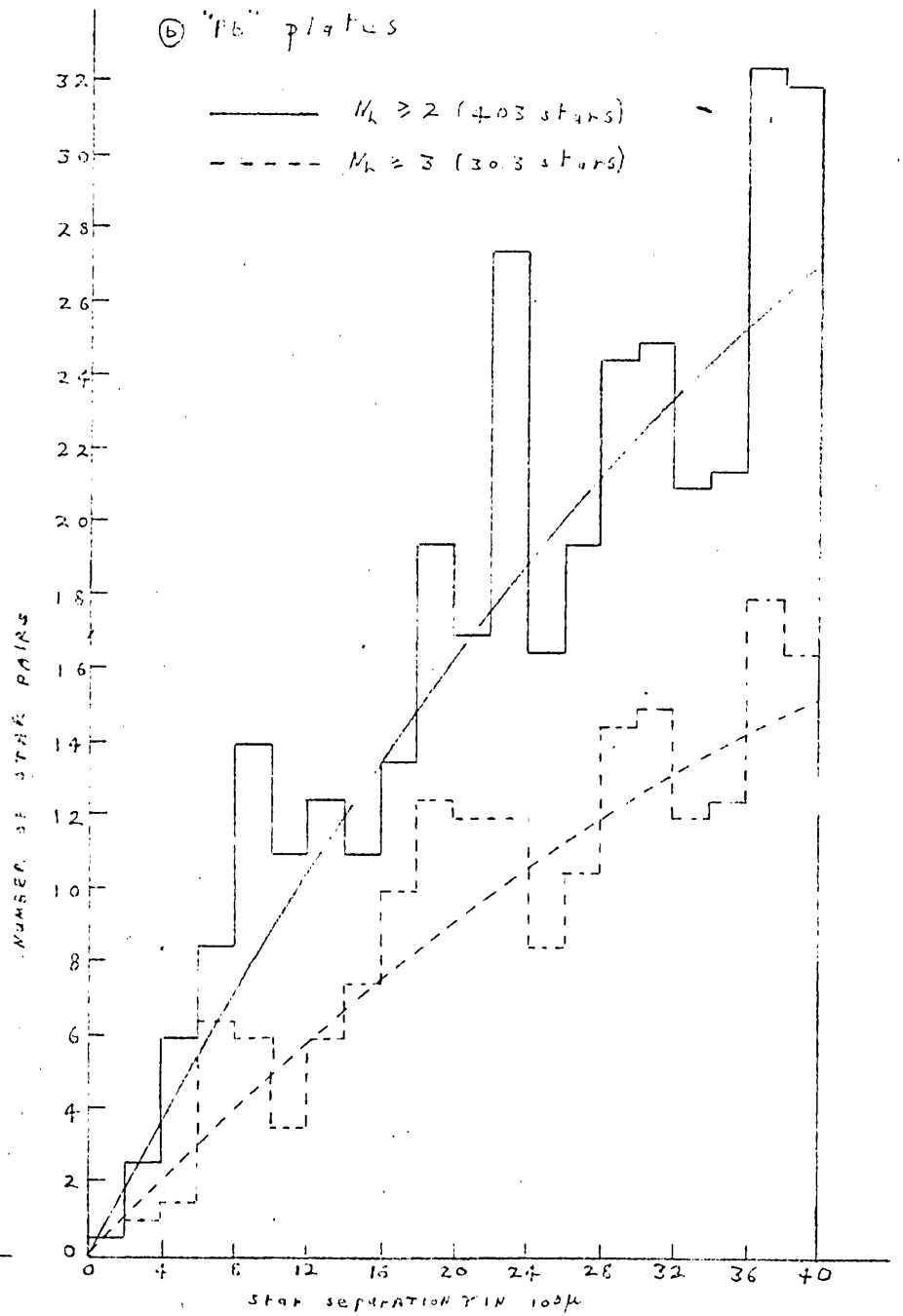
Evaluating I(18) a value of $\frac{q}{p}$ is obtained of 0.65.

This means that the anomalous distribution observed for Group B can be explained if 2-track stars are relatively more difficult to find at longer distances from other stars. If the efficiency is 100% for "close" 2-track stars, an efficiency of some 65% for distant 2-track stars is sufficient to explain the anomaly. Li was well aware of the possibility of preferentially inefficient searching affecting the distribution of star-pairs, but claimed that the searching efficiency was too high (> 98% for one group of "ice" plates) for this effect to explain the excess of star-pairs.

Nevertheless, it was decided to re-analyse two of the sets of plates described by Li in his 1950 paper. These are the "ice" plates and "Pb" plates, exposed under ice and lead at 3650 m. altitude. Li did not analyse quite all of the areas in these plates, and it was not possible to find out exactly which areas he had chosen. He mentions for the "ice" plates 1,126 stars on 77.5 in.^{2} (on 155 areas), and for the "Pb" plates 374 stars on 16 in.^{2} (on 32 areas). The average number of stars per area in each group is therefore 7.3 and 11.7 respectively. In the present analysis the "ice" plates contained 1,291 stars on 170 areas and the "Pb" plates 403 stars on 36

Fig I.8. Distribution of star separations for Li's "ice" and "Pb" plates





areas. The average numbers are now 7.6 and 11.2. It can therefore be concluded that although there are now a few more stars in each group, the results of the analysis can safely be compared with those obtained by Li.

Both these groups of plates were 100 μ C.2, and all the areas were 1" x ½".

Li had recorded the actual separation r between star-pairs. It was therefore preferable, on repeating the analysis, to use the actual distance r, instead of the "perimetral" separation s. The co-ordinates of the stars in each area were plotted on graph paper, especially noting all 2-track stars, with a multiplying factor of 10. The star-pair separations were then measured with a ruler and expressed in 200 μ intervals up to 4000 μ. Histograms were then drawn for the two sets of plates, with and without 2-track stars included in the analysis. These histograms are shown in Figures I.8(a) and I.8(b) together with the "expected" distribution $Q^1(r)dr$ given by equation I(3). With 2-track stars included, both the "ice" plates and "Pb" plates show an excess of close star-pairs ($r \lesssim 1500$) of 2×10^{-2} close pairs per star. This is identical with Li's results, as was to be expected.

On subtracting 2-track stars from the analysis, the excess completely disappeared for the "Pb" plates (Figure I.8(a)), but remained for the remaining 1,009 stars on the "ice" plates. This excess was 2.5×10^{-2} close pairs

per star and was equal to 25 close pairs more than the expected number of 100 close pairs. The average number of large stars ($\geq$ 3-tracks) per area on the "ice" plates is 6.4. If it is assumed that certain types of large stars, with 3 or 4 tracks, are more difficult to see than others, then a preferentially inefficient searching, similar to that assumed for the 2-track stars, will explain the observed excess. Using an equation similar to I(18) it can be shown that the efficiency for stars at large distances from other stars must be less than 75%, if one half of the stars with more than 2 tracks have this preferential searching inefficiency. The greatest efficiency capable of explaining the remaining star-pair excess must assume that all stars in the plate have this preferential searching efficienoy. This efficiency is then 89% for stars at long distances from other stars and, owing to the small probability (0.1) of finding stars within 1500 μ of each other on these plates, the overall searching efficiency will be $\sim$ 90%. A searching efficiency greater than this cannot explain the remaining excess.

However, it was for this group of "ice" plates that Li assumed a conservative lower limit of the searching efficiency of 98%, With a more probable efficiency of 99%. One tenth of the "ice" plates were carefully re-searched and the original efficiency for stars with more than 2 tracks was found to be 80% only. The remaining excess

for the "ice" plates can now be explained by preferential inefficient searching. This explanation is strengthened by the fact that the additional stars found were mainly at larger distances than 1500 μ from other stars, and there was a decrease in the total number of excess star-pairs.

The expected number of star-pairs within a certain separation is proportional to $\sum_i n_i(n_i-1)$, the summation being carried out over all the areas. For the areas re-searched, originally

$\sum_i n_i(n_i-1) = 646$ and the observed number of close star-pairs was equal to 11.

After re-searching the areas the value of

$\sum_i n_i(n_i-1) = 1112$ and the observed number of close star-pairs is now equal to 13.

Thus, while the expected number of close star-pairs has increased by a factor of 1.7, the actual number has increased by a factor of only 1.2. Originally for the "ice" plates there remained an excess of 25 close pairs over the 100 expected, or a ratio of 1.25 times the number expected. If the above trend for the re-searched plates was uniform over all the"ice"plates, it would therefore be more than sufficient to explain the remaining excess of close star-pairs.

There is thus no conclusive evidence that there

exists a double-star effect of the magnitude reported by Li. It was previously shown that the expected number of excess star-pairs was q x 10^{-3} for a separation of less than 1500μ, assuming a regenerative process, with q not greater than 2, but such an excess would not have been observed in the present analysis, owing to the small number of stars involved. The statistical problem of determining such an excess is discussed in the next section.

In explaining the large excess of double stars reported by Li, it has been stated that scanners have a greater probability of finding difficult events in a short period following the discovery of an event. R.M. Tennent (1952) has confirmed this effect and reported that deflections near large stars were more often recorded than those at great distances from large stars. There is also the possibility that in rejecting possible deflections on π-μ decays from the 2-track stars, the research worker might introduce some bias in favour of those nearer large stars. As far as is known, there was no really strict criterion for 2-track stars in the areas used by Li, and this makes their inclusion in the analysis rather unsuitable.

The absence of a large anomalous double-star effect has recently been confirmed by Barbanti Silva, Bonacini, Depietri, Lovera and Perilli Fedeli (1952). They analysed 1,359 stars in 73.5 cm^2 of 200 μ G.5 plates exposed under

paraffin at 3500 m. and also 1,603 radioactive stars in 23 cm.^{2} of emulsion. They measured the star-pair separations up to 1000 μ and for the cosmic ray stars they found a probability 0.43 for the distribution being random, on applying a χ^2 test. The corresponding probability for radioactive stars was 0.33. Thus there is no significant deviation from a random distribution of the cosmic ray stars, as the radioactive stars are almost certainly randomly distributed. These workers concluded that their statistics were insufficient to confirm any excess of star-pairs, but they would have found an excess of the magnitude of that reported by Li.

The detection of double stars by the photographic plate technique can only be easily applied for separations up to 1 mm. However, the shower and regenerative processes will also cause associated pairs with separations of the order of centimetres. Harding (1952) investigated the double-star effect using scintillation counters of potassium iodide. He used a bias setting such that the scintillation bursts corresponded with the production of stars in nuclear emulsions. The crystals were of dimensions 3.1 x 3.1 x 1.2 cm. and were separated by 2 mm. lead. Coincidences between the two counters were noted with the crystals side by side and one above the other. Random coincidences due to the finite resolving time of the coincidence unit was quite negligible. He showed that

the majority of the coincidence events must have been produced by events other than double stars and found no positive evidence for any double stars. He concluded that the frequency of double stars detected by the crystals must be very much smaller than that reported by Li.

5. The Statistical Problem of the Double-star Effect

In designing an experiment to determine an excess of close star-pairs, the excess must be clearly discernible from the random number of star-pairs. For an area with N_i stars the number of random pairs has been shown to be proportional to $N_i(N_i-1)$, while the number of non-random excess pairs within a certain distance can be expressed as $N_i \alpha$. It would therefore seem that the fewer stars occurring on each area, the more clearly will the excess stand out against the random background, as the latter increases far more rapidly with increasing N_i.

Consider n identical areas (in size) each having N_i stars on it, where N_i varies with i. Li and Perkins (1948) have shown that the distribution of star frequencies over areas of the dimensions of 1 cm. conform to the Poisson distribution. If the average number of stars in the n area is m, then the probability of finding N_i stars in an area equals $P_m(N_i)$

$$\text{where} \quad P_m(N_i) = e^{-m} \frac{m^{N_i}}{N_i^{1}}$$

The number of random star-pairs with separations $\leq r$ are given by Q(r) in equation I(2), and this may be written

$$Q(r) = N_i(N_i-1)\ f(r,a,b)$$

Therefore, the total number of random star-pairs in all n areas is equal to

$$n \sum_{N_i=0}^{\infty} P_m(N_i)(N_i-1)\ f(r,a,b)$$

$$= n\ f(r,a,b) \sum_{n_i=0}^{\infty} e^{-m} \frac{m^{N_i}}{(N_i-2)!}$$

$$= n\ m^2\ f(r,a,b) = n\ m^2 \beta \qquad \text{where } \beta = f(r,a,b)$$

The total number of stars in the n areas is equal to n m, and the number of excess star-pairs given by the regenerative process is equal to $n\ m\ \alpha$, where α is given by N(x) of equation I(12). If this excess is to be significant, it is desirable that the excess of star-pairs should be at least twice the root mean square deviation of the random number of star-pairs.

$$\therefore \quad n\ m\ \alpha > 2\sqrt{n\ m^2 \beta}$$

$$\therefore \quad n > 4\beta/\alpha^2 \qquad \text{I(19)}$$

It can be seen, therefore, that the detection of an excess of close star-pairs is independent of the actual number of stars in each area and depends only on the

number of areas. Of course, the total number of stars in the areas searched must be sufficient to give a reasonable number of excess star-pairs so as to be able to determine the magnitude of the excess with any accuracy. Thus, the excess should be at least 20, to give an accuracy of 25%. To facilitate efficient searching, however, it is desirable that the searchers should find at least one event in each line of searching, and the most suitable number of stars in an area 1" x ½" would be between 30 and 50 stars. If the number of stars is much above this, the events become difficult to find in the background of single tracks. The areas analysed by Li had an average of 8.5 stars per area, including 2-track stars, and this could account for the inefficient searching.

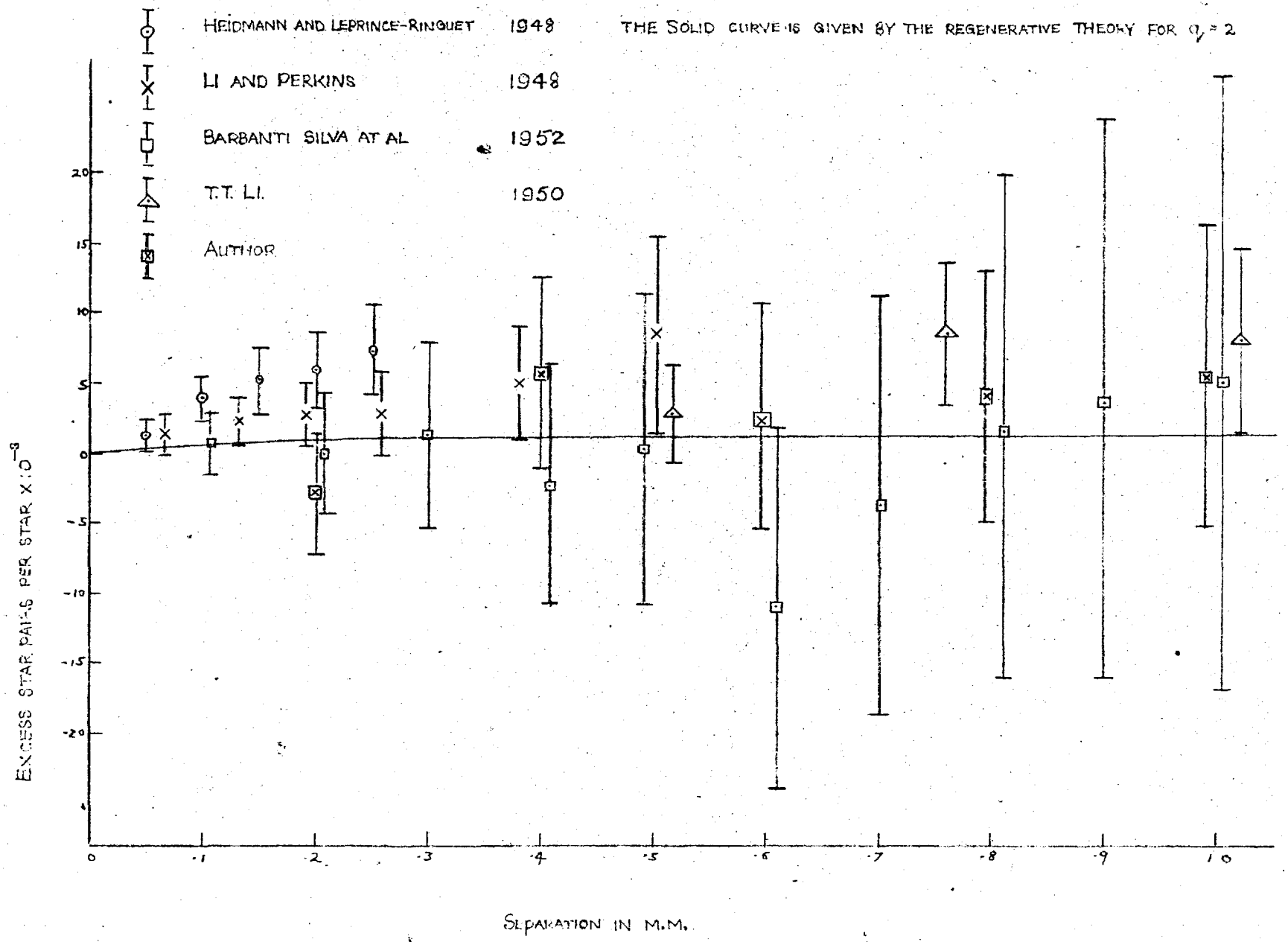
For a separation of 1500 μ in 1" x ½" areas on 100 μ plates $\beta = 1.1 \times 10^{-2}$ and $\alpha = 10^{-3}$. Substituting these values in equation I(19) we find $n > 1.1 \times 10^{+4}$. It would therefore be necessary to analyse 10^4 areas in order to establish the star-pair excess expected from the regenerative process. The excess reported by Li, with $\alpha = 2.5 \times 10^{-2}$, would be observed with n greater than 70. In the continued analysis of areas and the re-analysis of Li's areas described in Section 3, some 200 areas were taken. This would clearly resolve an excess corresponding to α greater than 1.5×10^{-2}. No

excess was observed and from the analysis it can be concluded that any excess of star-pairs is less than 10^{-2} star-pairs per star for separations $\leq 1500\,\mu$.

In their original work, Li and Perkins (1948) defined a quantity $(P-Q)/\sqrt{Q}$, where P is the observed number of star-pairs within a certain separation and Q the expected random number. This quantity gives the statistical significance of the particular excess (P-Q), and the values found by Li and Perkins and Leprince-Ringuet and Heidmann were given in Figure I.1. The quantity of physical significance, however, is not $(P-Q)/\sqrt{Q}$, but $(P-Q)/\Sigma N_i$, where ΣN_i is the total number of stars in the area. It has already been shown in this section that by increasing the number of areas sufficiently the statistical significance of any slight real excess of star-pairs can be increased to any desired value. For example, if $(P-Q)/\sqrt{Q} = 1$ for n areas, then by taking 100 n identical areas this function will increase to 10.

The real significance of the $(P-Q)/\sqrt{Q}$ function has not been entirely realised by some workers. Addario and Tamburino (1950) described an analysis of 84 stars of 3 or more prongs, in 100 μ C.2 plates exposed at 29,000 m. They calculated values of $(P-Q)/\sqrt{Q}$ and compared their values with those of Li and Perkins and Heidmann and Leprince-Ringuet. They then claimed a quantitative agreement with the values obtained at mountain elevation.

FIG I. 9. EXCESS OF STAR PAIRS OBSERVED BY VARIOUS AUTHORS



However, the only real comparison can be between values of $(P-Q) / \Sigma N_i$, and Addario and Tamburino did not give sufficient data for this to be calculated, neglecting to state the area of emulsion searched. As they only had 84 stars their value of the excess will not be of great statistical accuracy.

The values of $(P-Q) / \Sigma N_i$ found by all the observers previously mentioned, except Addario and Tamburino, are given in Figure I.9, and can be compared with the values predicted by the regenerative process. Those referred to as Author, apply to the Lead Cone (Group A) and Li's Lead Blocks (Group B) (with 2-track stars excluded), described in Section 3. These values are shown for star separations up to 1200 μ.

It can be seen that the results of the present analysis (Author) and the recent results of Barbanti Silva et al. show no evidence of any excess greater than that given by the regenerative theory. There is an excess for separations less than 500 μ given by the original results for Heidmann and Leprince-Ringuet, and Li and Perkins, but it may be remembered that these results included 2-track stars. Both these sets of plates were exposed vertically, moreover, and this effectively increases the number of secondaries remaining in the plate by a factor of 2 or 3, owing to the downward collimation of the shower particles.

It was pointed out in Section 3 that any anomalous distribution of stars in a photographic plate is most likely due to the simultaneous creation of 2 or more stars in the plate. The analysis of star-pair distributions would not show any effect, however, if many of the stars are created simultaneously with separations of the order of centimetres. At least one half of the stars formed in the regenerative process, and most of the stars formed in any shower process come into this category.

An apparatus was designed by N.C. Barford (1950) to study the production of stars as a function of time. This apparatus consists of two circular plates, rotating with respect to each other with a very close separation. The period of rotation is of the order of 3 weeks. Stars formed in one emulsion can be traced through to the opposite emulsion, and from the angular displacement of the two plates, the times of the formation of the stars can be determined. It is further possible, in principle, to do this not only for stars, but for single "grey" proton tracks, if the background is not too large. The maximum resolution in time available was one part in 10,000, using the total revolution of the plates. Stars formed in these rotating plates can therefore be regarded as having been created in one of 10,000 time cells. The proability p of finding any star in a particular cell

is then equal to $^{1}/_{10,000}$.

If there are N stars in the plates, the probability of finding 2 stars in 1 particular cell is equal to $^{N}C_{2}\ p^{2}$, and so the probability of finding 2 stars in any cell equals $^{N}C_{2}\ p$. If N is fairly large, so that N^{2} is large compared with N, then the random number of star-pairs in all the time cells is equal to $N^{2}p/2$.

The actual number of stars created simultaneously can be expressed as $N\alpha$. We are therefore expecting an excess of $N\alpha$ star-pairs, while the random number expected is $N^{2}\ p/2$. These conditions are very similar to those existing in the spatial analysis of star-pairs, discussed at the beginning of this section.

The condition for an excess to be observed is analogous to equation I(12) with n equal to 1,

$$\text{that is,} \quad 1 > p\ /_{\alpha}{}^{2}$$

Hence, using one pair of rotating plates, the minimum value of α which can be determined is $\alpha = \sqrt{2p}$ or $\alpha = 1.4 \times 10^{-2}$. The maximum regenerative effect gives α equal to 4×10^{-3} and it has previously been shown that the shower contribution is unlikely to be more than 1×10^{-3} simultaneous stars per star. The rotating plate model could therefore be used to confirm the absence of any anomalous time correlation in star-production of the order of 10^{-2} excess pairs per star.

Discussion and Conclusion

The nuclear emulsion technique has one great disadvantage over the counter and cloud-chamber techniques, in investigating statistical problems similar to the double-star effect. This is the human element which comes into the scanning of the emulsions. It has been shown that the bias errors introduced by the searchers can be of the same order of magnitude as the excess reported by the early workers in this field.

The stars formed in nuclear emulsions are also unsuitable for determining any correlation in groups of particles passing through the emulsion, as the mean free path for star-production is much longer than the thickness of the plates. If a very large number of particles pass simultaneously through the emulsion, then only a slight anomaly in the spatial distribution will be observed. In principle, the problem is similar to a coincidence counter experiment, where each counter has an efficiency of 10^{-3} in detecting particles. The large number of particles required to explain the original excess of star-pairs would be easily detected using counters or cloud chambers, but no such numbers have been observed in experiments at mountain altitudes. If the anomalous excess does exist, then one must assume that some stars in nuclear emulsion are formed by a different process from the usual nucleonic or mesonic interaction.

However, there is no reason to believe that the original excess of star-pairs cannot be ascribed to biasing errors of the searchers, especially for 2-track stars. There is, it is true, a possibility that 2-track stars do contribute a real excess of star-pairs of magnitude 10^{-2} per star, by some mechanism as yet unknown. In order to repeat the analysis with a reasonable area of emulsion (200 1" x ½" areas) and a scanning efficiency of at least 99%, about 4 scanner-years would be required.

It can be concluded that the results reported by the previous workers offer no conclusive evidence for an anomalous star-pair effect. In order to prove the absence of any anomalous excess, greater than that given by a simple regenerative process, a great scanning effort would be required. In the light of the preceding discussion this would hardly be justified.

II. THE LEAD CONE EXPERIMENT

Introduction

Information on the star-producing component of the cosmic radiation may be obtained from three sources. The first is the nature of the stars produced, the second is the effect of absorbers on the radiation and the third is the angular distribution of the radiation. Experiments dealing with the first two aspects have been described (e.g. Barton, George and Jason 1951; Brown et al. 1949; Rosser and Swift 1951) but the experimental conditions have been geometrically unsuitable for giving information about the third. The experiment described here was designed particularly for the last purpose, although in the course of the work interesting results have been obtained for the other two.

The angular distribution of the charged component producing stars has been previously given by Page (1950), who reported a $\cos^2 \Theta$ zenith angle dependence at mountain altitudes. However, the statistics were rather poor, and this experiment shows that the charged particles producing stars are rather more collimated than this.

The lead cone absorbers used in this experiment were designed so that radiation with zenith angles greater than a certain angle could reach the plates without passing through the absorber, while radiation with zenith

FIG II.1. GEOMETRICAL DETAILS OF A Θ° CONE

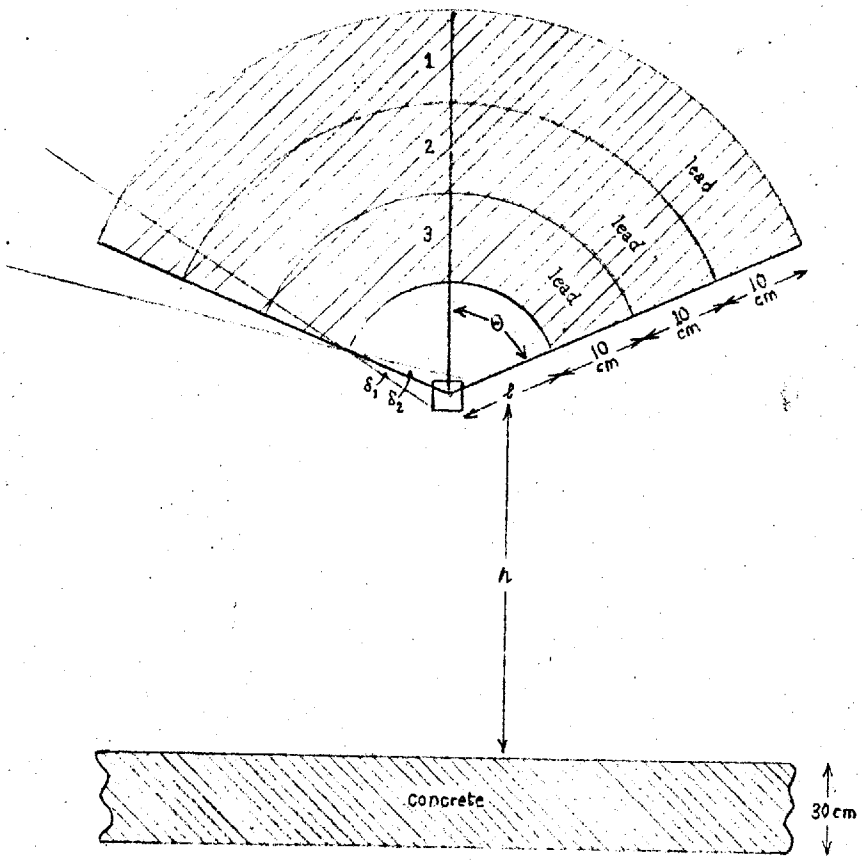


TABLE II.1. GEOMETRICAL DETAILS

Θ (°)	0	10	20	40	60	90
δ_1 (°)	—	2·2	2·8	5·2	7·9	0
δ_2 (°)	—	2·0	3·0	5·4	7·4	15·0
t (cm)	—	30	25	15	10	1·5
h (cm)	27·7	26·3	26·9	28·7	28·5	28·0

angles less than this angle had to penetrate the total thickness of absorber. By varying this cone angle, certain angular properties of the radiation can be studied.

1. Experimental Details

Ilford G.5 nuclear emulsion plates (double-sided 200 μ and single-sided 400 μ) were exposed at the Jungfraujoch (3570 m., 47° geomagnetic N) during 1950 and 1951 under inverted lead cones.

The lead absorbers were in the form of truncated lead cones, with various half-angles from 0° to 90°. Each cone was split into 3 shells of 10 cm. thickness so that absorption under 1020 and 30 cm. of lead could be investigated. The plates were stacked vertically below the cones, and only those parts of the emulsions were searched which lay within a vertical circular cylinder of diameter 2 cm. and height 2 cm. at the apex of each cone. The essential features of the experimental arrangement are shown in Figure II.1.

For a cone of half-angle Θ we can define angles δ_1 and δ_2 such that any undeviated ray reaching the searched cylinder of emulsion with declination less than $\Theta - \delta_1$ must pass through the total thickness of lead, while if it is greater than $\Theta + \delta_2$, it can pass through no lead. Values of δ_1 and δ_2 are given in Table II.1 for the various values of Θ using 30 cm. lead (shells 1,

Fig. II.2 Photograph of a 40°, 10 cm, lead cone.



2 and 3). For 20 cm. (shells 1 and 2) and 10 cm. (shell 2), these values of δ_1 and δ_2 are less. The probable error in the Ⓗ co-ordinate is clearly less than δ_1 or δ_2 and we may certainly say that the angular measurements have a precision within 10%. Also shown in Table I are the various distances of the plates from the innermost lead shell (ℓ cm.) and from the concrete roof above which the cones were suspended (h cm.).

Each set of plates was sealed at approximately 15°C. in an atmosphere of 30° to 40° relative humidity, and maintained at 10° to 20°C. using thermostatically controlled heating elements throughout the experiment to obviate fading.

The photograph of a typical lead cone is shown in Figure II.2. The method of suspension of the cones and of the plates is shown. At the apex of this cone can be seen the thermostatically heated container, which holds the plate box.

The boxes containing the plates, the heating elements, and the scaffolding supporting the cones, contributed approximately 1 gm. cm^{-2} of absorber extra, but this has been neglected throughout.

The emulsion was developed by the temperature cycle method to a minimum grain density of 30 to 40 grains per 100 μ of track. In the succeeding analysis those plates were rejected which were so distorted as to impair

searching efficiency or the classification of stars. As scattering measurements were not used in the analysis, a degree of distortion causing effective scattering of straight tracks by a few degrees in a 100 μ length was not too serious. However, in one batch of plates the excessive scattering gave straight tracks a sinusoidal appearance, with a half wavelength of about 10 μ. The exposure under the lead cones was therefore repeated for this batch.

The emulsion thickness of one-third of all the plates was measured before and after the development, using a thickness gauge. Care was taken to measure the glass thickness of each plate separately. This was done using a microscope fine focussing adjustment, which was calibrated using glass slides of known thickness. As the same immersion oil was used in both cases, errors introduced by the different refractive indices cancel out. From this a shrinkage factor 2.5 $\pm$ 0.05 was calculated and used to determine the initial thickness of the emulsion in the remaining plates, which were measured only after development. Variations of 10% or more from the nominal emulsion and glass thickness were common. The nominal "400 μ" emulsion was found to have an average thickness before development of 417 μ, while for the "200 μ" emulsion the initial thickness was found to be 184 μ. The variations in thickness of the emulsion were

sufficient to cause appreciable errors in the star-production rate, if the nominal thicknesses had been assumed.

2. Scanning of the Emulsions

Great importance was attached to the scanning of the plates. It has already been shown in Part I of this thesis that searching inefficiency can cause serious errors in work requiring statistical accuracy. Inefficient searching soon showed up as irregularities in the plots of star-production rate against cone angle, and this problem was therefore considered in detail. As far as possible emulsion areas exposed under a particular cone were scanned by at least two scanners, to avoid any personal error for the star-production rate under that cone.

A really efficient scanner requires a certain minimum power of concentration. It seems that girls of very high or very low intelligence do not make very good scanners, especially for the type of work required in the lead cone experiment, where there is little to arouse the interest of the scanner. The most efficient scanners in this department seem to combine the minimum of interest in the physical significance of the events found with an intelligent awareness of any unusual event. Searchers lacking concentration were found to miss even stars with more than 10 tracks, and the results found by such searchers were not used in this experiment.

Some specimen areas of the emulsion were carefully

scanned twice and, assuming the overall efficiency of these to be 100%, it was found possible to divide the 6 searchers concerned into 2 groups. The 4 experienced scanners, who scanned the great majority of the areas, were 95% to 100% efficient, and the 2 inexperienced scanners were 80% to 90% efficient in finding 3 and 4-pronged stars. In the analysis of these small stars a correction factor of 1.1 was there applied to those found by the latter. As this affected only a small fraction of the results, the overall correction factor is in most cases nearly 1.0 (see Tables II.2 and II.3), and none of the conclusions is invalidated if no such correction is made. The total scanning effort required was some 70 scanner-weeks, not including those areas which were scanned by inefficient scanners and later neglected.

The plates were scanned at 250 x magnification, and all the events recorded, including 2-track stars, were checked by the author at 800 x magnification. Any event showing 3 or more tracks of grain density greater than 1.5 x minimum and length greater than 4 μ were used in the analysis unless

(a) all such tracks were less than 70 μ long, in which case the event was assumed to be a radioactive disintegration,

(b) one track could have been caused by a slow meson travelling towards the centre of the event - a

Tables II.2, 3, 4 and 5.

N_h = number of heavily ionising particles;

n_s = number of shower particles;

n = neutral primary;

p = charged primary.

Table II.2. Nuclear Disintegrations under 20 cm. Lead at 5570 m.

Cone Semi-angle	Thickness d cm.	Exposure Days	Corrected Days	Vol. V cc. of Emul.	Number of heavy tracks N_h / Type of Star n_s	3	4	5	6	7	8	9	10	11	12	13	14	15	16	17	18	19	≥20	Total	Searching Factor $3 \leq N_h \leq 4$
0°	10	37	39.2	0.343	0(n)	77	57	18	10	3	4	2	3	1	-	2	-	1	-	-	-	-	-	178	1.0
					0(p)	2	3	5	2	2	-	2	2	-	-	-	-	-	-	-	-	-	-	18	
					≥1(n)	2	2	2	-	-	-	-	-	-	-	-	1	-	-	1	-	-	-	8	
					≥1(p)	-	2	-	1	-	-	-	-	-	1	1	1	-	-	-	-	-	-	6	
0°	30	46	46.4	0.862	0(n)	241	139	76	33	14	13	8	7	6	1	3	2	2	1	2	-	-	-	548	1.0
					0(p)	17	21	11	10	7	2	2	2	-	2	1	-	-	-	-	-	-	-	75	
					≥1(n)	22	12	5	5	3	4	2	-	1	3	-	-	-	-	-	-	-	1	58	
					≥1(p)	5	6	4	4	2	1	4	1	3	1	1	2	-	-	-	1	-	1	36	
10°	30	46	46.5	1.009	0(n)	269	160	80	38	28	6	5	5	1	8	2	2	1	1	1	-	-	1	608	1.0
					0(p)	16	19	12	8	5	4	3	1	2	2	1	1	-	-	2	-	-	-	76	
					≥1(n)	10	7	3	1	1	-	1	1	1	3	1	-	1	1	-	-	-	-	31	
					≥1(p)	3	3	4	1	1	2	-	1	1	1	-	1	-	1	1	-	-	-	20	
20°	30	46	47.2	0.343	0(n)	67	51	21	19	7	2	2	3	-	-	-	-	-	-	-	-	-	-		1.0
					0(p)	4	10	3	4	3	-	1	1	-	-	1	-	-	-	-	-	1	-	28	
					≥1(n)	3	7	2	-	2	-	-	-	1	1	1	2	-	-	-	-	-	-	19	
					≥1(p)	2	1	-	2	1	-	1	2	-	-	-	1	-	-	-	-	-	1	11	
40°	30	46	47.9	1.116	0(n)	213	111	58	31	10	14	4	5	2	1	1	-	-	-	-	-	-	-	450	1.0
					0(p)	16	8	3	6	7	-	1	5	1	-	-	-	-	-	-	-	-	-	47	
					≥1(n)	8	4	1	-	-	2	1	-	-	-	-	-	-	-	1	-	-	1	18	
					≥1(p)	6	6	2	1	2	1	-	1	2	-	-	-	-	-	-	-	-	1	22	
60°	30	46	50.3	0.338	0(n)	47	27	11	5	1	1	-	-	-	-	-	-	-	-	-	-	-	-	92	1.0
					0(p)	3	5	6	-	1	-	-	-	-	-	-	-	-	-	-	-	-	-	15	
					≥1(n)	-	2	-	-	1	-	-	1	-	-	1	-	-	-	-	-	-	-	5	
					≥1(p)	-	-	1	1	-	-	-	-	-	-	-	-	-	-	-	-	-	-	2	
90°	30	46	50.8	1.5	0(n)	190	98	42	13	11	9	4	3	3	2	-	1	-	-	-	-	-	-	376	1.0
					0(p)	9	15	6	5	2	3	-	-	1	-	-	-	-	-	-	-	-	-	41	
					≥1(n)	6	4	2	3	1	-	-	1	-	2	-	-	-	1	1	-	-	-	21	
					≥1(p)	2	-	4	2	1	1	1	-	1	2	1	-	-	1	-	1	-	-	17	

Table II.3. Nuclear Disintegrations under 30 cm. Lead at 3570 m.

Cone Semi-angle	Thickness d cm.	Exposure Days	Corrected Days	Vol. V cc. of Emul.	Type of Star n_s	Number of heavy tracks N_h 3	4	5	6	7	8	9	10	11	12	13	14	15	16	17	18	19	≥20	Total	Searching Factor $3 \leq N_h \leq 4$
0°	20	51	51.8	0.596	0(n)	170	95	52	27	16	6	4	3	2	3	–	2	–	1	–	1	–	–	382	1.00
					0(p)	16	10	15	2	5	4	2	1	3	–	–	–	1	–	–	–	–	–	59	
					≥1(n)	7	8	4	2	2	1	2	–	1	3	–	–	1	–	–	–	1	–	32	
					≥1(p)	4	6	2	2	2	2	–	–	2	1	–	–	–	1	1	–	–	–	23	
10°	20	51	51.9	0.655	0(n)	182	116	50	20	8	5	9	4	1	4	2	1	–	–	–	–	–	1	403	1.00
					0(p)	14	5	12	11	7	1	1	–	1	1	1	–	–	–	–	–	–	–	54	
					≥1(n)	5	5	4	5	2	1	2	2	1	1	1	–	–	1	–	–	1	–	31	
					≥1(p)	6	2	9	2	4	2	3	1	1	1	1	2	–	1	1	1	1	1	39	
20°	20	51	52.1	0.145	0(n)	39	21	11	5	2	1	3	–	1	1	1	1	–	–	–	–	–	–	86	1.00
					0(p)	3	6	1	–	1	–	1	1	–	–	–	–	1	–	–	–	–	–	14	
					≥1(n)	3	3	1	–	–	1	–	–	–	–	–	–	–	–	–	–	–	–	8	
					≥1(p)	2	–	1	1	–	–	1	–	–	–	–	–	–	–	–	–	–	–	5	
40°	20	51	52.6	0.881	0(n)	202	108	49	28	9	3	6	3	1	1	–	–	1	–	–	–	–	1	412	1.04
					0(p)	11	12	11	6	3	3	3	–	3	2	1	–	–	2	1	–	1	–	59	
					≥1(n)	6	2	3	2	1	1	3	2	–	–	1	2	–	–	–	–	1	1	25	
					≥1(p)	1	5	3	2	1	1	1	1	–	–	–	–	–	–	–	–	1	1	17	
60°	20	51	52.7	0.146	0(n)	40	8	3	8	2	2	–	1	–	–	–	–	–	–	–	–	–	–	64	1.00
					0(p)	3	–	–	1	1	–	–	–	–	–	–	–	–	–	–	–	–	–	5	
					≥1(n)	1	1	–	–	–	–	–	–	1	–	–	–	–	–	–	–	–	–	4	
					≥1(p)	–	–	–	–	–	–	–	–	1	–	–	–	–	–	–	–	–	–	1	
90°	20	51	53.8	1.06	0(n)	188	83	62	18	15	9	6	1	–	3	2	1	–	–	–	–	–	–	388	1.05
					0(p)	12	19	5	7	8	1	–	1	–	1	1	–	1	–	–	–	–	–	56	
					≥1(n)	4	3	2	1	2	1	3	1	1	–	1	–	–	–	1	–	–	1	21	
					≥1(p)	6	2	2	1	2	1	2	1	1	–	–	–	–	–	–	–	–	–	18	

Table II.4. Nuclear Disintegrations under No Lead at 3570 m.

Number of Heavy Tracks N_h	3	4	5	6	7	8	9	10	11	12	13	14	15	16	17	18	19	20	$3 \leq N_h \leq 6$	$7 \leq N_h$	$3 \leq N_h \leq 6$	$7 \leq N_h$	$3 \leq N_h \leq 6$	$7 \leq N_h$
Type of Star n_s																			Bristol				Manchester	
0(n)	488	291	146	70	33	23	14	13	9	4	5	4	3	2	2	1	–	–	995±32	113±11	600±11	101±4	835±25	116±9
0(p)	35	34	31	14	14	6	6	5	3	2	1	–	1	–	–	–	–	–	114±11	38±6	54±3	45±3	70±7	46±6
≥1(n)	31	22	11	7	5	5	4	–	2	6	–	1	1	–	1	–	1	1	71±8	27±5	31±2	32±2	72±7	37±5
≥1(p)	9	14	6	7	4	2	4	1	5	3	2	3	–	1	1	1	–	1	36±6	29±5	29±2	33±2	45±6	18±4
Total	563	361	194	98	56	36	24	19	19	15	8	8	5	3	4	2	1	2	1216	207	714	211	1022	217

Corrected exposure 84.3 cm^3 days.

Searching factor 1.01 ($3 \leq N_h \leq 4$).

Table II.5. Nuclear Disintegrations under 30 cm. Lead Hemisphere at 3570 m.

Number of Heavy Tracks N_h	$3 \leq N_h \leq 6$	$7 \leq N_h$	Manchester $3 \leq N_h \leq 6$	Manchester $7 \leq N_h$
Type of Star n_s				
0(n)	343±19	33±6	256±8	24±2
0(p)	35±6	6±2	26±2	11±2
1(n)	15±4	6±2	16±2	10±2
1(p)	8±3	9±3	16±2	10±2
Total	401	54	314	55

Corrected exposure 76.2 cm^3 days.

Searching factor 1.00 ($3 \leq N_h \leq 4$).

σ -star, and

(c) it could be interpreted as a proton-proton scatter.

Quite a number of 3-track stars which at first sight seemed to be radioactive were found to have a steeply dipping track with a length of over 100μ. The scanners were warned to look out for such events, although inexperienced ones did tend to miss them.

3. Results

These are tabulated for all cone angles and thicknesses in Tables II.2 and II.3, which show the 20 cm. and 30 cm. cone results respectively. Plates under no absorber were exposed during the experiments with 20 cm. and 30 cm. and the stars observed in them are given separately in Tables II.2 and II.3. Also shown in Table II.3 are the results with no absorber for plates exposed in the experiment with 10 cm. of lead. The plates under the 10 cm. cones have not been used in the analysis, as the searching effort required was too great. In Tables II.4 and II.5 the combined starintensities under no absorber, and under the 30 cm. hemispherical shell is summarised, and can be compared with the results of other observers.

Classification

The usual classification of tracks in terms of their grain density, g, relative to minimum grain density, g_m,

was employed. The numbers of "minimum" tracks ($g \leq 1.5\ g_m$), "grey" tracks ($1.5\ g_m \leq g \leq 7\ g_m$) and "black" tracks ($7\ g_m \leq g$) were recorded for each star. The minimum tracks correspond to proton energies of greater than 330 MeV and meson energies greater than 50 MeV. The grey tracks correspond to protons with energies between 330 and 25 MeV and mesons from 5o to 4 MeV. The black tracks correspond to protons of less than 25 MeV and mesons of less than 4 MeV.

If at least 1 of the minimum tracks lay in the upper hemisphere, it was assumed that the disintegration was oaused by a charged particle (a p-star), and the number of shower particles (n_s) was taken as 1 less than the number of minimum tracks. If not, it was assumed that the primary particle was neutral (producing an n-star), and n_s was taken equal to the number of minimum tracks. It has previously been shown that about 10% of the shower particles are emitted upwards (Camerini, Davies, Fowler, Franzinetti, Muirhead, Lock, Perkins and Yekutieli 1951) and some of the stars classified as p-stars will actually have been produced by neutral radiation. However, this classification of stars was used by Brown et al. (1949) and Rosser and Swift (1951) and can be safely used in comparing the rates of star-production. The size of a star is defined by the number of "heavy" prongs, N_h, where N_h is the sum of the grey and black tracks.

Errors and Corrections

The small correction factor for searching inefficiency has already been discussed. All the plates used in the Lead Cone experiment were several days at sea-level and after the exposure at the Jungfraujoch. To correct for the sea-level exposure an absorption length in air for the radiation produoing all types of stars of 135 g cm.$^{-2}$ has been assumed (Bernabdini, Cortini and Manfredini 1949). This gives a star-production rate at sea-level of one-twelfth that found at the Jungfraujoch. From the plates exposed without absorbers at the Jungfraujoch the sea-level production rate was found to be 1.5 stars cm.$^{-2}$ day^{-1}. The number of stars in each batch of plates due to the sea-level exposure was then estimated. This correction has been expressed in terms of a total equivalent exposure time at the Jungfraujoch, for each particular batch of plates considered. For a given sea-level exposure the equivalent number of days at mountain altitudes depends on the star-production rate under the particular cone, and it can be seen in Tables 2 and 3 that the corrected exposure time increases with the angle of the cone.

It must be emphasised that all the numbers of stars given in the Tables 2, 3, 4 and 5 are of stars found and checked - corrections are applied only in the subsequent analysis.

In calculating star-production rates the statistical errors due to random fluctuations were calculated as follows. If N events were observed, the errors were assumed to be $\pm \sqrt{N}$ if $N > 40$, while for smaller values of N the fiducial limits discussed by Regener (1951) were used. If the true mean were found (from an infinite distribution of stars), it would have a probability of 0.84 of lying within the above limits.

4. Analysis of the Results

In this initial analysis of the results the star-producing component will be treated as a whole, and the resulting angular distribution obtained will be averaged over all the particles. The following simple assumptions are made:

(a) star-producing radiation travels in straight lines;

(b) if a primary particle in this radiation interacts in the absorber, giving rise to a secondary particle itself capable of producing a star, the latter continues in the same direction as the former (this will be called a collimated secondary);

(c) the intensity of radiation at any angle traversing a distance d in the absorber suffers an overall reduction $\alpha(d)$ of its original value, where $\alpha(d)$ is independent of angle.

It will be assumed that the angular distribution of the radiation is proportional to $\cos^m \Theta$ steradian^{-1} in

the upper hemisphere with zero intensity in the lower hemisphere, where Θ is the zenith angle.

Consider an inverted lead cone of half-angle Θ and thickness d. If we ignore absorption, the flux of particles reaching a given volume of emulsion with zenith angles between θ and $\theta + d\theta$ can be expressed as

$$a\, 2\pi \sin\theta \cos^m\theta \, d\theta$$

where a is some constant.

Those particles passing through the lead cone, that is, with zenith angles from 0 to Θ, will suffer an overall reduction α (d), while those with angles between Θ and $\pi/2$ will reach the emulsion unaffected by the absorber. The number of particles reaching the emulsion is therefore equal to

$$\int_0^{\Theta} 2\pi\, a\, \alpha(d) \sin\theta \cos^m\theta \, d\theta + \int_{\Theta}^{\frac{\pi}{2}} 2\pi\, a \sin\theta \cos^m\theta \, d\theta$$

$$= \frac{2\pi a}{m+1}\left[\alpha(d)\,(1 - \cos^{m+1}\Theta) + \cos^{m+1}\Theta\right]$$

The rate of star-production at the apex of such a cone is therefore of the form:

$$N(\Theta) = N(0)\ \alpha(d)\left[1 + \cos^{m+1}\Theta\ \left(\frac{1}{\alpha(d)} - 1\right)\right] \qquad \text{II(1)}$$

Whatever the value of m, α (d) is given by

$$N\left(\frac{\pi}{2}\right) = N(0)\ \alpha\ (d) \qquad \text{II(2)}$$

If for different values of d the experimental results

FIG. II. 3 Rate of production of all stars with $N_s \geq 3$ under 20 cm of lead.

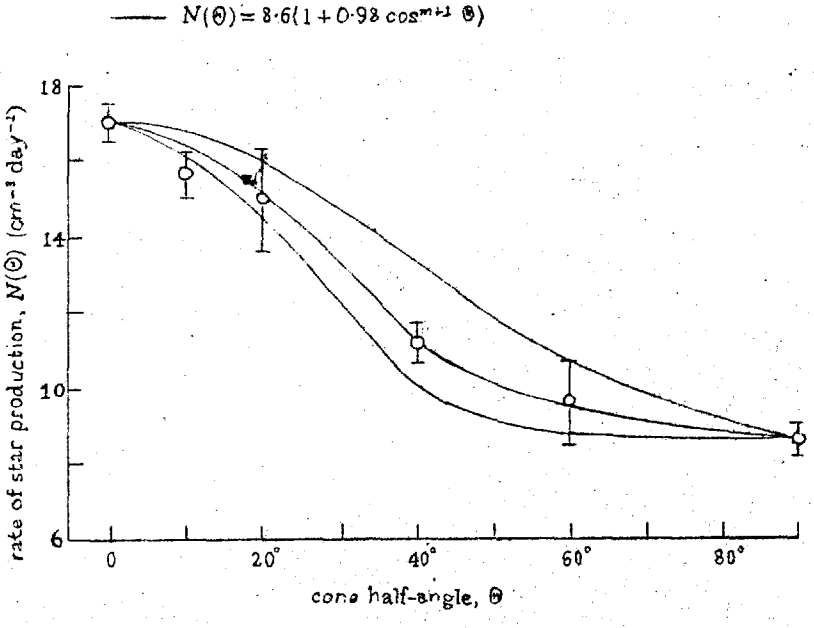
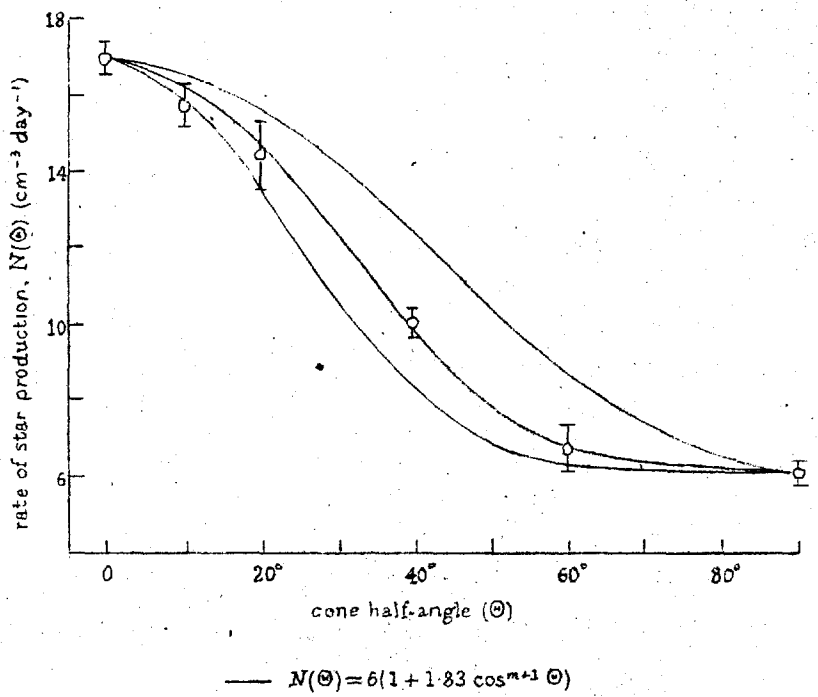


FIG. II. 4 Rate of production of all stars with $N_s \geq 3$ under 30 cm of lead.



satisfy a variation of type (1) for the same values of m, the zenith angle law of distribution will be verified (subject to the assumptions already mentioned). If, in addition, for variations of d, there is a constant satisfying

$$\alpha(d) = e^{-\frac{d}{\lambda}} \qquad \text{II(3)}$$

one will be justified in talking of effective exponential attenuation and in defining λ as the attenuation path-length.

Various classes of stars were examined to see how well laws II(1) and II(3) were obeyed and to determine the relevant values of m and λ. Typical curves showing star-production rates under each cone are given in Figures II.3 and II.4. In order to obtain the most accurate values of m and λ the following procedure was adopted. N(0) was taken as the experimental value at $\Theta = 0$, combining all the results from emulsion with no absorber. For the two hemispheres of lead (20 cm. and 30 cm.) two values of the attenuation length were then obtained from the formula

$$\frac{d}{\lambda} = \log \left[N(0) \,/\, N(\tfrac{\pi}{2}) \right]$$

derived from II(2) and II(3). If they were consistant their weighted mean was taken as λ.

In order to obtain an accurate value of λ at least 1 c.c. of 0° and 90° cone emulsions were searched. A

FIG II.5. MAXIMUM RESOLUTION ANGLES Θ_M

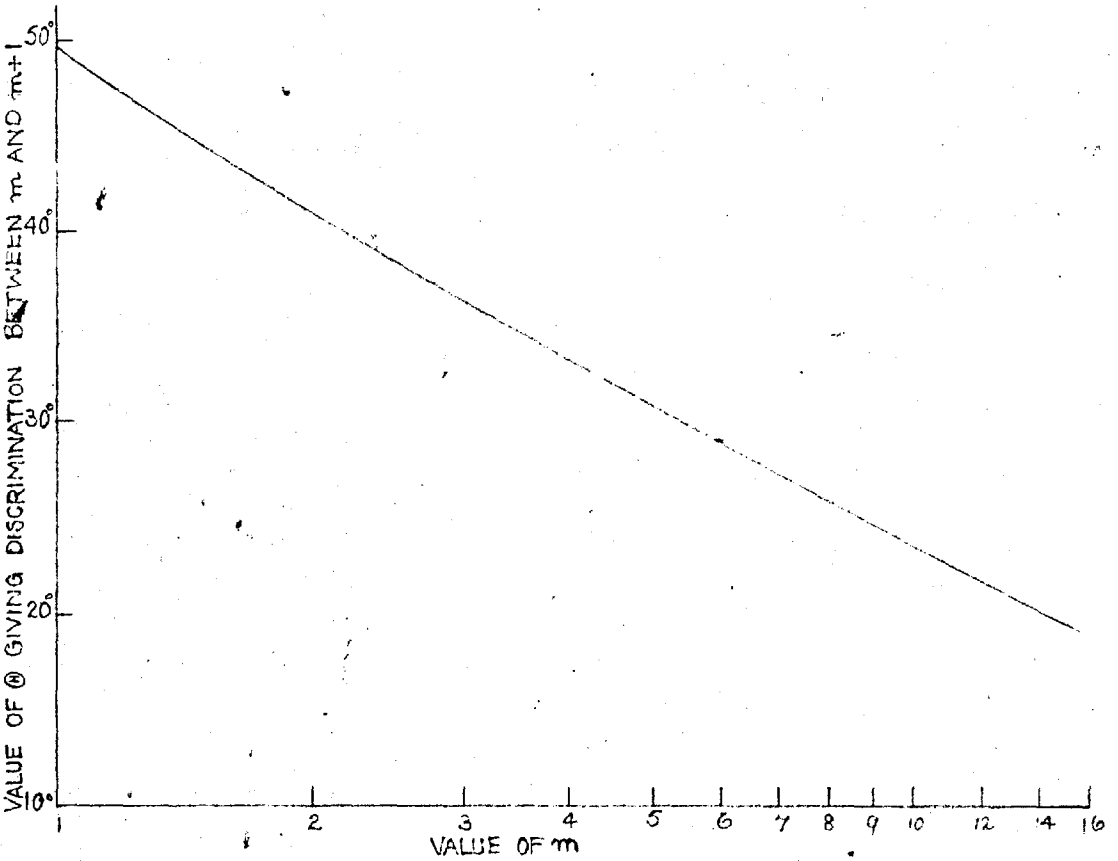
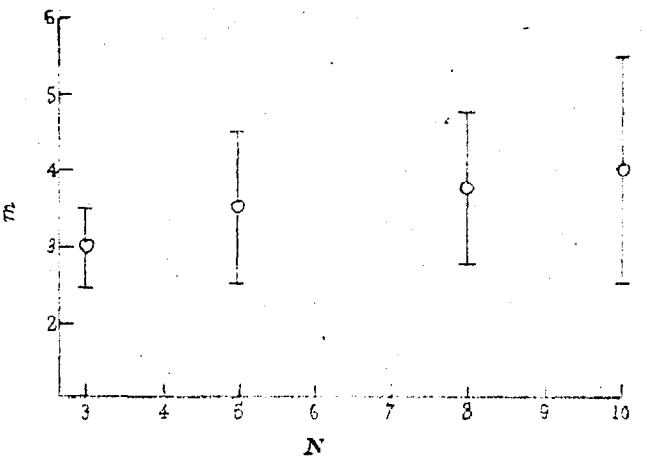


FIG. II.6. ANGULAR DISTRIBUTION EXPONENT, m, FOR STARS WITH $N_h \geq N$



few areas (2 cm. x 2 cm.) from each cone were searched to see if the production rates were consistent with curves of ~~Figure~~ type II(1) With the values of N(0) and previously determined, curves of ~~Figure~~ type II(1) were constructed for various values of m, and the production rate of all stars with $N_L \geq 3$ gave a preliminary value of $m \approx 3$, both for the 20 cm. and 30 cm. curves.

Additional searching was therefore concentrated on that cone Θ_m which gave the best discrimination between a $\cos^m \Theta$ and a $\cos^{m+1} \Theta$ law. This angle Θ_m is given by the maximum value of $C(\cos^{m+2} \Theta - \cos^{m+1} \Theta)$ where C is given by II(1) and equals $N(0)(1 - \alpha(d))$. By differentiating this expression we find

$$\Theta_m = \cos^{-1} \frac{m+1}{m+2} \qquad \text{II(4)}$$

These maximum resolution angles are shown in Figure II.5 and it is apparent that the cone giving best discrimination for values of m from 1 to 5 is the 40° cone. The cones with angles nearest to this are the 20° and 60°. The 20° cone would be important in determining the value of m only for very high collimation, with m between 10 and 20. Owing to the great scanning effort required it was not possible to obtain good statistics for the other cones as well.

For the total star-producing component the above method of analysis gave a value of λ of 330 ± 15 gm cm.$^{-2}$

and for m of $3 \pm \frac{1}{2}$. This value of λ is in good agreement with the earlier values of 310 ± 20 gm cm.$^{-2}$ (George and Jason 1949) and 305 ± 7 g cm.$^{-2}$ (Rosser and Swift 1951). Values of m and λ have similarly been calculated for different categories of stars, the final values being taken as the weighted mean of the values best fitting the results for 20 cm. and 30 cm. absorber.

5. The Angular Distribution

This experiment was designed to determine the angular distribution of the total star-producing component; the statistics, however, are not really good enough to permit an exhaustive analysis of the variation of the angular distribution with star size. Nevertheless, there are some indications of a variation of collimation with star size.

For the lowest energy stars (with $3 \leq N_h \leq 4$) the exponent $m = 2.5 \pm 0.5$ as compared with the average value of 3.0 ± 0.5. The values of m for various classes of stars are given in Figure II.6. Although all these values are consistent with $m = 3.0 \pm 0.5$, they are also consistent with an increase in m with increasing star size. This would mean that the high-energy radiation is more collimated than the low-energy component, as would be expected from the following considerations.

The high energy nucleons in the atmosphere are strongly collimated in the downward direction because of

the absorption effect. In nuclear interactions the high-energy secondaries are known to be more collimated about the primary direction than those of low energy, and hence are more collimated about the vertical. In addition, the large stars have a greater proportion of charged primaries than have the small stars; since these charged primaries suffer ionisation as well as nuclear collision losses, passage through the atmosphere above 3570 m. will tend to collimate them more than the neutral primaries.

It has been assumed that m = 2 (e.g. Harding 1951, Schopper, Höcker, and Rössle 1951) on the basis of measurement by Coates and Herz (1941) and Page (1950). The former were, however, of "straight line tracks" at sea-level, and were presumably mostly caused by μ -mesons. The latter measurements were of charged primaries only, based upon some 60 p-stars. In neither case is there a direct measure of the angular distribution of the total star-producing radiation, most of which is neutral at 3570 m.

It has been possible in this analysis to investigate the angular distribution of the charged primaries by two independent methods. First, p-stars were analysed by the method discussed in the previous section, using the 20 cm. and 30 cm. lead cones. This gave the value $m = 4.0 \pm 1$. This is not a direct measure of the angular distribution because of the secondary processes in the lead absorber. To obtain this directly the zenith angles of the primaries

FIG II.7a. ANGULAR DISTRIBUTION OF CHARGED PRIMARIES OF STARS UNDER NO ABSORBER AT 3570m.

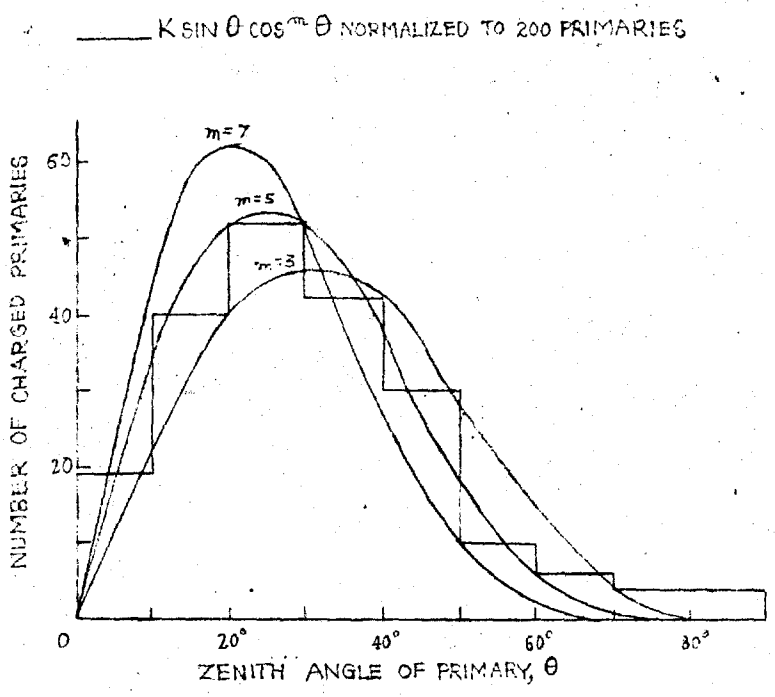


FIG II.7b DISTRIBUTION OF ANGLES OF DIP

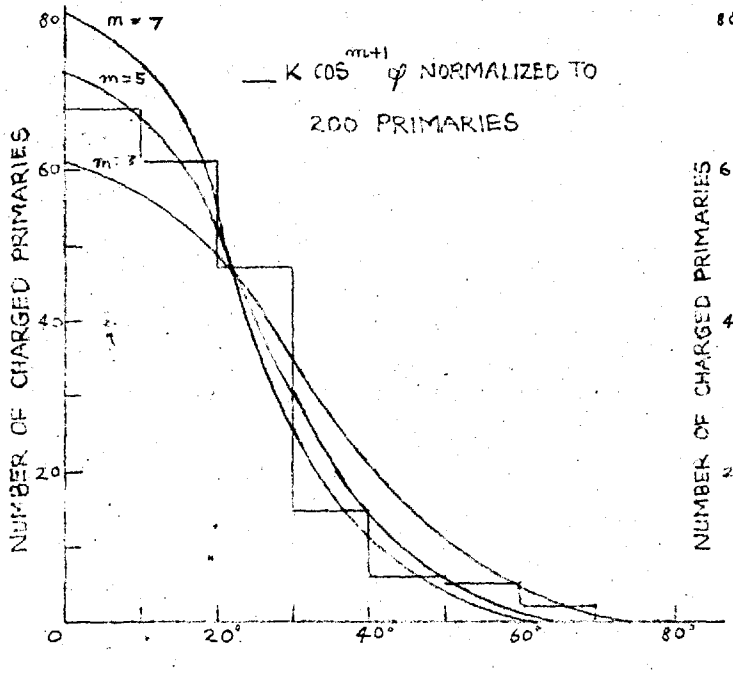
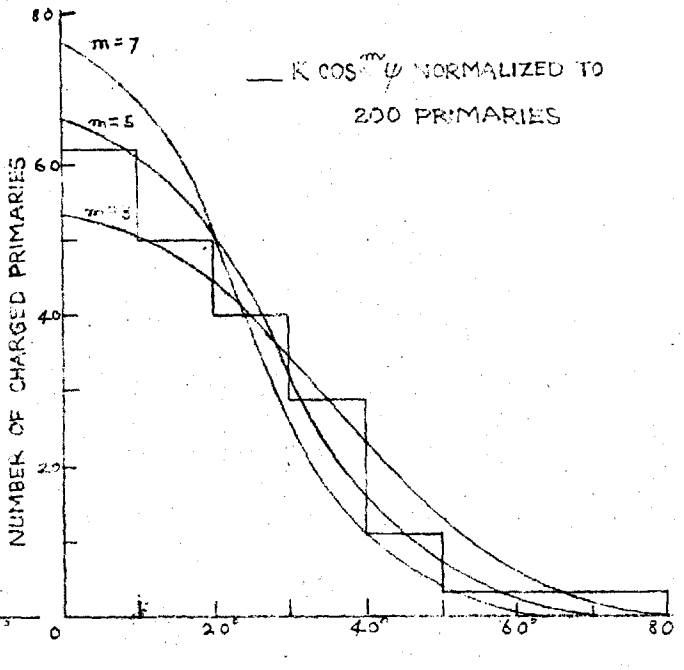


FIG II.7c. DISTRIBUTION OF PROJECTED ANGLES



of 200 p-stars found under no absorber were determined in the following way.

Firstly, the projected angle ψ is measured, where ψ is the inclination to the vertical of the projection of the track on the plane of the emulsion. Secondly, the angle of dip φ, which the primary makes with the plane of the emulsion, in the undeveloped emulsion, is found, making allowance for the shrinkage factor caused by development. The zenith angle Θ is then given by $\cos \Theta = \cos \varphi \cos \psi$.

The zenith angle distribution of 200 charged primaries is shown in Figure II.7(a), together with the theoretical distributions expected on a $\cos^m \Theta$ steradian^{-1} law, for several values of m. This shows a value of $m = 5.0 \pm 1.0$, in contrast with the value of $m = 2$ reported by Page.

It is possible that charged primaries dipping very steeply with respect to the plane of the emulsion will be missed in the analysis of the stars under the oil objective. However, in distortion-free emulsions, it was quite easy to observe primaries with angles of dip up to 70°, as the rocking motion of the microscope fine adjustment enables one to follow the primary to or from the star. Indeed, it is often easier to see a dipping track than one lying in the plane of the emulsion, as the former can be seen for a longer period of time.

The observed distribution of angles of dip, and projected angles are shown in Figures II.7(b) and II.7(c), together with the theoretical curves. If primaries with large angles of dip were preferentially missed in the checking of stars, then the number observed with large angles of dip should be less than that expected on a $\cos^m \theta$ steradian^{-1} zenith angle distribution law. However, both the histograms in Figures II.7(b) and II.7(c) are consistent with $m = 5.0 \pm 1.0$. As previously mentioned, some 10% of the shower particles are emitted upwards, more or less isotropically in the upper hemisphere, and the majority of these will have been classed as charged primaries. This will cause an apparent loss in collimation of the charged primaries, and the real value of m will therefore not be less than 5.0 ± 1.0, and possibly slightly greater.

This may be compared with the angular distribution of the charged particles producing showers determined by Walker (1950), who used a counter array at a similar altitude. From the nature of his apparatus the counts $A^1 B^1 C^3$ will include large stars of great energy. This angular distribution has $m = 7.3 \pm 1.0$.

It is also of interest to compare the corresponding distribution at great altitude. Lord (1951) has given the angular distribution of charged star primaries at 28,700 m., 54°N (Magnetic). This is very nearly given

by a cos θ steradian^{-1} zenith angle distribution law. These primaries will become more collimated in penetrating the atmosphere. If one assumes an attenuation mean free path $\lambda = 135$ g cm.$^{-2}$, then the number of primaries having zenith angles between θ and $\theta + d\theta$ is reduced by a factor $\exp(-\frac{a}{\lambda} \sec\theta)$, where a g cm.$^{-2}$ is the depth in the atmosphere. The differential angular distribution at 3570 m. can therefore be obtained by transforming the corresponding distribution at 28,700 m., multiplying by this factor $\exp(-\frac{a}{\lambda} \sec\theta)$.

On applying this simple transformation to give the simple air attenuation down to 3570 m., the distribution up to 60° zenith angle is best given by a $\cos^{4.5}\theta$ law, which compares very well with the value found here for the charged primaries.

It is important to realise that the effective angular distribution of the total star-producing component, as determined by absorption in the lead cones, is the true angular distribution of the primaries above the lead only if the assumption of collimated secondaries is true. The general problem of non-collimated production of secondaries is quite complicated and will be discussed more fully in Part III of this thesis, when the effect of isotropic emission of secondaries is studied.

6. Absolute Rate of Star Production at the Jungfraujoch

The rate of production of all stars with $N_\mu \geq 3$ in nuclear emulsion of 17.0 ± 0.4 cm.$^{-3}$ day^{-1} is greater than previously reported. For comparison the stars recorded by the Bristol and Manchester groups (Brown et al. 1949, Rosser and Swift 1951) are shown in Tables 4 and 5. These are corrected to the same exposure time, and in the latter case for the difference in altitude also. It can be seen that the differences involve small stars only, and in fact this experiment records twice as many 3-pronged stars as reported by the Bristol groups. There is very good agreement for production rates of stars with more than 7 tracks, both with and without absorber.

In the classification of 3-track stars any track of length greater than 4 μ was accepted, while one of 4 μ or less was defined as a recoil. The Manchester and Bristol groups have not stated their definition of a recoil and may have regarded 3-track stars containing one track between 4 μ and 10 μ in length as a 2-track star with a recoil. This could possibly explain the discrepancy in the number of 3-track stars found. Tidman and Hodgson (1952) have analysed the 3-track stars found under no absorber in the lead cone experiment, and using their results it is apparent that one-tenth of these

stars have one track with length between 4 μ and 10 μ. However, the production rate found here for 3-track stars is 260% of that reported by the Bristol group and 140% of that reported by the Manchester group. The discrepancy cannot be explained by the particular choice of criteria in the classification of the stars and there can be little doubt that it is caused by the increased efficiency in finding the small stars.

Brown et al. (1949) had analysed their stars and showed that the total energy carried away by particles in the black and grey energy region, making allowance for neutrons, could be represented by the energy versus size law, $E = 37N_h + 4N_h^2$ for stars with 4 or more tracks. Extrapolating this law to stars with 3 tracks gives a mean energy of 147 MeV. However, Tidman and Hodgson (1952) have analysed the 3-track stars found in this work and they obtained a mean energy of 186 MeV. It is therefore probable that the Bristol group tended to miss small stars having grey tracks.

7. Attenuation of the Star-Producing Radiation

The star-production rates under no absorber and under the 20 cm. and 30 cm. hemispheres are shown in Figure II.8. for various classes of stars. It can be seen that for all classes of stars the results are consistent with exponential attenuation, and there is no sign of the anomalous increase under 20 cm. lead reported

FIG II. 8 STAR PRODUCTION RATES UNDER 20 cm AND 30 cm HEMISPHERES

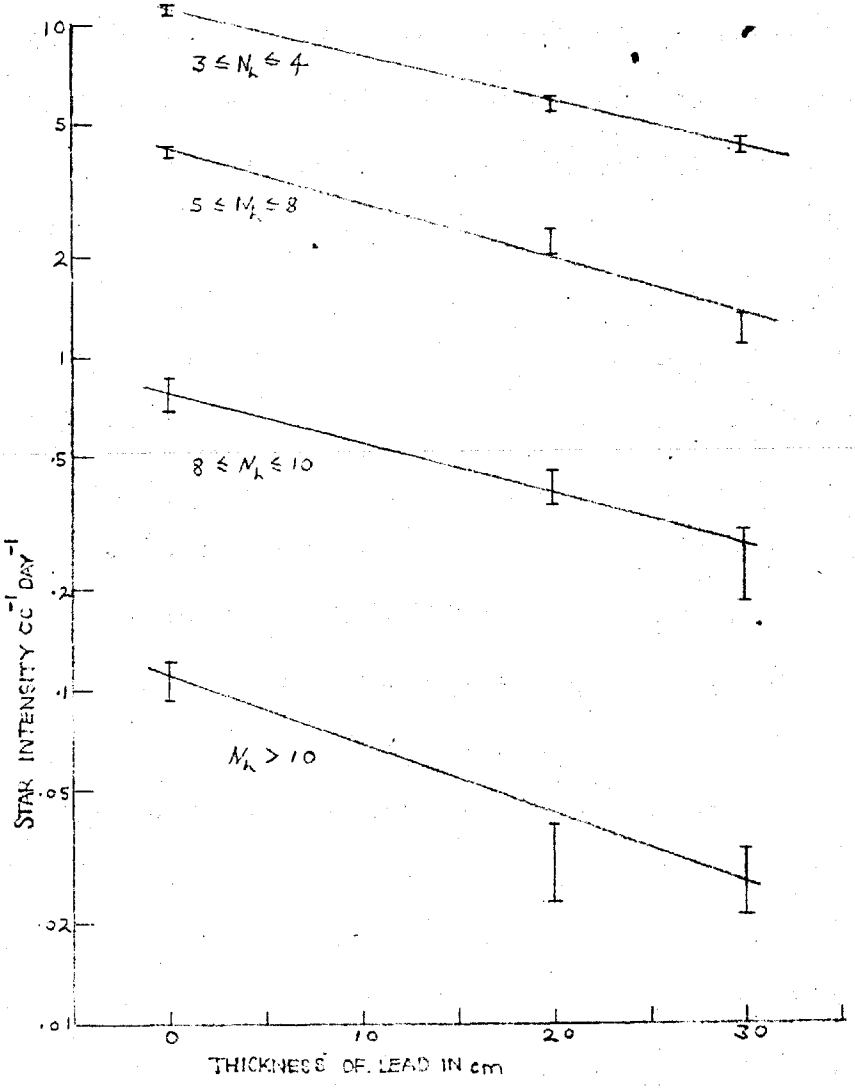


FIG II. 9a ATTENUATION LENGTH FOR STARS WITH $N_h \geq N$

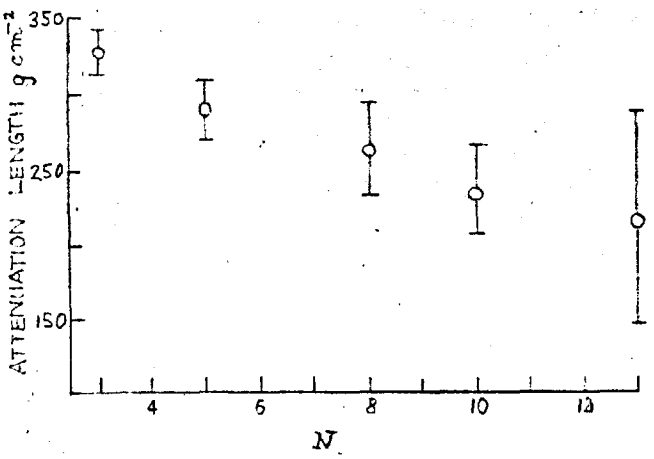
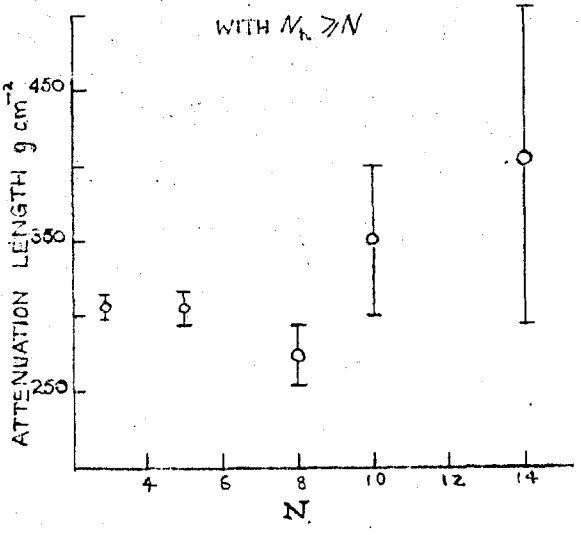


FIG II. 9.b ROSSER AND SWIFT 1951
ATTENUATION LENGTH FOR STARS WITH $N_h \geq N$



by Schopper et al. (1951) for stars with 2 or more prongs. In any case, under the conditions of the experiment one would not have expected to observe the transition effects for small thicknesses of absorber, reported by Shapiro, Stiller, Birnbaum and O'Dell (1951) and Schopper et al. (1951).

Figure II.9(a) shows the attenuation length in lead for different types of stars, obtained from the results shown in Figure II.8. The attenuation length for all the stars with $N_L \geq 3$ is 330 ± 15 gm cm.$^{-2}$. However, the size distribution under the absorber is not identical with that above the absorber. The results show a larger proportion of small stars under the absorber similar to that found with air as the absorber by Addario and Tamburino (1949), but not observed at a slightly lower altitude by Rosser and Swift (1951).

This results in a definite trend towards smaller attenuation lengths for large stars, as can be seen in Figure II.9(a). For small stars only ($3 \leq N_L \leq 4$) produced by neutral radiation the attenuation length is 370 ± 30 g cm.$^{-2}$, while for stars with more than 12 tracks it is somewhat lower, at $210 \, ^{+80}_{-70}$ g cm.$^{-2}$. This smallest length, 210 g cm.$^{-2}$, may be compared with the "geometrical" mean free path of 150 g cm.$^{-2}$ based on a nuclear radius $4 = 1.45 \times 10^{-13} A^{\frac{1}{3}}$ cm.

There can be little doubt that the increase in

proportion of the small stars does exist, as there are reasonably large numbers of the small stars (3- and 4-track stars forming 65% of the total). However, the statistics for the large stars is very poor (stars with more than 12 tracks forming less than 2.5% of the total) and it is rather important to see if the continuing decrease in attenuation length with increasing star size is significant. For this category of large stars ($N_h \geq 13$) the results are based on a total of 33 stars without absorber, 8 stars under the 20 cm. hemisphere and 6 stars under the 30 cm. hemisphere. Using these numbers one finds an attenuation length of 210 g cm.$^{-2}$. An attenuation length of 300 g cm.$^{-2}$ would have required roughly 11 $\pm$ 2 stars under each absorber, taking into account statistical fluctuations in the 33 stars without absorber. The significance of the lowest value of the attenuation length thus depends upon the probability of the two observed numbers of stars, 6 and 8, not being statistical fluctuations of a random distribution of stars having an average of between 9 and 13 stars in the given volume of emulsion. If one takes the lower value 9 of the mean number of stars, then both the observed values 6 and 8 lie within the root mean square value, and the results are therefore just consistent with an attenuation length of 300 gm cm.$^{-2}$.

If, however, we include the result of Brown et al.

(1949) for stars with more than 12 tracks, the new production rate above the absorber should give rise to 37 ± 2 stars in the volume of emulsion which contained the 33 stars. The numbers under the 20 cm. and 30 cm. hemispheres corresponding to an attenuation length of 300 g cm.$^{-2}$ is 12.5 ± 1.0. The results are then not quite as easy to explain by statistical fluctuations.

However, Rosser and Swift reported no change in the size distribution under 30 cm. of lead and actually found an increase in the attenuation length for stars with $N_h \geq 15$. They found a value of 400 ± 100 g cm.$^{-2}$ for these large stars compared with 307 ± 7 g cm.$^{-2}$ for all stars with $N_h \geq 3$. Their results are shown in Figure II.9(b) and show no sign of the trends found in the present experiment. Although their results for small stars might be suspect because of inefficient searching, there is no reason to doubt the results for large stars. In fact, as seen from Table II.5, the corrected production rates for stars with 7 or more tracks are almost identical with those found in this experiment.

In view of the discrepancy between these two experiments, it is not possible to confirm the presence of the decrease of attenuation length with increasing energy. Such an effect could have been caused by statistical fluctuations in the small number of stars observed.

A great deal of information is available on the

the attenuation of the radiation producing high energy bursts in ionisation chambers (Bridge, Hazer, Rossi and Williams 1948; Fahy and Schein 1949; Fahy 1951; Stinchcomb 1950 (a), 1950 (b), 1951). These bursts are usually caused by electron cascades from the neutral π^0 mesons, produced in high energy nuclear interactions, though a certain proportion are caused by μ -mesons, especially at lower altitudes. Hence these bursts include events corresponding to large stars in nuclear emulsions. The earlier results gave an attenuation mean free path in lead of the order of 440 ± 60 g cm.$^{-2}$. However, on correcting for those bursts caused by μ -mesons and air showers, these observers gave an attenuation mean free path of about 350 ± 50 g cm.$^{-2}$, as is shown in Table II.6.

Table II.6. Attenuation mean free path of Radiation producing Bursts

Observer		Attenuation mean free path in lead
Bridge et al.	1948	345 g cm.$^{-2}$
Fahy & Scheir	1949	434 g cm.$^{-2}$
Fahy	1951	346 ± 36 g cm.$^{-2}$
Stinchcomb	1950 (a)	440 ± 65 g cm.$^{-2}$
Stinchcomb	1951	350 ± 40 g cm.$^{-2}$

There is thus no sign of any decrease in the attenuation mean free path for these high energy nuclear interactions. However, these bursts cannot be directly compared with the large stars in emulsion, as they correspond to a higher energy region.

A more direct comparison with stars in emulsion is given by the pulses produced in scintillation counters. The size of the pulse will be more or less proportional to the number of heavy tracks in the star, and the material of the scintillation crystal, often silver iodide, is very similar to the silver bromide component of the emulsion. Michaelis (1952), in a private communication, has reported a variation in the attenuation mean free path of the particles producing pulses in scintillation crystals. His results are shown in Table II.7.

Table II.7. Attenuation mean free path for Various Pulse Sizes reported by Michaelis (1952)

Pulse Size in MeV	43 - 65	65 - 86	86 - 108	108
Attenuation m.f.p. in lead in g cm.$^{-2}$	380	380	340	280

This shows the same trend as that reported in the lead cone experiment; the statistics, however, are rather poor for the higher energy pulses. The value of 380 g cm.$^{-2}$ for the lower energy pulses is in good agreement with the

value of 370 ± 30 g cm.$^{-2}$ obtained in the present work for stars of 3 and 4 heavy tracks. The group containing the largest pulse energy will probably include most stars with more than 5 or 6 heavy tracks. The corresponding attenuation mean free path for stars with more than 4 tracks was found to be 290 ± 20 g cm.$^{-2}$.

In view of the above evidence no real conclusion can be drawn about the presence of this decrease in the attenuation mean free path. Although the very-high-energy events as typified by bursts give an attenuation mean free path of about 350 g cm.$^{-2}$, there is still a possibility that the above effect does exist for stars with about 15 heavy tracks. A very suitable method of solving this problem is offered by the scintillation counter. High statistical results can be obtained by using large enough crystals with sufficient exposure times, and the method does not require the effort of skilled searchers as does the emulsion technique. It is intended to investigate the attenuation of the radiation causing large pulses in the near future, using the lead hemispheres of the lead cone experiment.

If this variation of the attenuation with energy does exist, then it will have an important bearing on any theory of the nucleon cascades in the star-producing radiation. For if we assume that this radiation has a differential energy spectrum of the form

$$dN = K E^{-\gamma} dE$$

even the fairly general law that a nuclear collision of a primary of energy E yields n_1 secondaries of $\alpha_1 E$, n_2 of energy $\alpha_2 E$, etc., themselves capable of producing further stars, where n_1, n_2 ..., α_1, α_2 ... are constants, would merely reproduce the same power distribution at all thicknesses of absorber and therefore give the same effective attenuation for radiation of all energies. A cascade model for interactions in lead is developed in Part IV of this thesis. Under certain conditions this model does lead to an increase of attenuation with the nucleon energies.

In addition to this cascade model, one could also assume that there is a low-energy cut-off to the primary spectrum at the Jungfraujoch which is greater than the minimum energy required for a 3-pronged star. Interactions in the lead would then cause a filling up of the spectrum with a corresponding relative increase in the numbers of small stars.

III. THE GEOMETRICAL PROPERTIES OF THE NUCLEAR INTERACTIONS IN THE LEAD CONES

1. Introduction

In the lead cone experiment, described in Part II of this thesis, the attenuation of star-producing radiation is studied using cone shaped lead absorbers of various angles and thicknesses. From the observed rates of star-production under the various cones it is possible to deduce certain features about the angular distribution of the primary particles incident on the absorbers. The preliminary analysis described in Part II, Section 4, assumed that in interactions within the lead absorber secondary particles continued in the same direction as the primary. This assumption of collimated secondaries permits an investigation of the angular distribution of the primaries which is independent of the actual properties of the nuclear interactions. The following work shows the effect of a non-collimated emission of secondaries on the theoretical lead cone absorption curves. In general, this leads to a different interpretation of the experimental curves and will modify to a certain extent the conclusions on the angular distribution of the radiation.

It will be assumed that the interactions in the lead absorber can be represented by a one-stage cascade process. That is, each primary can make one collision

in the absorber, producing secondaries energetic enough to form stars. As the 30 cm. lead absorber has a thickness of more than 2 interaction lengths, there is a reasonable chance of a second or even a third stage cascade developing. However, if a primary particle interacting in the lead produces a secondary particle, and this has sufficient energy to produce tertiary particles in a further interaction in the absorber, themselves energetic enough to produce stars, then it can be assumed that the secondary particle is more or less collimated in the direction of the primary. It is well known that high energy interactions in the lead will produce collimated events, from the point of view of high energy secondaries, but in the succeeding work no account is taken of any variation in angular properties with the energy of the incident radiation. The energy considerations of the cascade in lead are discussed in the last part of this thesis.

The following simple assumptions will be made in the succeeding work of Part III:

(a) star-producing radiation travels in straight lines through the absorber until it suffers nuclear interaction. The interaction mean free path is taken as the geometric value (150 g cm.$^{-2}$) and this will give an upper limit to the effect of the cascade process inside the absorber;

(b) the angular distribution of the primaries above the cones can be represented by a $\cos^m \Theta$ steradian^{-1} law in the upper hemisphere and zero in the lower hemisphere, where Θ is the zenith angle.

We will first consider a one-stage cascade with collimated emission of secondaries, which is a particular case of the general analysis given in Part II, Section 4. In the remainder of Part III will be considered the effect of isotropic emission of secondaries in interactions in the lead absorber.

Effects due to ionisation loss by the charged star-producing particles will be ignored.

2. One-Stage Cascade assuming Collimated Secondaries

The attenuation mean free path of star-producing radiation in lead is known to be greater than the interaction mean free path. The latter has been shown experimentally to be nearly geometric - 150 g cm.$^{-2}$ (Walker Walker and Greisen 1950, Boehmer and Bridge 1952), while this experiment yields an attenuation mean free path of 330 $\pm$ 15 g cm.$^{-2}$. This can be explained if secondaries capable of producing further stars are produced in interactions in the lead. This category of secondaries will include primaries passing right through a nucleus unaffected, due to a partial transparency of the nucleus, or elastically scattered primaries, as well as nucleons

emitted in nuclear disintegrations.

Let λ_g g cm.$^{-2}$ be the geometric interaction mean free path of the radiation, and in a nuclear disintegration we will assume an average of n_c secondaries to be emitted. The number n_c refers to collimated secondaries. These secondaries themselves cannot produce disintegrations with secondaries energetic enough to cause stars, but will be attenuated by nuclear interaction in the lead absorber.

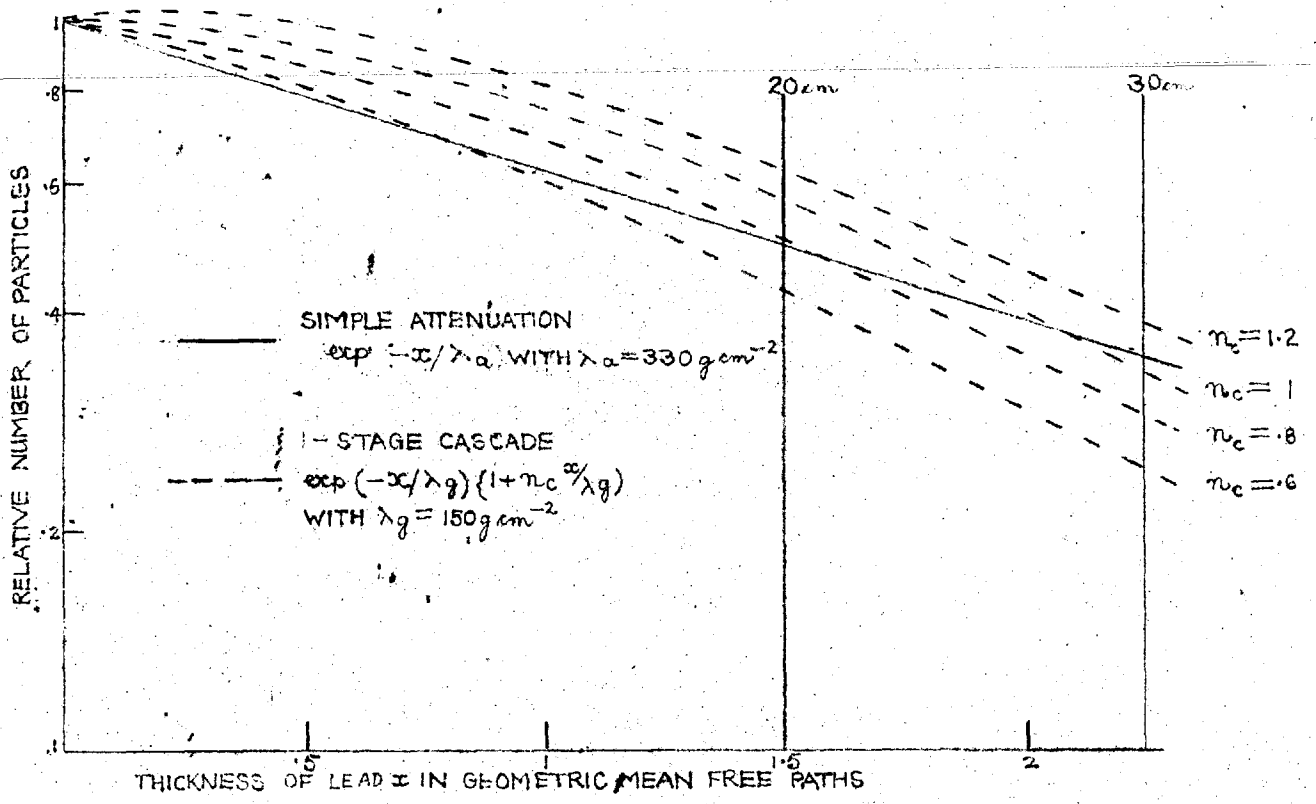
Suppose there are N primary particles incident on an absorber of thickness d g cm.$^{-2}$. Then the number of star-producing primaries emerging from the absorber will be

$$N \exp(-\frac{d}{\lambda_g}) (1 + n_c \frac{d}{\lambda_g}) \qquad \text{III(1)}$$

The second term in the brackets gives the number of secondary particles emerging, while the first term represents the proportion of primary particles traversing the absorber without interaction. For an absorber of 30 cm. thickness $\exp(-\frac{d}{\lambda_g}) = 0.105$, that is, one-tenth of the primary particles emerge without interaction.

The expression III(1), neglecting the initial constant N, is equivalent to the term $\alpha(d)$ in equation II(1), which is the general equation giving star-production rates for the interaction mechanism assuming collimation of secondaries. The rate of star-production at

FIG. III.1. 1 STAGE CASCADE ASSUMING COLLIMATED SECONDARIES



the apex of a cone of semi-angle Θ and thickness d is then given by $N(\Theta)$

$$\text{where } N(\Theta) = N(0)\left[(1 - \cos^{m+1}\Theta)\exp(-\frac{d}{\lambda_g})\times \left\{1 + n_c\frac{d}{\lambda_g}\right\} + \cos^{m+1}\Theta\right] \qquad \text{III(2)}$$

This equation will obviously yield the same value of m as the more general equation II(1) in interpreting the star-production rates under the various cones. As is to be expected, the production rate under the hemisphere is given by

$$N(90^\circ) = N(0)\exp(-\frac{d}{\lambda_g})\left\{1 + n_c\frac{d}{\lambda_g}\right\} \qquad \text{III(3)}$$

However, the observed star-production under the 20 cm. and 30 cm. hemispheres was consistent with exponential attenuation with a mean free path of 330 ± 15 g cm.$^{-2}$. That is

$$N(90^\circ) = N(0)\exp(-\frac{d}{\lambda_a}) \qquad \text{III(4)}$$

where λ_a is the experimentally observed attenuation mean free path.

The functions III(3) and III(4) are plotted in Figure III.1, the former being shown for several values of n_c. The two curves both give the observed attenuation under the 20 cm. and 30 cm. hemispheres, for values of

n_c between 0.8 and 1.0. The one-stage cascade can therefore explain the observed attenuation if an average of 0.9 collimated secondaries are emitted from each primary interaction in the lead.

For the 30 cm. cone $\frac{x}{\lambda_g} = 2.25$, and we have just shown that $n_c = 0.9$. It is apparent from equation III(1) that over two-thirds of the star-producing particles under the 90° hemisphere are really secondaries from interactions in the lead. This is an upper limit to the secondary effect, but it is important to consider the effect on the lead cone absorption properties if the secondaries are permitted to have an angular distribution about the primary direction.

3. Isotropic Emission of Secondaries

It was decided to consider only the case of isotropic emission of secondaries, as any other type of angular distribution (except the collimated case) leads to very complicated mathematics. It is known that the grey tracks emitted from stars with sufficient energy to produce further stars are certainly not isotropically emitted, and can be represented by a $\cos \Theta$ zenith angle distribution or even higher degree of collimation about the direction of the primary (Camerini et al. 1951). The above assumption of isotropic emission will thus give an upper limit to the effect of non-collimated production

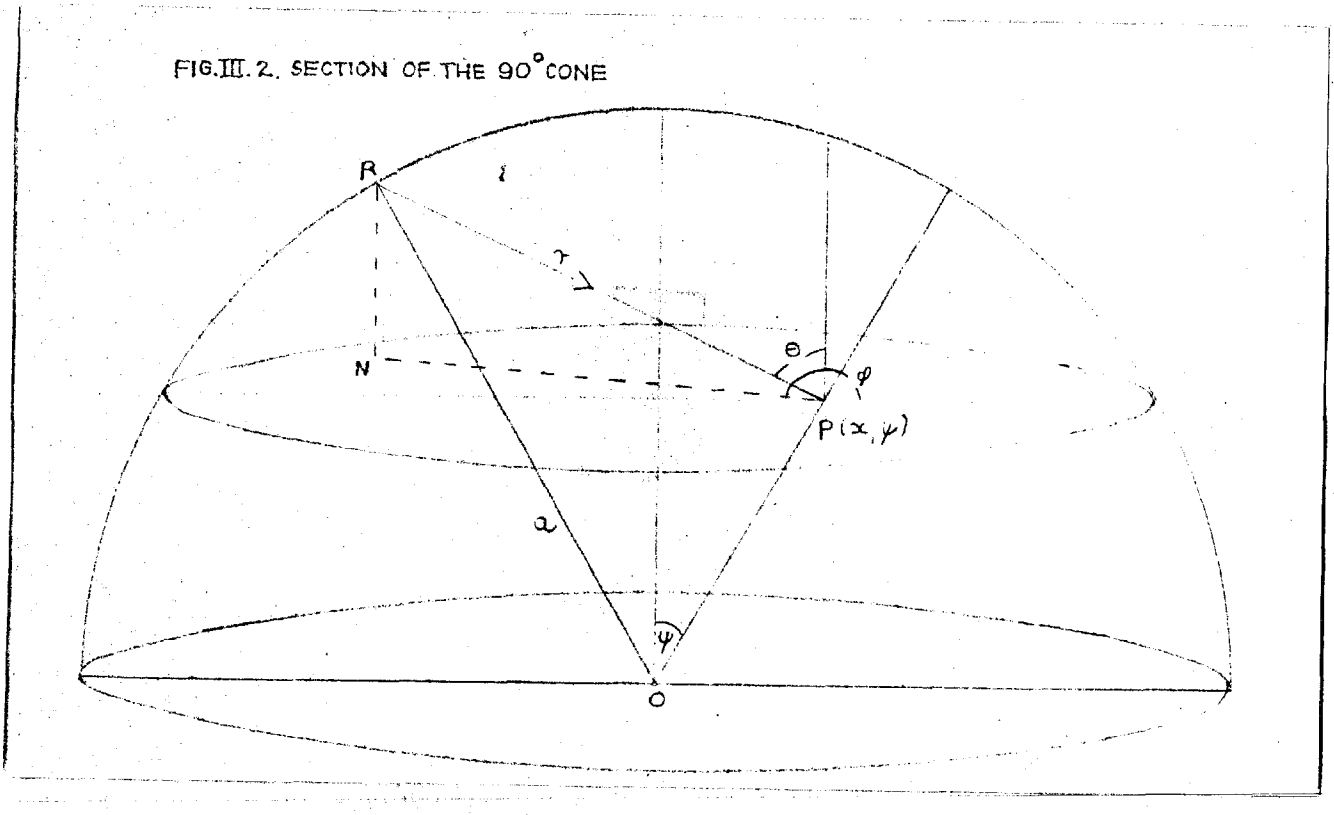
of secondaries.

It will therefore be assumed that in each primary interaction in the lead an average of n_i secondaries are emitted isotropically in the downward hemisphere with respect to the direction of the primary. Those secondaries emitted in the upper hemisphere cannot reach the plates, and so will not be considered here.

The problem will be treated as a one-stage cascade, as in the previous section. However, the calculations have only been made for the 30 cm. cone, as the cascade effect is more pronounced for the greater thickness of lead. The 90^o cone and 40^o cone have been considered in detail as these are the ones of greatest use in determining the exponent m in the $\cos^m \theta$ law describing the angular distribution of the star-producing radiation.

4. Calculation of Secondary Contribution assuming Isotropic Emission, under a 90° Cone

Figure III.2. Section of the 90° Cone.



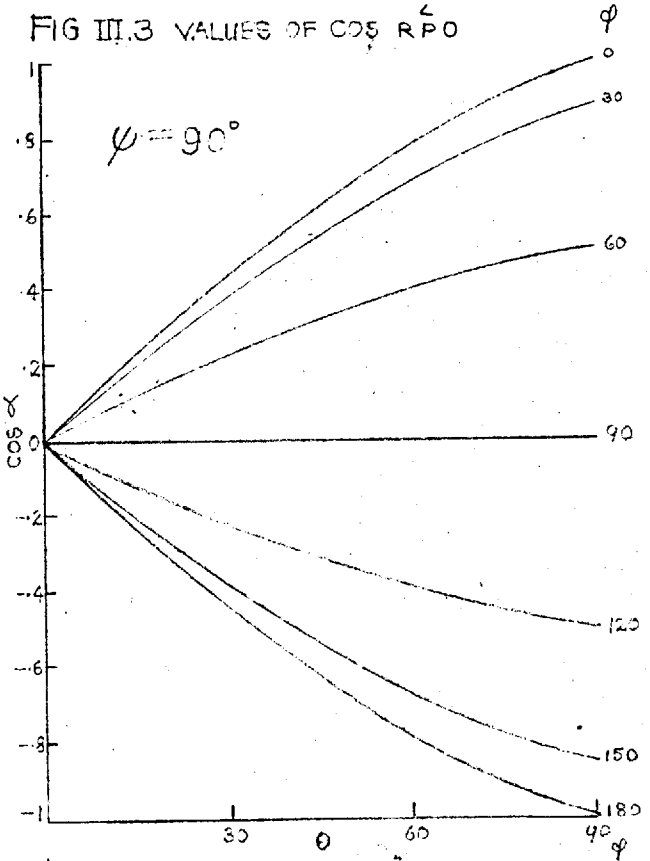
A schematic drawing of the 90° cone is shown in Figure III.2. The thickness of the cone, measured in g cm.$^{-2}$, is denoted by a. The star-producing radiation is travelling downwards with a $\cos^{m}\theta$ steradian^{-1} zenith angle distribution and can interact in the lead absorber with an interaction mean free path λ_{g} = 150 g cm.$^{-2}$. A certain proportion, $\exp(-a/\lambda_{g})$ of the

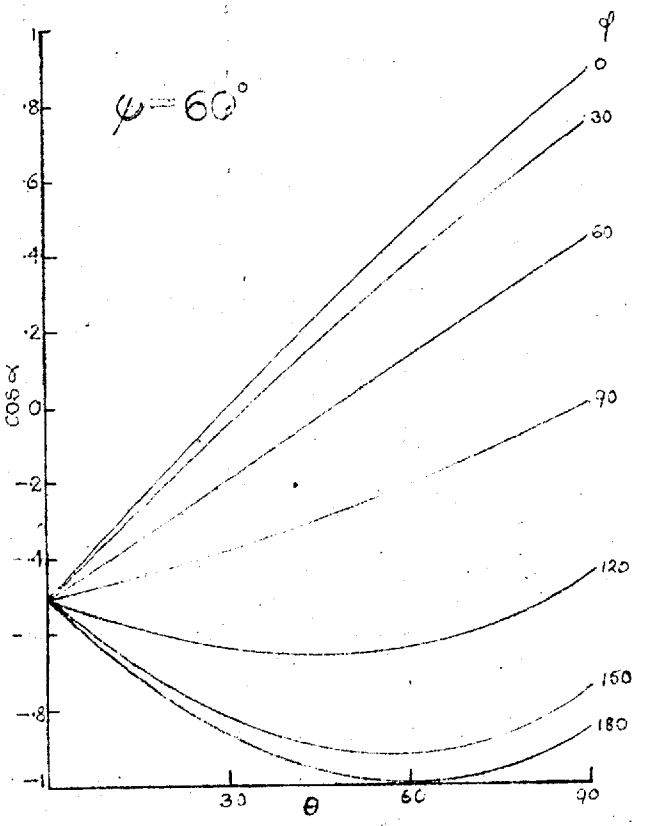
primaries will reach the centre O without interaction. Whenever interaction occurs, however, the secondaries are isotropically emitted in the downward hemisphere. Any point within the lead hemisphere will thus be associated with a certain density of nuclear interactions, caused by the primary radiation. A certain proportion of the secondary radiation can then reach the plates at O, depending on the solid angle subtended by the plates, and also on the remaining thickness of absorber to be traversed.

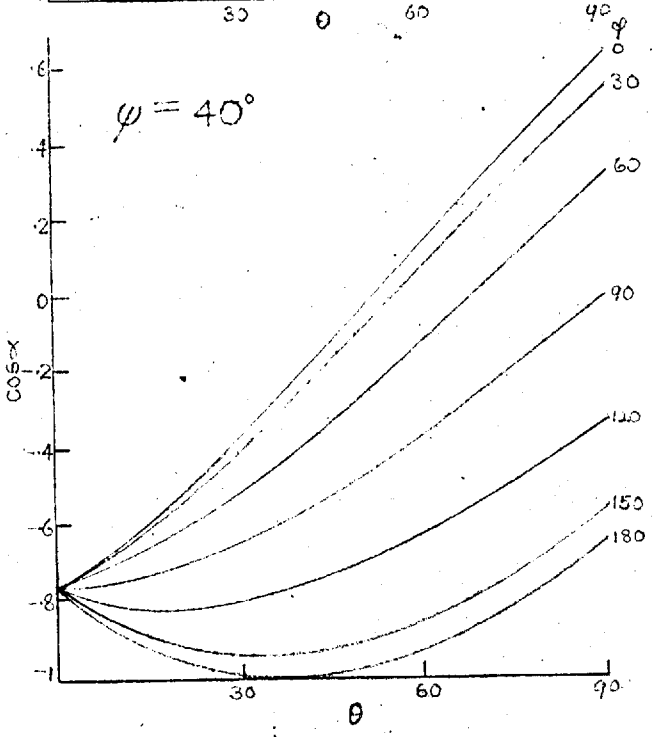
We will consider a typical point $P(x, \psi)$ inside the lead hemisphere, where P lies anywhere on the circle defined by x, the distance from O, and the zenith angle between the vertical through O and the line OP. Unless there is a directional asymmetry of the incident radiation, all such points $P(x, \psi)$ can be treated identically for a given x, ψ, independent of the position on the circle. Incident particles interacting at P must have traversed a certain thickness of lead and the number reaching P without interaction can therefore be found by assuming exponential attenuation with the interaction mean free path.

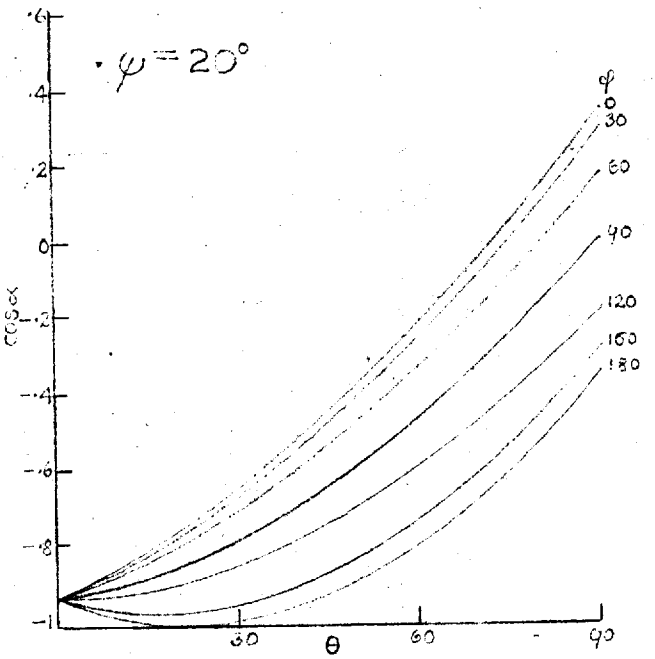
The number of particles reaching unit area, in the horizontal plane, at P, and making zenith angles between Θ and $\Theta + d\Theta$ and azimuthal angles between φ and $\varphi + d\varphi$ can be expressed as

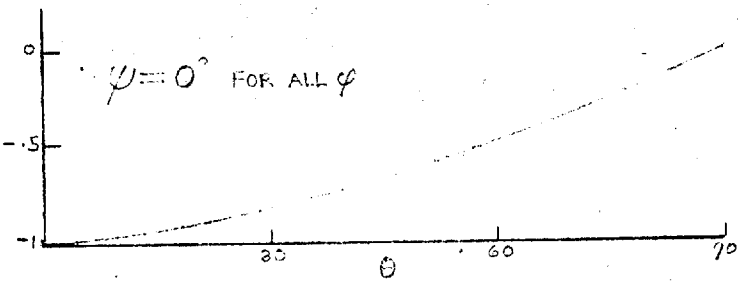
FIG III.3 VALUES OF COS $\angle RPO$











$$N \cos^m \theta \sin \theta \exp(-r/\lambda_g)\, d\theta\, d\varphi \qquad \text{III(5)}$$

where the azimuthal angle φ is measured from the vertical plane through P and O, and r is the distance the particle has to travel in the lead before reaching P. N is some arbitrary constant.

Let the point where the radiation enters the hemisphere be denoted R. Then the distance RP(r) is a function of θ , φ , x and ψ .

From the triangle RPO it can be shown that

$$r = x \cos \widehat{RPO} + \sqrt{x^2 \cos^2 RPO + a^2 - x^2} \qquad \text{III(6)}$$

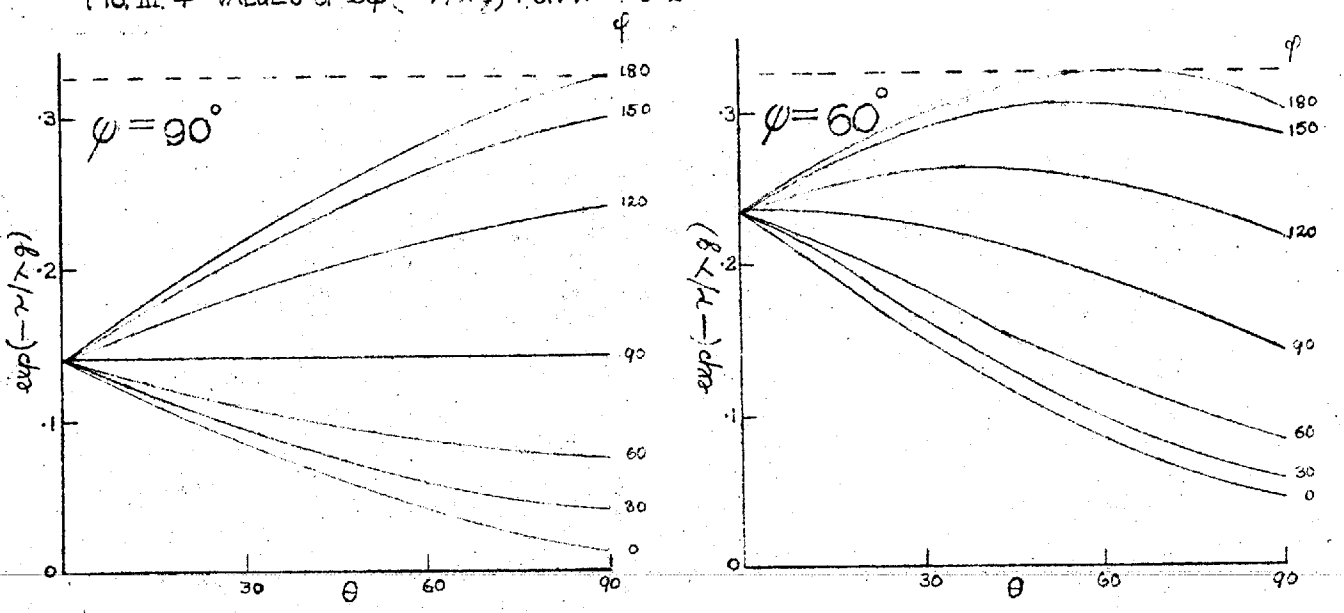
$$\text{where } \cos \widehat{RPO} = \sin\theta \sin\psi \cos\varphi - \cos\theta \cos\psi \qquad \text{III(7)}$$

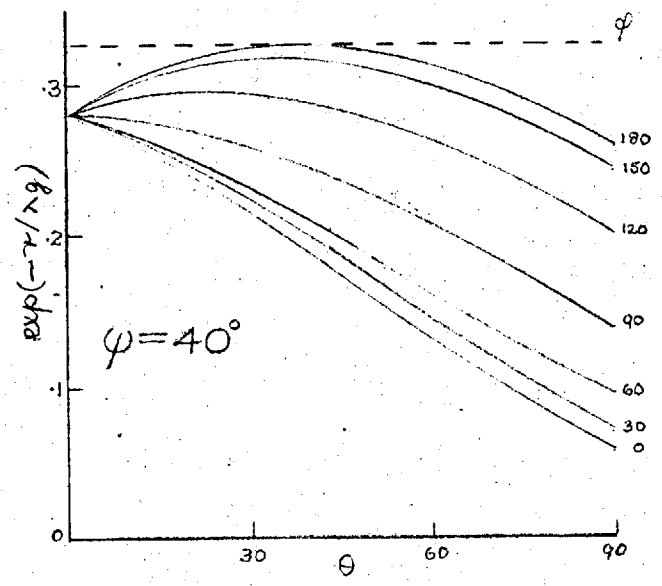
The number of disintegrations formed at P per cc. can therefore be obtained by integrating III(5) over the values of θ and φ, and is given by $I(x,\psi)$ where

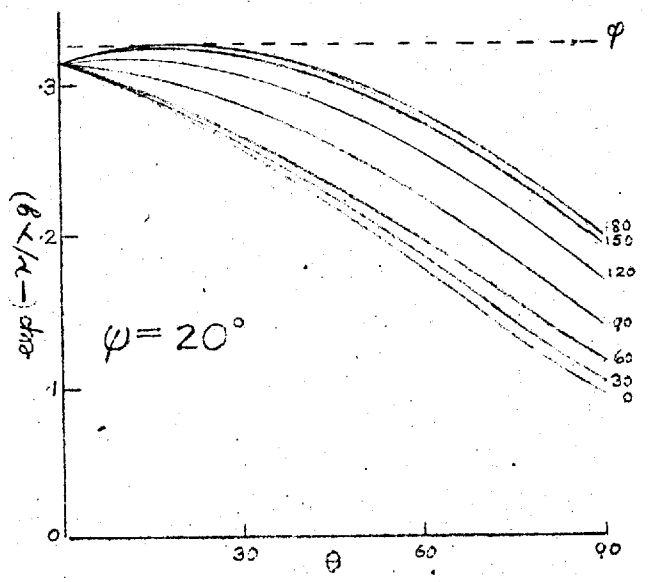
$$I(x,\psi) = \frac{2N}{\lambda} \int_{\varphi=0}^{\pi} \int_{\theta=0}^{\frac{\pi}{2}} \cos^m \theta \sin\theta \exp\left\{ -\frac{1}{\lambda_g}\, r(\theta,\varphi,x,\psi) \right\} d\theta\, d\varphi \qquad \text{III(8)}$$

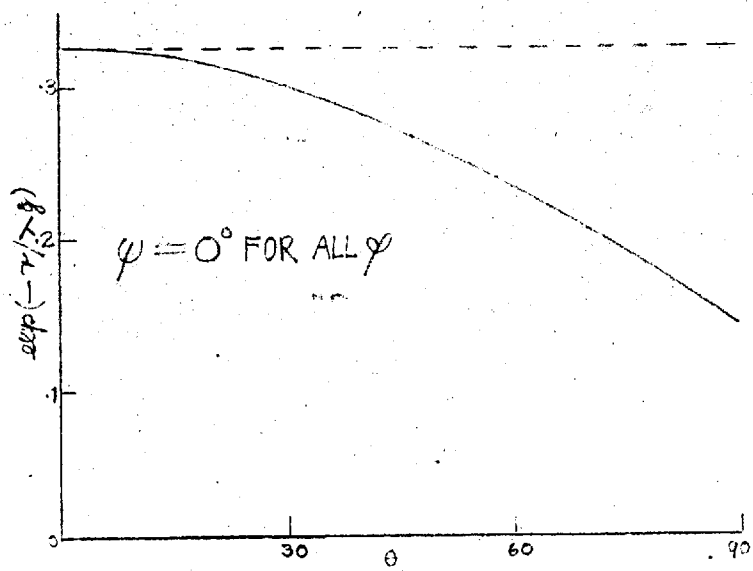
In evaluating this integral for a particular value of x, ψ , values of $\cos \widehat{RPO}$ and $r(\theta,\varphi,x,\psi)$ had to be computed over the full range of θ and φ . Curves of the factor $\cos \widehat{RPO}$ are shown in Figure III.3 as a continuous function of θ , for different values of φ

FIG. III. 4 VALUES OF $2\varphi(-\tau/\lambda\varphi)$ FOR $X = .5$ a







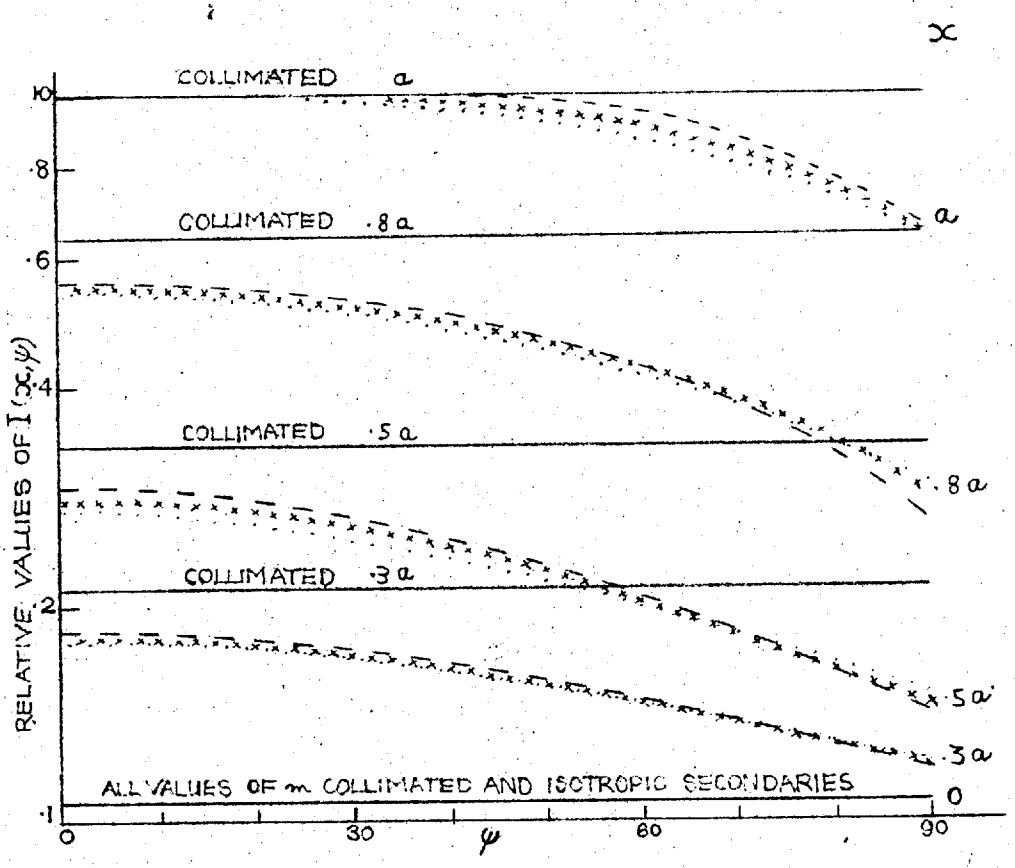


and ψ. Using these curves it was possible to compute values of $r(\theta, \varphi, x, \psi)$ using equation III(6).

The values of $\exp\left\{ -\frac{1}{\lambda_g} r(\theta, \varphi, x, \psi) \right\}$ for $x = 0.5a$ are shown in Figure III.4. As is to be expected, the attenuation is nearly always greater than that corresponding to the minimum path length of 0.5a in the straight line through P and O. The minimum attenuation of 0.325 is shown by the broken line in Figure III.4. For equal numbers of secondaries from each interaction, one would therefore expect that less secondaries could reach O than in the corresponding collimated case, for in the latter case all the primaries must travel in the radial line through P towards O, this being the shortest possible distance through the absorber.

The expression in III(8) has been integrated for each value of x and ψ by the following procedure. The exponential part was integrated over the range of φ for the four values of θ, 20°, 30°, 40° and 60°. The values at $\theta = 0^\circ$ and 90° are not necessary as the $\cos^m \theta \sin \theta$ term is zero at these two angles. Then was performed the integral over the range of θ for the three angular distributions $\cos \theta$, $\cos^3 \theta$, and $\cos^6 \theta$. Thus for each value of $I(x, \psi)$ it has required seven graphical integrations. However, $I(x, \psi)$ has been evaluated for five values of ψ and four values of x: a total of twenty different functions. Hence, in evaluating the

FIG III.5 VALUES OF $I(x,\psi)$ FUNCTION

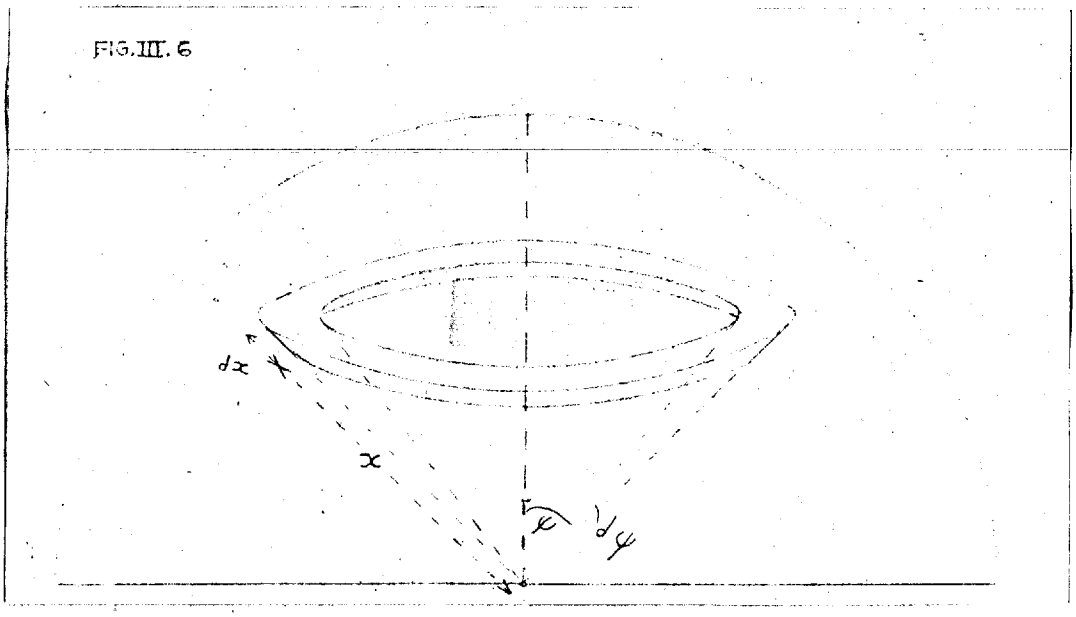


$I(x, \psi)$ function throughout the hemisphere a total of 140 separate graphical integrations were required.

The values of the $I(x, \psi)$ functions are shown in Figure III.5 for the three angular distributions of the primaries. This is expressed as a continuous function of ψ, for the five values of x, a, 0.8 a, 0.5 a, 0.3 a, 0. The horizontal lines denote the corresponding functions assuming collimated secondaries. It may be noticed that the total variation in the curves as one goes from a cos θ to a $\cos^6 \theta$ primary distribution is not very great.

Assuming isotropic emission (in the lower hemisphere) of n_i star-producing secondaries from each nuclear interaction, the number produced in an elemental torus of volume $2\pi x^2 \sin\psi \, d\psi \, dx$ (Figure III.6) is equal to

FIG. III. 6



$$n_i \, I(x, \psi) \, 2\pi x^2 \sin\psi \, d\psi \, dx$$

The number of these secondaries reaching O depends on the solid angle subtended by the emulsion, and the remaining distance of lead (x g cm.$^{-2}$) to be traversed. Hence, the number of secondaries reaching an elemental area ds at O from this elemental torus , and thus having zenith angles between ψ and $\psi + d\psi$ is given by

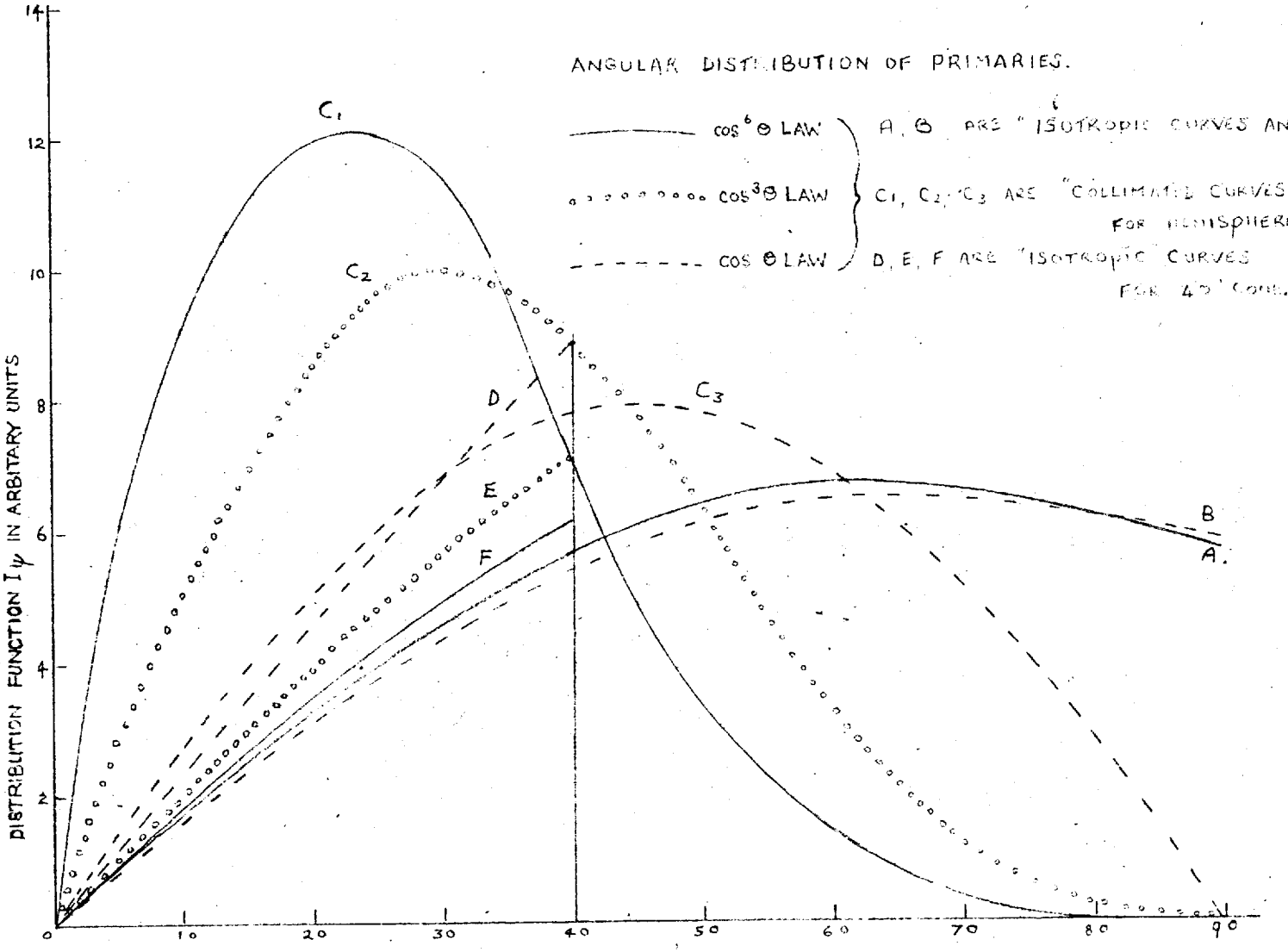
$$n_i \; I(x,\psi) \; 2\pi x^2 \sin\psi \; d\psi \; dx \; \exp(-x/\lambda_g) \; ds/2\pi x^2$$

Therefore, the total number of secondaries reaching unit area of the emulsion at O with zenith angles between ψ and $\psi + d\psi$ is given by $I_\psi \; d\psi$, where

$$I_\psi \; d\psi = \frac{n_i}{} \sin\psi \; d\psi \int_0^a I(x,\psi) \exp(-x/\lambda_g) \; dx \qquad \text{III(9)}$$

This has been evaluated graphically for the five values of ψ 0°, 20°, 40°, 60° and 90°. The I_ψ function gives the angular distribution of the secondary radiation reaching the plates. Values of this function have been calculated assuming a $\cos\theta$ and $\cos^6\theta$ zenith angle distribution of primaries and are shown in curves B and A of Figure III.7. It is apparent that the angular distribution of the secondaries does not vary appreciably with the corresponding distribution of the primaries. This is completely different from the results obtained with a strictly collimated production of secondaries, for these secondaries have the same angular distribution of the primaries. The I_ψ functions equivalent to a $\cos\theta$,

FIG III. 7. ANGULAR DISTRIBUTION FUNCTION I_ψ



$\cos^3\theta$ and $\cos^6\theta$ zenith angle distribution for collimated secondaries are shown in Figure III.7, normalised to the same area as the curves A and B.

In both the isotropic and collimated cases the numbers of primaries traversing the absorbers without interaction are the same, and so the difference between the two will depend on the number of secondaries under the various cones. One would therefore expect to find relatively more stars under a small angled cone for the collimated than in the isotropic case, on studying Figure III.7. The total number of secondaries under the 90° cone is the same for the two types of secondary production, due to the normalisation mentioned above. The problem of the general cone, for isotropic production of secondaries, is discussed in the next section.

The total flux of secondary radiation entering unit area of the emulsion from the hemisphere is obtained by integrating I_ψ over the range of ψ. The result is not very sensitive to the angular distribution exponent m of the primaries from m=1 to m=6, and can be expressed as

$$0.75\ N\ n_i\ \exp(-\ a/\lambda_g)\ a/\lambda_g \qquad \text{III(10)}$$

where N is the number of primaries which reach unit area of the plate without absorber.

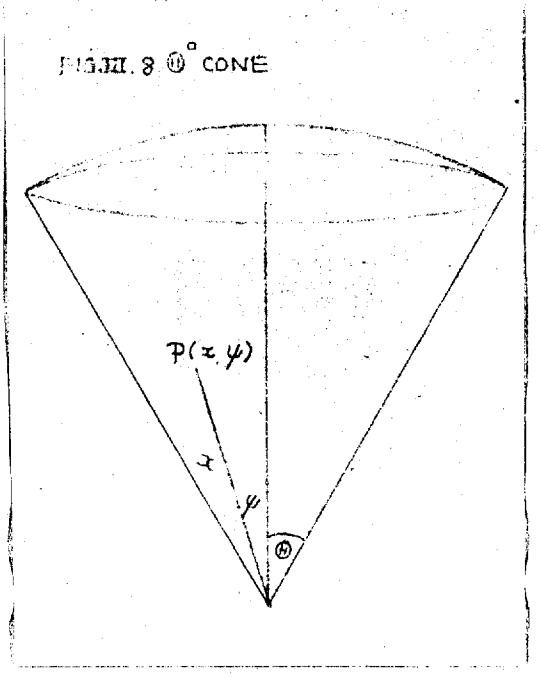
If this is compared with the second term of relation III(1) it can be seen that the effect of isotropic

emission reduces the number of secondaries by a quarter, as compared with the collimated case. Hence, to explain the experimentally observed attenuation of the total star-producing radiation, the isotropic mechanism requires one-third as many secondaries again as the collimated mechanism. That is, each primary interaction in the lead produces an average of 1.2 secondaries distributed isotropically in the lower hemisphere, compared with the 0.9 secondaries required for collimated production. These numbers of secondaries can be compared with the maximum number for stars in emulsion, discussed in Part I, § 2. It was shown that the upper limit to q, the average number of star-producing secondaries, could be fixed at $q = 2$. The above number of secondaries is certainly possible.

5. Isotropic Emission of Secondaries in a General Cone of Semi-Angle Ⓗ.

In the last section was shown the result for the angular distribution of the secondary radiation under the 90° cone (Figure III.7). For the collimated case, curves C and D, the number of secondaries under a cone of semi-angle Ⓗ is simply obtained by integrating the curve from 0° to Ⓗ $^{\circ}$. However, in considering isotropic emission of secondaries, a separate absorption calculation is necessary for each cone.

Figure III.8.



Consider a general cone with semi-angle Θ (Figure III.8). Primary radiation reaching a point $P(x, \psi)$ inside the cone and having zenith angles less than Θ must have passed through the spherical cap of the cone and the geometry is similar to that discussed in the last section for the hemisphere. However, for zenith angles greater than Θ the primaries can enter through the conical surface, and so have a shorter path length than is the case for the hemisphere, with correspondingly less absorption. Hence, for a typical point $P(x, \psi)$ the density function $I(x, \psi)$, giving the number of nuclear disintegrations per unit volume of lead, is greater in a Θ° cone than the corresponding function for the 90° cone.

It follows that the number of secondaries arriving at

0 with zenith angles less than Θ will be greater than the corresponding number for a 90° cone. The angular disribution of secondaries under a 40° cone is derived in the next section, and for comparison the results are shown in Figure III.7. Curves D, E and F correspond to $\cos \theta$, $\cos^3 \theta$ and $\cos^6 \theta$ zenith angle distributions of the primaries, and are obtained from the same total number of incident primaries as the calculation for the hemisphere. It can be seen that the less collimated the primary particles the greater the difference between the 40° and 90° curves. This is to be expected, for the less the collimation of the primaries, the more can enter the cone through the conical sides.

In the next section the problem of the 40° cone is discussed in detail, as this is the one of greatest use in determining the angular distribution of the primary radiation.

6. Isotropic Emission of Secondaries - 40° Cone

The 40° 30 cm. lead cones were truncated, and had an external radius of 45 cm. and an inner radius of 15 cm. The radius of the external spherical cap is thus 1.5 times that of the 30 cm. hemisphere. In calculating distances from points on this spherical cap to points within the 40° cone the geometrical relations derived for the 90° cone can be used (III(6) and III(7)), though all distances must

FIG. III. 9 a. 40° CONE

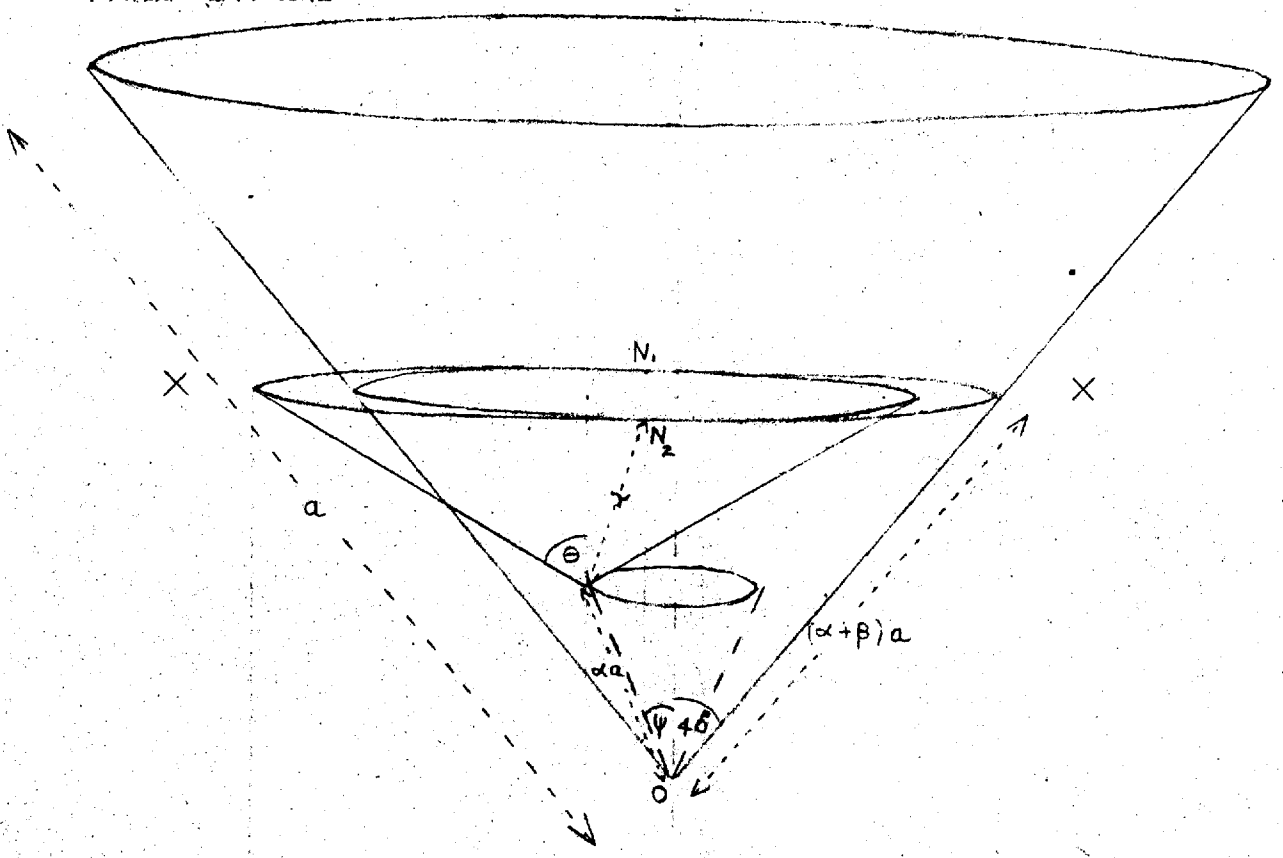
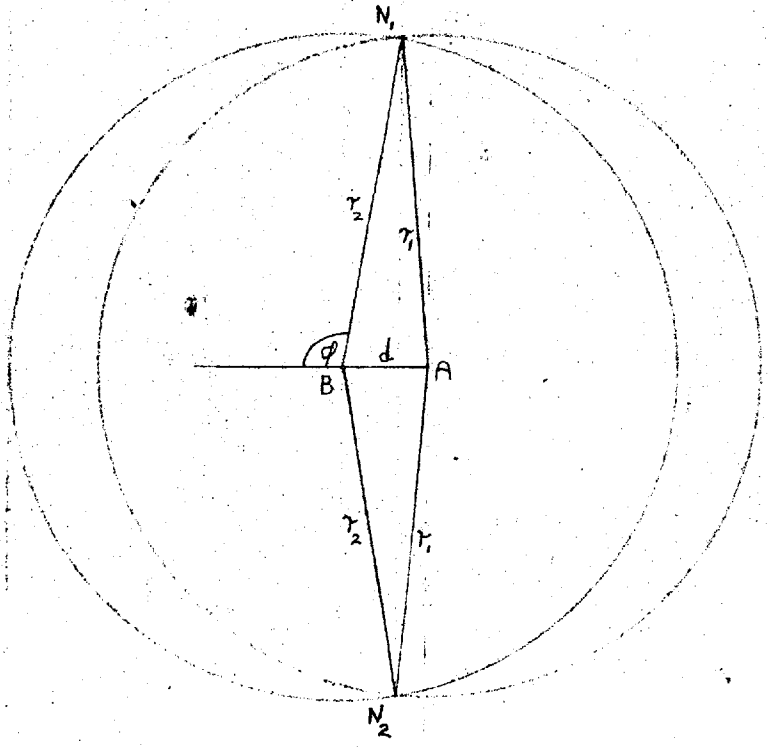


FIG. III 9. b.
SECTION ACROSS XX



be multiplied by the above factor.

In Figure III.9(a) is shown a section of the 40° cone. It must be remembered that the lead absorber lies within radial distances from O between 15 cm. and 45 cm. Consider a typical point $P(x, \psi)$ inside the cone, where x is equal to α a. For P to be within the absorber α must lie between $\frac{1}{3}$ and 1. Primaries reaching P with zenith angles less than 40° cut the spherical cap, and so can be treated in the same way as for the 90° cone, discussed in Section 4.

However, primaries with zenith angles greater than 40° can cut the conical sides, and the geometrical relationship between r, the distance traversed through the absorber, and the variables φ, θ, x and ψ, have to be derived. These variables are exactly analogous to those used in Section 4.

All particles reaching P from outside the absorber with zenith angle Θ will lie along the sides of an inverted vertical cone of semi-angle Θ and apex at P. If Θ is greater than 40°, then the Θ° cone and the 40° cone will intersect along a certain ellipse in space. For the particular case of P lying on the vertical axis of the 40° cone, the intersection of the two cones will be a circle in the horizontal plane. Consider a horizontal section XX across the two cones (Figure III.9(b)) and cutting the 40° cone at a distance $(\alpha + \beta)a$ from the apex O. The cross-sections of the two cones will be two circles, with centres

A and B (for the 40° and Θ° cones respectively) and these two circles will intersect at two points N_1 and N_2, these being real or imaginary.

Primaries entering the 40° cone at N_1 or N_2 and reaching P will have travelled the same distance r through the absorber. The zenith angle of these primaries is of course Θ, and the azimuthal angle φ can be calculated from the triangle ABN_1 (Figure III.9(b)).

$$\varphi = \cos^{-1} (r_1^2 - r_2^2 - d^2) / 2\, r_2\, d \qquad \text{III(11)}$$

where

$$r_1 = \begin{matrix}\text{radius of } 40^{\circ} \\ \text{cone section}\end{matrix} = (\alpha+\beta)\, a \sin 40^{\circ} \qquad \text{III(12)}$$

$$r_2 = \begin{matrix}\text{radius of } \Theta^{\circ} \\ \text{cone section}\end{matrix} = a\{(\alpha+\beta)\cos 40 - \alpha \cos\psi\}\tan\Theta \qquad \text{III(13)}$$

$$d = \begin{matrix}\text{distance bet-} \\ \text{ween centres} \\ \text{A and B}\end{matrix} = \alpha\, a \sin\psi \qquad \text{III(14)}$$

Combining equations III(11), III(12), III(13) and III(14) it can be shown that

$$\varphi = \cos^{-1}\left\{\frac{(\alpha+\beta)^2 - \alpha^2 \frac{\sin^2\psi}{\sin^2 40} - (\alpha+\beta)^2 \frac{\tan^2\Theta}{\tan^2 40} - \alpha^2 \frac{\cos^2\psi}{\sin^2 40}\tan^2\Theta + 2\alpha(\alpha+\beta)\frac{\cos\psi}{\sin 40}\frac{\tan^2\Theta}{\tan 40}}{2\alpha(\alpha+\beta)\frac{\tan\Theta}{\tan 40}\frac{\sin\psi}{\sin 40} - 2\alpha^2 \tan\Theta \frac{\cos\psi \sin\psi}{\sin^2 40}}\right\} \qquad \text{III (15)}$$

while the distance r is given by

$$r = a \sec\Theta \left((\alpha+\beta)\cos 40 - \alpha \cos\psi \right) \qquad \text{III(16)}$$

Using relations III(15) and III(16) it was possible to obtain values of r corresponding to different values of φ and Θ. This has been done by varying the parameters α and β to give real values of φ. α can take any value between 1 and $\frac{1}{3}$, while $(\alpha + \beta)$ must be equal to or less than 1.

This calculation has been performed for the three values of ψ, 40°, 0° and 20°, and the relations III(15) and III(16) simplify considerably for the first two of these.

(a) $\psi = 40^\circ$.

This applies to points P lying along the conical sides of the 40° cone. r and φ are now given by

$$r = \beta \, a \cos 40 \, / \cos \Theta \qquad \text{III(17)}$$

$$\varphi = \cos^{-1} \left\{ \frac{2\alpha + \beta - \beta \tan^2 \Theta \, / \tan^2 40}{2\alpha \tan \Theta \, / \tan 40} \right\} \qquad \text{III(18)}$$

Having chosen a value of Θ greater than 40°, values of r corresponding to different values of φ can be calculated from III(17) and III(18) by varying β and α. In particular, if we choose $\beta = 0$, some of the primaries will not pass through any lead at all, and this will be true for all φ outside the region $\varphi_0 \leq \varphi \leq 2\pi - \varphi_0$ where $\varphi_0 = \cos^{-1} (\tan 40 \, / \tan \Theta)$.

For $\Theta = 60^\circ$, $\varphi_0 = 61^\circ$ and hence one-third of the primaries arriving at a point P, on the conical surface of

the 40^0 cone with zenith angles of 60^0, do not pass through any of the absorber. For zenith angles of 90^0, this fraction is increased to one-half.

(b) $\varphi = 0^0$.

This applies to points lying along the axis of the cone, and hence the distance r is independent of the azimuthal angle ϕ. Equation III(16) simplifies to

$$r = 2a \sin 40 \,/\, \sin(\theta - 40)$$

(c) $\varphi = 20^0$.

The relations III(15) and III(16) become slightly simplified, and r and ϕ are now given by

$$r = a \sec\theta \left\{ (\alpha + \beta) \cos 40 - \alpha \cos 20 \right\}$$

$$\phi = \cos^{-1}\left\{ \frac{(\alpha+\beta)^2 - \frac{\alpha^2}{4}\sec^2 20 - (\alpha+\beta)^2 \frac{\tan^2\theta}{\tan^2 40} - \alpha^2 \frac{\tan^2\theta}{\sin^2 20} + \alpha(\alpha+\beta)\frac{\tan^2\theta}{\sin 20 \tan 40}}{\alpha(\alpha+\beta)\sec 20 \frac{\tan\theta}{\tan 40} - \alpha^2 \frac{\tan\theta}{\tan 40}} \right\}$$

Using the above results the new density functions $I(x, \varphi)$ have been calculated for the 40^0 cone, using a similar method as described for the 90^0 cone. Then using the $I(x, \varphi)$ functions the angular distribution functions, I_φ, of the secondaries reaching the emulsion at 0 were calculated.

The resulting I_φ functions, for $\cos\theta$, $\cos^3\theta$ and $\cos^6\theta$ zenith angle distributions of primaries are shown

in Figure III.7. By integrating the I_ψ functions over the range of ψ, from 0° to 40°, one obtains the total flux of secondaries under a 40° cone. This can be expressed as a certain fraction, f_{40°, of the number of secondaries under the 90° cone.

For primaries of high collimation, $\cos^3\theta$ to $\cos^6\theta$ zenith angle distributions, this fraction f_{40° does not vary very much, and in fact the I_ψ function tends asymptotically to that of the hemisphere as the collimation increases. This is because less of the primaries can enter the cone by its conical sides. However, if we assume collimated production of secondaries, the corresponding fraction f_{40} increases with the collimation of the primaries. Hence, for primaries having any reasonable degree of collimation (greater than a $\cos^2\theta$ distribution, say) the number of secondaries obtained from the collimated mechanism is greater than the corresponding number assuming isotropic production of secondaries.

Similar calculations have been made for a 60° cone, and the resulting fraction f_{60} obtained for a $\cos^3\theta$ zenith angle distribution of secondaries. The general effect on the lead cone absorption curves will be considered in the next section.

It is of interest to consider a cone of very small angle, say with semi-angle 5°. Under certain conditions the number of secondaries assuming isotropic production

is actually greater than the corresponding number assuming collimated production.

For such a small cone, angle Θ, the density function $I(x,\varphi)$ is practically unaffected by depth in the lead, since the great majority of primaries enter from the sides. The number of isotropic secondaries reaching the apex can be calculated from equations III(8) and III(9) and is equal to

$$\frac{2\pi N n_i}{m+1}(1-\cos\Theta)(1-e^{-\frac{a}{\lambda}}) \qquad \text{III(19)}$$

while the corresponding number assuming collimated secondaries is equal to

$$\frac{2\pi N n_c}{m+1}(1-\cos^{m+1}\Theta)\left(\frac{\alpha}{\lambda}e^{-\frac{a}{\lambda}}\right) \qquad \text{III(20)}$$

For a $\cos^3\theta$ distribution of primaries, thickness a = 30 cm. lead and semi-angle $\Theta = 5^0$, then the number of secondaries is proportional to 0.36 n_c and 0.34 n_i for the collimated and isotropic cases respectively. However, in order to give equivalent numbers of secondaries under the 90^0 cone, $n_i = 1.33\ n_c$. If, therefore, we express the number of secondaries as the fraction f_Θ of the number under the 90^0 cone, then the fraction for the isotropic mechanism is 1.25 times greater than the fraction for the collimated mechanism.

7. Effect of the Isotropic Production of Secondaries on the Lead Cone Absorption Curves

The concept of isotropic production of secondaries can considerably affect the simple analysis of the lead cone absorption curves, discussed in Part II, § 4. The shapes of the absorption curves were analysed to give a value of m, in the $\cos^m \theta$ zenith angle distribution of the primaries. However, it will be shown that the theoretical absorption curves assuming isotropic secondaries are different from those assuming collimated secondaries.

Consider a lead cone of semi-angle Θ and thickness a. The number of primaries reaching the apex at O is equal to $N_p(\Theta)$ where

$$N_p(\Theta) = N_p(0) \left\{ \cos^{m+1} \Theta + (1 - \cos^{m+1} \Theta) \exp(- a/\lambda) \right\} \quad \text{III(21)}$$

for a value of a = 30 cm. of lead, $\exp(- a/\lambda) = 0.105$, and so

$$N_p(\Theta) = N_p(0) \left\{ \cos^{m+1} \Theta + (1 - \cos^{m+1} \Theta) 0.105 \right\} \quad \text{III(22)}$$

This number of primaries is independent of the angular distribution of the secondaries. The number of secondaries arriving at the apex, $N_s(\Theta)$, can be expressed as $f_\Theta \; N_s(\pi/2)$, where $N_s(\pi/2)$ has been shown experimentally to equal 0.25 $N_p(0)$, for a 30 cm. hemisphere.

For a collimated production of secondaries f_Θ equals $(1 - \cos^{m+1} \Theta)$. The calculations of f_Θ assuming isotropic

FIG III. NUMBER OF SECONDIES PRODUCED UNDER 30cm, @ ° LEAD CONE ASSUMING A

$\cos^3\theta$ DISTRIBUTION LAW OF PRIMARIES

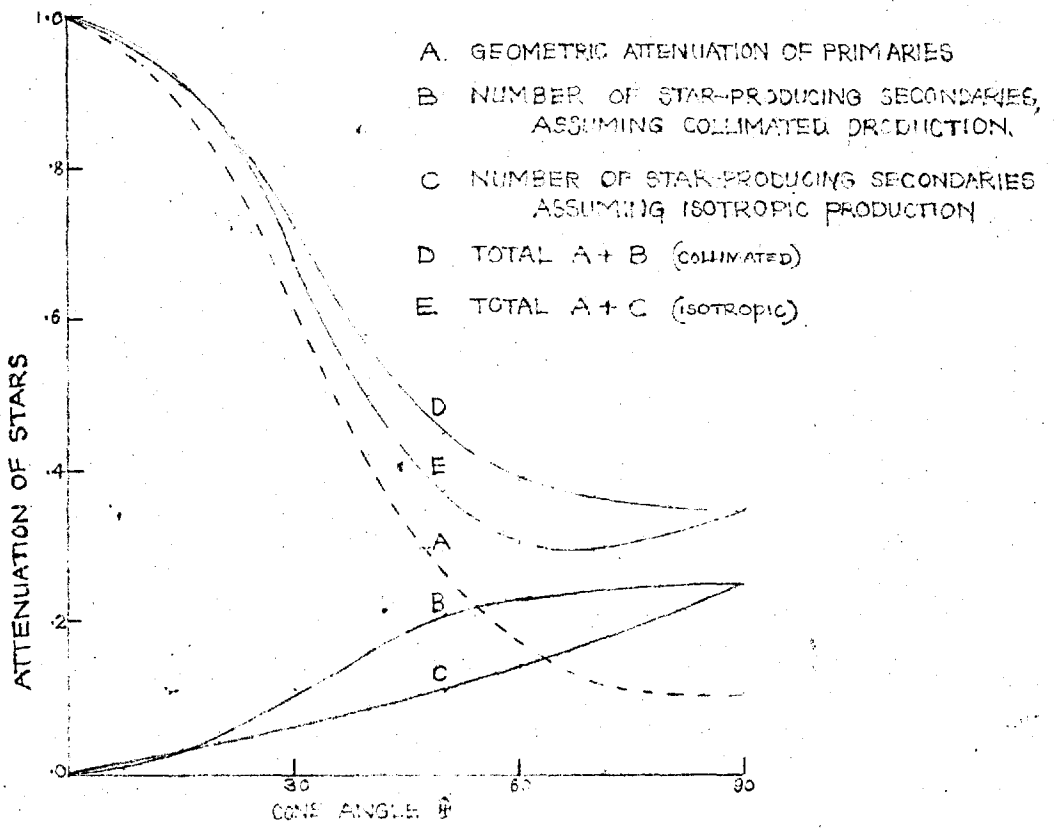
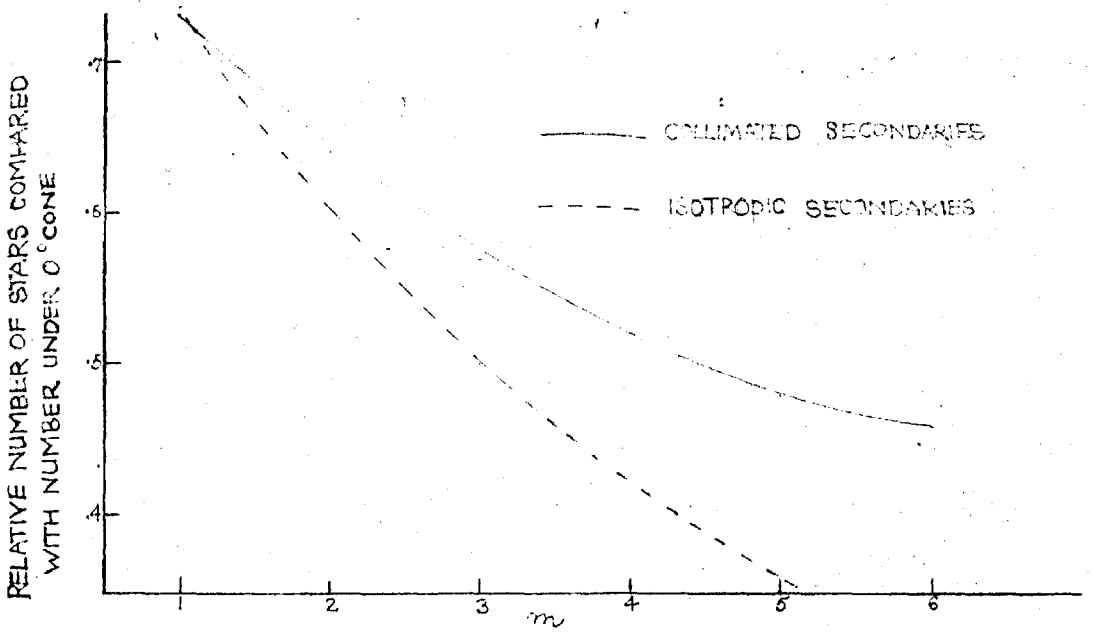


FIG III. 11. ATTENUATION UNDER 40° CONE FOR ISOTROPIC AND COLLIMATED SECONDARIES



production of secondaries have been described in the previous three sections for 30 cm. lead cones.

In Figure III.10, curves B and C show the number of secondaries expected under cones of semi-angles Θ, for the collimated and isotropic cases respectively. They have been calculated assuming a $\cos^3 \theta$ zenith angle distribution of the primaries. Apart from the initial cross over at about 15°, discussed at the end of the last section, the collimated curve B rises more rapidly than the isotropic curve. Consequently the curve showing total flux of star-producing radiation for the collimated case (D) will generally lie above that corresponding to isotropic secondaries (E). These curves of total flux, D and E, are obtained by adding to the primary flux curve A, curves B and C respectively.

The isotropic curve of total flux E shows some interesting features. It intersects the collimated curve D at a value of $\Theta \sim 15^\circ$, and actually has a minimum value at about 65°, in contrast with curve D. This implies that the addition of lead between 65° and 90° increases the isotropic secondary contribution at a greater rate than the attenuation of the primary radiation within these angles. For a $\cos^3 \theta$ distribution of primaries only 3% of the primaries lie between 65° and 90° with respect to the vertical, and this minimum is therefore understandable.

However, the great bulk of the searching was

concentrated in the emulsion under the 0°, 40° and 90° cones. There is therefore insufficient statistics for the 60° cone to show the presence of a minimum corresponding to isotropic production of secondaries. Although the statistics are not of great weight, there is no sign of such a minimum, as can be seen from Figures II.3 and II.4.

In these figures II.3 and II.4 it may be noted that increased collimation of primaries (that is, larger values of m) correspond to lower absorption curves. Any degree of isotropic emission of secondaries also causes a lowering of the absorption curves, for cone semi-angles $\sim 40^{\circ}$, and hence the initial analysis of Part II, § 4 will overestimate the value of m.

This is clearly shown in Figure III.11, which gives the expected attenuation under a 40° cone, 30 cm. thick, for values of m between 1 and 5, assuming isotropic and collimated secondaries. The curve corresponding to isotropic secondaries lies well below the collimated curve at large values of m, but the curves actually cross at $m = 1.1$. Hence, for values of m greater than 1 the collimated assumption always gives less attenuation than the isotropic assumption, and for a given attenuation, the collimated curve will give a greater value of m. For example, an experimental attenuation of 0.5 represents a $\cos^{4.5}\theta$ law assuming collimated secondaries, but only a $\cos^{3}\theta$ law assuming isotropic secondaries.

The difference between corresponding values of m increases rapidly with the index m. However, increasing collimation of primaries implies increasing energy, with corresponding collimation of secondaries, and the experimental attenuation curve should tend towards the upper collimated curve.

The initial analysis showed an effective $\cos^3 \theta$ law for the total star-producing component. If the secondary radiation is isotropic, then the true distribution is represented by a $\cos^{2.2} \theta$ law.

This difference between the true and effective angular distributions increases as

(a) the proportion of non-collimated secondaries to primaries entering the emulsion is increased (by decreasing the attenuation length for the primaries),

(b) the angular distribution of secondaries changes from collimated towards isotropic.

It has been shown above that the extreme possibilities for (a) and (b) (that the attenuation length is geometrical, and the emission of secondaries is completely isotropic) give a value of m for the total star-producing component of 2.2. This is the least true value that could give the apparent value of 3.0, derived from the simple analysis. An attenuation length of 210 g cm.$^{-2}$, instead of 150 g cm.$^{-2}$, with the secondary distribution still isotropic would increase this to m = 2.5, and with some degree of secondary

collimation it would rise still further towards m = 3.

A more detailed knowledge of the production of secondaries is required before the angular distribution of the primaries can be established with certainty. However, there is evidence that the true value of m cannot be much less than the effective value m = 3, from the fact that the experiments under 20 cm. and 30 cm. of lead both gave this result. Since the proportion of secondaries is very different in the two cases, their effect in determining the effective distribution cannot be very great.

For the larger stars only, the problem is much more complicated, for charged primaries here play a much greater part and one can no longer neglect ionisation losses. The general effect of these is to sharpen the overall collimation and thus counteract the effect of non-collimated secondary production. To judge from the effective and true angular distributions obtained in Part II, §5 for p-stars, the former effect may be slightly the greater.

IV. A ONE-DIMENSIONAL NUCLEON CASCADE MODEL IN LEAD, LEADING TO AN ENERGY VARIATION OF THE ATTENUATION

1. Introduction

The lead cone experiment showed signs of a decrease in the attenuation mean free path with increasing energy (Part II, Section 7) although this could have been due to statistical fluctuations. In this part of the thesis a cascade model is developed which can produce the above results. This model is very sensitive to slight changes in the basic parameters and under certain conditions the cascade can be made independent of energy. The mathematics have been made as simple as possible and the physical implications of the cascade can be seen at each stage of the formulation of the model.

Several authors have developed cascade models giving a description of the nucleon cascade in the atmosphere (Messel and Ritson 1950; Mellel 1951; Thomson and Hodgson 1951).

Messel considers a basic nucleon-nucleon interaction, in which an incident nucleon gives rise to two emergent nucleons, with a cross-section depending only on the ratio of the energies of the emergent nucleons to that of the primary. He then develops the cascade theory in homogeneous nuclear matter, which is analogous to star-production within a nucleus, and then continues the development in

inhomogeneous nuclear matter. From this theory it can be shown that a primary nucleon, incident on a nucleus, causes the emission on the average of a given number of nucleons, and that their energy distribution, expressed as a fraction of the primary energy, is independent of the primary energy. This means that the number of nucleons emitted in a given energy band, whose limits are proportional to the primary energy, is independent of the primary energy.

Thomson and Hodgson in a rather simpler analysis formulate a convenient model for star production in developing their cascade picture. In this model 1.7 nucleons are assumed to be emitted on the average from each nuclear interaction, each secondary nucleon possessing one-quarter of the energy of the primary. The majority of shower particles are π-mesons; most of these decay in flight before causing stars in the atmosphere, and so are not effective in the cascade process. However, it is very probable that the number of secondary nucleons per interaction increases with the energy of the primary, instead of remaining constant as Thomson and Hodgson assume. Since the majority of air nuclei in the atmosphere have only 14 nucleons, and at most 16, the assumption of constant numbers of secondaries can be expected to give reasonable agreement between theory and experiment for a cascade in the atmosphere, but when the medium is lead, this assumption can hardly be justified for there are now 210 nucleons per nucleus.

Both of these theories give a good picture of the nucleon cascade in the atmosphere, and the values for the neutron : proton ratio at different depths agree well with experimental results. Similar laws governing the production of secondaries are used in the two theories. That of Thomson and Hodgson assumes a constant number of secondaries with energy directly proportional to the primary energy; while that of Messel can be represented by the general law that a nuclear collision of a primary of energy E yields on the average n_1 secondaries of energy c_1 E, n_2 secondaries of energy c_2E, etc., where n_1, n_2..., c_1, c_2... are constants.

Under these initial conditions, it can be shown (see Section 2) that if the initial energy spectrum has the form $N(E)dE \propto E^{-\gamma} dE$, it will remain a power law with the same exponent throughout the atmosphere if ionisation and obliquity effects are neglected. If ionisation is taken into account, it will effectively remove low energy protons from the cascade, and should decrease from top to bottom of the atmosphere. In fact, Thomson and Hodgson calculated this effect in their theory and their results show a decrease in the index from 3, three-quarters of the way up the atmosphere, to 2.2 at sea-level. This result means that there is a relative increase in low energy nucleons, as one follows the cascade upwards to the top of the atmosphere.

This conclusion is in contradiction to the experimental work with photographic plates, which have been performed with balloons (Lord 1951; Camerini, Coor, Davies, Fowler, Lock, Muirhead and Tobin 1949). These all show a rapid increase in the proportion of very-high-energy events as compared with similar experiments at lower altitudes. It is clear that the above simple mechanism for star production is not suitable for explaining energy distributions in the nucleon cascade.

In a recent paper, Camerini et al. (1951) have described 200 stars in G.5 nuclear emulsion, each of which was produced by a charged particle whose track was long enough to permit an energy determination. These stars were analysed in detail, and from their results it can be shown that the number of grey and shower particles (capable of producing secondary stars) can be represented by a power law in the energy range 100 MeV$\leq$E$\leq$10,000 MeV. If N_{gs} is the number of these particles, then

$$N^{(E)} \propto E^{0.75} \qquad \text{IV(1)}$$

The average energy of these particles is represented by a power law of the form

$$E_1 \propto E^{0.35} \qquad \text{IV(2)}$$

These two relations hold for stars produced in nuclear emulsions, and chiefly for the heavy elements silver and

bromine. In developing the following cascade theory for lead, it will be assumed that the numbers and average energies of the secondary particles can be represented by equations similar to IV(1) and IV(2).

The theory of the nucleon cascade is developed in Section 2 for a purely neutronic cascade, and in Section 3 the assumptions made in formulating the cascade are discussed and suitable values given to the constants in the theory. The results for the neutron cascade are given in Section 4 and the attenuation is compared with experimental results. Under certain conditions the neutronic cascade leads to an increase in the proportion of low energy secondaries. However, ionisation loss by the protons tends to reduce the low energy component and so counteracts the above effect.

The effects of ionisation will be discussed in Section 5 for a cascade in 30 cm. of lead and the final nucleon intensities under the absorber are given. In Section 6 these nucleon intensities are interpreted in terms of the distribution of star sizes, and the final comparison between theory and experiment is set out in Section 7.

2. The cascade model in lead, neglecting ionisation.

The cascade will be considered in one dimension only. All the nucleons taking part in the cascade are assumed to have the same mean free path for nuclear interaction in

the lead (λ gm. cm.$^{-2}$).

If a nucleon of energy E (expressed in 100 MeV units) interacts with a lead nucleus, it will be assumed that the number of star-producing secondaries n(E) and their mean energy E can be represented by the following relations:

$$n(E) = mE^{\psi} \qquad \text{IV(3)}$$

$$E_1 = xE^{\beta} \qquad \text{IV(4)}$$

A differential energy spectrum of the form $N(E)\,dE = N_0E^{-\gamma}\,dE$ is assumed for the incident nucleons, and it will be shown that this power law changes as a result of the cascade. Ionisation effect will be neglected in this initial treatment.

Consider a cascade in a lead absorber y gm./cm.^{2} thick. This can be expressed as α-interaction paths in lead, where $\alpha\lambda = y$.

It will be assumed that an incident particle of energy E produces n(E) particles all of the average energy E_1, where E_1 and n(E) are given by III(3) and III(4). In actual practice it is known that the secondaries are produced with a distribution of energies about the average energy, However, if the energy distribution of secondaries is taken into account, the mathematics becomes rather complicated, involving the use of the Mellin transforms. Messel (1951) in his theory does consider the energy distribution of secondaries, but even for the particular case

where the form of the energy distribution is independent of energy the mathematics is rather elaborate. The solution for the general relations IV(3) and IV(4) would be exceedingly laborious. As the cascade is so sensitive to small changes in the basic parameters (Section 4), many of which are not known for interactions in lead, it was not thought worth while considering the effect of the energy distribution.

The secondaries, of energy E_1, can in turn interact in the lead, each producing $n(E_1)$ secondaries of energy $(E_1)_1$, etc. Thence nucleons in the energy range E to E+dE found under the absorber will consist of two components. A proportion $e^{-\alpha}$ of nucleons in the energy range E to E+dE will pass through the absorber without interaction. A second portion will consist of secondaries and tertiaries, etc. which are cascade products from higher energy particles interacting in the lead. Since the average energy of secondaries equals xE, a final nucleon of energy E can have been produced by primaries above the lead of energies:

$(\frac{E}{x})^{\frac{1}{\beta}}$ for 1st-order cascade

$(\frac{E}{x^{1+\beta}})^{\frac{1}{\beta^2}}$ for 2nd-order cascade

$(\frac{E}{x^{1+\beta+\beta^2}})^{\frac{1}{\beta^3}}$ for 3rd-order cascade

For an nth-order cascade, the primary energy corresponding to a final energy E is given by E_n

where $$E_n = \left(\frac{E}{x^{p_n}}\right)^{\frac{1}{\beta^n}} \qquad \text{IV(5)}$$

and $$p_n = 1 + \beta + \beta^2 + \ldots + \beta^{n-1} = \frac{1-\beta^n}{1-\beta} \qquad \text{IV(6)}$$

The number of nth-order cascade nucleons in the energy range E to E+dE below the absorber will depend on the following three quantities:

(a) the number of primaries in the energy range E_n to $E_n + dE_n$ incident on the absorber;

(b) the number of nucleons produced per interaction at each stage of the nth-order cascade leading to a final nucleon energy of E;

(c) the effect of absorption on all the components of the cascade.

(a) The first of these three quantities can be obtained by differentiating IV(5), and is given by

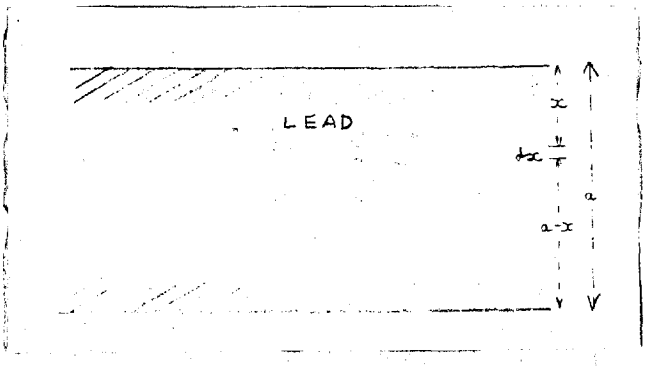
$$N(E_n)\, dE_n = N_0 (E_n)^{-\gamma}\, dE_n \qquad \text{IV(7)}$$

where $$dE_n = \left(\frac{1}{x}\right)^{\frac{p_n}{\beta^n}} \frac{1}{\beta^n}\, E^{\frac{1}{\beta^n}-1}\, dE \qquad \text{IV(8)}$$

(b) and (c) The combined effects of Absorption and Nucleon Multiplication at each stage of the cascade.

Consider a beam of nucleons, all of energy E, incident on an absorber g cm.$^{-2}$ thick. In the cascade process the secondary nucleons will all be assumed to retain the direction of the primary, and all the nucleons are assumed to have the same mean free path, λ g cm.$^{-2}$, for nuclear interaction.

Nucleons of energy E interacting with a lead nucleus give rise to $f_E(1)$ secondary nucleons, and each of these can give rise to $f_E(2)$ nucleons etc., $f_E(1)$, $f_E(2)$ .... being given by equations IV(3) and IV(4).



At a point x g cm.$^{-2}$ below the top of the absorber, the number of primaries interacting in an interval dx is equal to

$$N_o(E)\ \exp(-\ x/\lambda)\ \frac{dx}{\lambda}$$

The number of secondaries produced and reaching the bottom of the absorber without further interaction is therefore equal to

$$N_o(E)\ f_E(1)\ \frac{dx}{\lambda}\ \exp(-\ x/\lambda)$$

Thence the total reaching 0 is equal to

$$N_o(E)\ f_E(1)\ \frac{a}{\lambda}\ \exp(-\ a/\lambda\ )$$

Similarly, the number of secondaries interacting in an interval dy at y g cm.$^{-2}$ below the top of the absorber is equal to

$$N_o(E)\ f_E(1)\ \frac{y}{\lambda}\ \exp(-\ y/\lambda\ )\ \frac{dy}{\lambda}$$

The number of tertiaries reaching 0 is therefore equal to

$$N_o(E)\ f_E(1)\ f_E(2)\ \frac{1}{2!}\ \frac{a^2}{\lambda^2}\ \exp(-\ a/\lambda\ )$$

It can be similarly shown that the number of n^{th} order nucleons reaching 0 is equal to

$$N_o(E)\ \prod_{r=1}^{n} \left\{f_E(r)\right\}\ \frac{1}{n!}\ \left(\frac{a}{\lambda}\right)^n\ \exp(-\ a/\lambda\ ) \qquad IV(9)$$

However, this applies to a cascade generated by incident nucleons of energy E. In order to correspond with final nucleon energies of E, then $f_E(r)$ in relation IV(9) must be replaced by $f_{E_{\overline{n}}}$, where $E_{\overline{n}}$ is given by equation IV(5). The combined effects of absorption and nucleon multiplication are therefore represented by the $(n+1)^{th}$ term of the following series, for an n^{th} order cascade:

$$e^{-\alpha} + e^{-\alpha}\alpha\, f_{\underline{E}}(1) + e^{-\alpha}\frac{\alpha^2}{2!} f_{\underline{E}}(2) + \ldots$$

primary absorption — 1st stage cascade — 2nd stage cascade

$$e^{-\alpha}\frac{\alpha^n}{n!} \prod_{r=1}^{n} \left\{ f_{\underline{E}}(r) \right\}$$

n^{th} stage cascade

where $f_{\underline{E}}(1)$ is the number of secondaries each primary can produce, $f_{\underline{E}}(2)$ is the number of tertiaries each secondary can produce, etc., in an n^{th} order cascade leading to a final energy of E.

As primaries above the absorber are chosen so that each term of the above series corresponds to a final nucleon energy of E, then using relation IV(3)

$$\prod_{1}^{n} f_{\underline{E}}(r) = \prod_{r=1}^{n} \left\{ m(\underline{E})^{\gamma} \right\} \qquad \text{IV(10)}$$

Hence, combining the three quantities (a), (b) and (c), the total number of particles in the energy range E to E+dE, after a cascade in α interaction lengths in lead is given by $N_{\alpha}(E)\,dE$, where $N_{\alpha}(E)\,dE$ is equal to

$N_0 E^{-\gamma} \exp(-\alpha)\, dE$ +

attenuation of incident nucleons

$$\sum_{n=1}^{\infty} \left[N_0 E_{\overline{n}}^{-\gamma} dE_{\overline{n}} \cdot \exp(-\alpha) \frac{\alpha^n}{n!} \cdot \prod_{1}^{n} \left(m E_{\overline{r}}^{\psi} \right) \right] \qquad \text{IV(11)}$$

(a) number of incident nucleons in the appropriate energy range — (b) absorption factor — (c) multiplication factor

This can be somewhat simplified, using the relations derived above in this section.

From equation IV(11) the series terms equals

$$\left\{ N_0 \left(\frac{1}{E}\right)^{\gamma} dE \quad e^{-\alpha} \frac{\alpha^n}{n!} \tilde{\prod}_{1} m \left(E_{\overline{r}}\right)^{\psi} \right\}$$

$n=1$

where $E_{\overline{n}} = \left(\frac{E}{x^{pn}}\right)^{\frac{1}{n}}$ and $pn = \frac{1-\beta^n}{1-\beta}$

and $dE_{\overline{n}} = \left(\frac{1}{x}\right)^{\frac{pn}{\beta^n}} \frac{1}{\beta^n} E^{\frac{1}{n}-1} dE$

(a) determination of $\prod_{1}^{n} \left[m \left(E_{\overline{r}}\right)^{\psi} \right]$

$$\equiv m^n \left\{ E^{\left(\frac{\psi}{\beta} + \frac{\psi}{\beta^2} + \frac{\psi}{\beta^n}\right)} \right\} \left(\frac{1}{x}\right)^{\psi} \left(\frac{1}{\beta} + \frac{1+\beta}{\beta^2} + \frac{1+\beta+\beta^2}{\beta^3} + \frac{1+\beta+\ldots\beta^{n-1}}{\beta^n} \right)$$

$$\equiv m^n E^{\psi S_1} \left(\frac{1}{x}\right)^{\psi S_2}$$

where $S_1 = \frac{1}{\beta} + \frac{1}{\beta^2} + \ldots \frac{1}{\beta^n} = \frac{1}{\beta^n} p_n$

$$\zeta_2 = \frac{n}{\beta} + \frac{n-1}{\beta^2} + \ldots \frac{1}{\beta^n} = \frac{1}{\beta^n}\,(1 + 2\beta + 3\beta^2 + \ldots n\beta^{n-1})$$

$$= \frac{1}{\beta^n}\left(\frac{pn - n\beta^n}{1-\beta}\right)$$

$$\therefore \prod_1^n \left\{ m(E_r)^{\psi} \right\} = m^n \; E^{\left(pn \frac{\psi}{\beta^n}\right)} \left(\frac{1}{x}\right)^{\frac{\psi}{\beta^n}} \; \frac{pn-n\beta^n}{1-\beta}$$

The cascade series can now be written

$$\sum_{n=1}^{\infty} \left\{ N_o \left(1/\left(\frac{E}{x^{pn}}\right)^{\frac{1}{\beta^n}}\right)^{\gamma} \left(\frac{1}{x}\right)^{\frac{pn}{\beta^n}} \frac{1}{\beta^n} \; E^{\frac{1}{\beta^n}-1} \; dE \right.$$

$$\left. e^{-\alpha} \frac{\alpha^n}{n!} \; m^n \; E^{\frac{pn\psi}{\beta^n}} \left(\frac{1}{x}\right)^{\frac{\psi}{\beta^n}} \left(\frac{pn-n\beta^n}{1-\beta}\right) \right\}$$

The n^{th} term of this series can be grouped into terms containing $\frac{1}{x}$ and E

(i) $\frac{1}{x}$ term $= \left(\frac{1}{x}\right)^{\left\{\frac{pn}{\beta^n} - \gamma \frac{pn}{\beta^n} + \frac{\psi}{\beta^n} \quad \frac{pn-n\beta^n}{1-\beta}\right\}}$

$$= \left(\frac{1}{x}\right)^{\left\{\frac{pn}{\beta^n}(1-\gamma) \; + \; \psi\left(\frac{pn}{\beta^n} - n\right) / 1-\beta \right\}}$$

$$= \left(\frac{1}{x}\right)^{\left\{\frac{pn}{\beta^n}\left(1 - \gamma + \frac{\psi}{1-\beta}\right) - \frac{n\psi}{1-\beta}\right\}}$$

(ii) E term $= E^{\left\{-\frac{\gamma}{\beta^n} + \frac{1}{\beta^n} - 1 + \frac{pn\psi}{\beta^n}\right\}}$

$$= E^{-\gamma \left\{1/E\beta^{\left(\frac{\gamma}{n} - \frac{1}{\beta^n} + 1 - \gamma \; - pn\frac{\psi}{\beta^n}\right)}\right\}}$$

$$E \text{ term} = E^{-\gamma} \left\{ {}^{1}/_{E^{\left(\frac{1}{\beta^n}-1\right)}} \left(\gamma - 1 - \frac{\psi}{1-\beta} \right) \right\}$$

The final series term can now be written

$$\sum_{n=1}^{\infty} \frac{\alpha^n}{n!} \frac{1}{\beta^n} m^n x^{\left(\frac{pn}{\beta^n}\left(\gamma - 1 - \frac{\psi}{1-\beta}\right) + \frac{n\psi}{1-\beta}\right)} E^{-\left(\frac{1}{\beta^n}-1\right)\left(\gamma - 1 - \frac{\psi}{1-\beta}\right)}$$

and equation IV(11) becomes

$$N_{\alpha}(E)\, dE = N_o E^{-\gamma} \exp(-\alpha)$$

$$dE \left[1 + \sum_{n=1}^{\infty} \frac{\alpha^n}{n!} \frac{1}{\beta^n} m^n x^{\left(\frac{pn}{\beta^n} K + \frac{n\psi}{1-\beta}\right)} E^{-K\left(\frac{1}{\beta^n}-1\right)} \right] \qquad \text{IV(12)}$$

where $K = \gamma - 1 - \psi/(1-\beta)$ IV(13)

It can be seen from IV(12) that the attenuation of nucleons in a particular energy band is less than that given by the interaction mean free path, and in general varies with energy. This means that the inverse power law is no longer true under the absorber. However, the assumptions made by Thomson and Hodgson on star production are equivalent to making $\beta = 1$ and $\psi = 0$. Under these conditions $K(\beta^{-n} - 1) = 0$, and the series terms become independent of energy. The exponent of the power law will then be the same under the lead as above it.

3. Choice of Values of the Constants of the Theory

In this section the most suitable values of the constants λ , γ , m, ψ , x and β are disoussed.

The interaction in lead of particles producing penetrating showers of great multiplicity has been studied by Boehmer and Bridge (1952) and Walker, Walker and Greisen (1950). They both found an interaction mean free path of 150 gm/cm.^{2}, consistent with a geometric cross-section in lead. Camerini et al. (1950) found a geometrical cross-section for the production of secondary stars in emulsion by shower particles. For low energy protons in the energy region 300-400 MeV. Bernadini, Booth and Lindenbaum (1952) and Bernadini et al. (1950) found a value of only 50% of geometrical for the production of stars in emulsion. This phenomenon of nuclear transparency in light elements has been shown by Cook, McMillan, Peterson and Sewell (1949) for 90 MeV neutrons, and also by Fox, Leith, Wouters and Mackenzie (1950) and by De Juren (1950) for 270 MeV neutrons. It is unlikely that the transparency shown for light nuclei will be as great for lead nuclei as the latter have for more nucleons. It is therefore assumed that all nucleons taking part in the cascade have a geometric cross-section for nuclear interaction, and λ = 150 gm/cm.^{2}. This is probably quite true for nucleons with energies above 1 GeV, which play a leading part in

the cascade process.

If there is any degree of transparency for low energy nucleons, the theory will overestimate their attenuation. However, these nucleons will have a corresponding longer mean free path for star production in emulsion, and as the nucleon cascade will be compared with the observed star production in emulsion these two effects will tend to compensate each other.

It has been assumed in this theory that the secondaries of stars are travelling in the same direction as the primary. This is a reasonable assumption for secondaries of enough energy to participate further in the cascade in lead, as shower particles are known to be strongly collimated about the primary direction. However, nucleons of an energy corresponding to "grey" proton tracks have quite a broad angular distribution about that of the primary. These will have a corresponding greater path length in the lead, and it is therefore probable that the theory will overestimate the numbers of low energy nucleons. The effective loss due to isotropic emission of secondaries in the lower hemisphere has been calculated in Part III of this thesis and is only 25% for a hemispherical lead absorber 30 cm. thick. This effect can therefore be neglected in obtaining an approximate description of the cascade.

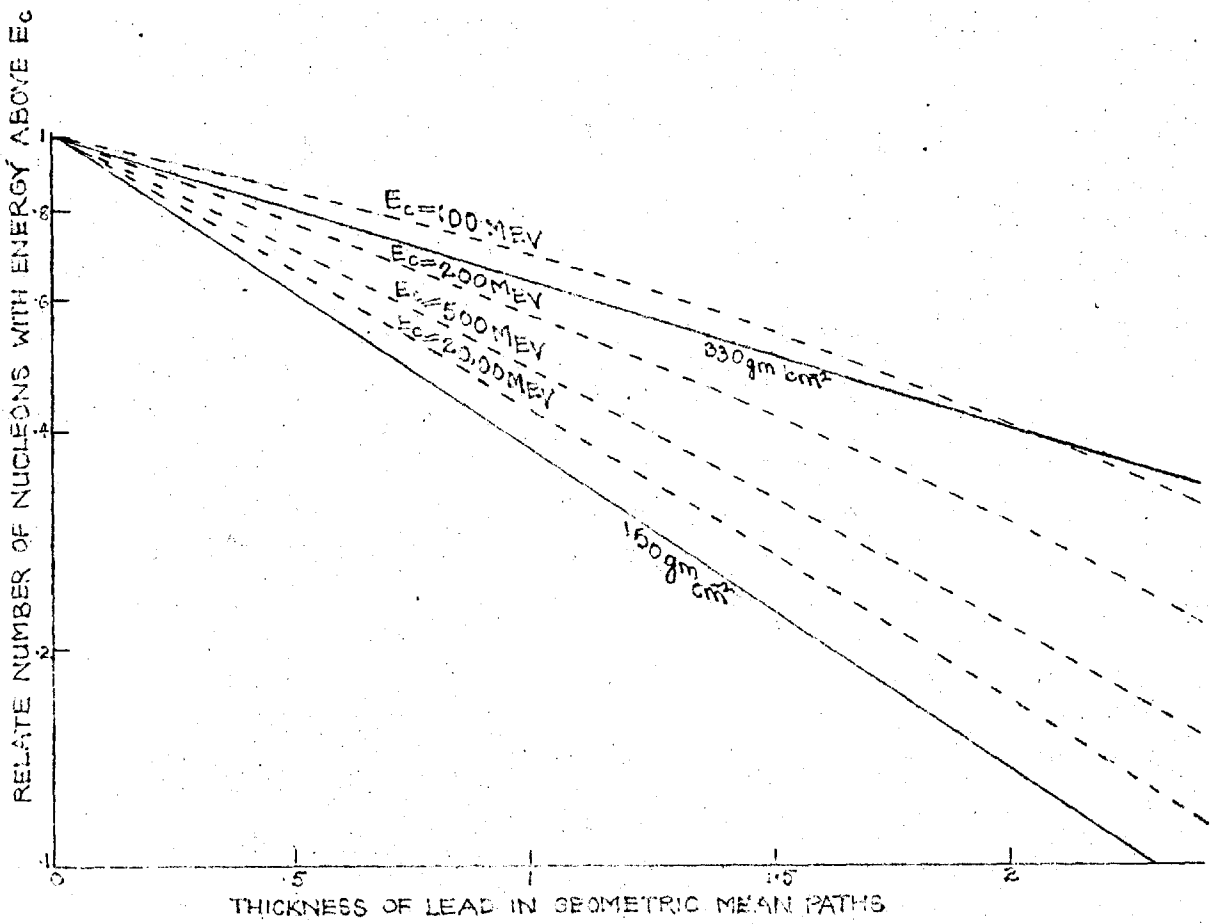
The results of Camerini et al. (1951) previously

discussed, showed that the number of "grey" and "shower" particles produced by particles of energy E could be represented by $N_{gs} = 0.3\ E^{0.75}$ with average energy $0.8\ E^{0.35}$, where E is measured in 100 MeV units. There are no similar experimental results for nuclear interactions in lead at the present time. These could be obtained by using wire-loaded emulsions (Danysz and Yekutieli 1951), or with lead foils (Hodgson 1951, Barbour 1951), but the searching time would be quite prohibitive if good statistical results are required. It will be assumed in the theory that the exponents in the two power laws are the same for lead as for emulsion. The above relations apply only for charged particles emitted from stars, and allowance has to be made for neutrons emitted. In the lead nucleus there are 50% more neutrons than protons, and allowing for neutrons in the "grey" track energy region (25-500 MeV), the number of neutrons is taken as 1.5 times the "grey" tracks. Fowler (1950) has shown that the majority of "grey" tracks are protons, but the proportion is only one-quarter for low energy shower particles (proton energies of 500 MeV to 800 MeV, and meson energies of 80 MeV to 1100 MeV). Assuming that the fraction of protons remains one-quarter for high energy shower particles, the correction for neutrons is found by taking three-eighths of the shower particles. For primary energies between 1 GeV, which produce four times as many

"grey" as "shower" particles, and 10 GeV, which produce roughly equal numbers of "grey" and "shower" particles, the neutron correction is approximately equal to the total number of "grey" and "shower" particles. Above this energy, the shower component may well exceed the grey component, and the neutron component will be overestimated. However, it was decided to equate the total in the neutron component to that of the charged component, and in equations IV(3) and IV(4), $m = 0.6$, $\varphi = 0.75$, $x = 0.8$, $\beta = 0.35$. This choice of constants can only be regarded as provisional estimates, and only a qualitative agreement between theory and experiment can be hoped for. In using these values it is assumed that high energy neutrons, protons and mesons, which all take part in the lead cascade, are equally effective in causing nuclear disintegrations in the lead.

Following Thomson and Hodgson, the exponent γ in the differential spectrum is taken as 2.5. This value was found for primary particles (Hoang 1951) and for the energy distribution of stars (Barton, George and Jason 1951). For those particles producing extensive air showers, with energies greater than 15 BeV, Hilberry (1941) found a value of γ of 2.75. However, the more recent experiment of Winchler, Stix, Dwight and Sabin (1950) for primary protons between 1 and 14 BeV has shown a value of 1.9. These results are not necessarily inconsistent, and

FIG IV.1 INTEGRAL ATTENUATION CURVES (NEGLECTING IONISATION)



——— EXPONENTIAL ATTENUATION WITH GEOMETRIC MEAN FREE PATH (150 gm cm^{-2}) AND EXPERIMENTAL MEAN FREE PATH (330 gm cm^{-2})

– – – – – INTEGRAL ATTENUATION CURVES WITH CUT OFF ENERGY E_c

it seems most probable that the exponent varies with energy, the spectrum flattening out below 1 BeV and becoming steeper at high energies.

4. Results for the Cascade (neglecting Ionisation)

The negative exponent of E in the series terms of IV(9) is equal to $K(\beta^{-n} - 1)$. Using the values discussed in Section 3, K is equal to 0.35 and as the energy tends towards infinity, the attenuation mean free path of the nucleons tends towards the interaction mean free path. The series terms in IV(12) have been evaluated for 30 cm. of lead (equal to 2.25 geometric mean free paths).

$$\text{series terms} = \underset{(n=1)}{2.5\ E^{-0.65}} + \underset{(n=2)}{1.86\ E^{-2.5}} + \underset{(n=3)}{0.3\ E^{-7.8}}$$

It can be seen that the series terms are rapidly converging with increasing n and E. For E = 200 MeV the series terms are approximately equal to 2 and the total attenuation of protons of this energy equals $3\ e^{-\alpha}$. For E = 2000 MeV the series terms equal 0.4 and the total attenuation equals $1.4\ e^{-\alpha}$. The integral attenuation curves for different lower cut off energies are shown in Figure IV.1. Also are shown the curves corresponding to geometric absorption (m.f.p. of 150 gm/cm^2) and the observed attenuation of all stars with more than 3 tracks discussed in Part II, Section 7 with a m.f.p. of 330 gm/cm^2.

Table IV.1. Values of Cascade Series for Different Values of γ.

Order n of Cascade	1	2	3	4	5	6	7
Value of γ							
2.15	2.98	4.5	4.52	3.3	1.97	1.01	0.43
2.2	$2.9\ E^{-0.09}$	$3.98\ E^{-0.36}$	$3.14\ E^{-1.12}$	$1.12\ E^{-3.3}$			
2.3	$2.70\ E^{-0.27}$	$3.1\ E^{-1.08}$	$1.45\ E^{-3.36}$	$0.12\ E^{-9.9}$			
2.4	$2.55\ E^{-0.47}$	$2.4\ E^{-1.8}$	$0.67\ E^{-5.6}$				
2.5	$2.45\ E^{-0.65}$	$1.86\ E^{-2.5}$	$0.3\ E^{-7.8}$				
2.7	$2.1\ E^{-1.02}$	$1.15\ E^{-3.95}$					

The increase in attenuation with energy agrees quite well with that reported in Part II, where it was shown that the number of 3 and 4-track stars under 30 cm. of lead is four times that expected on a geometric attenuation, but for stars with more than 13 heavy tracks the ratio was 1.5 times the geometric attenuation.

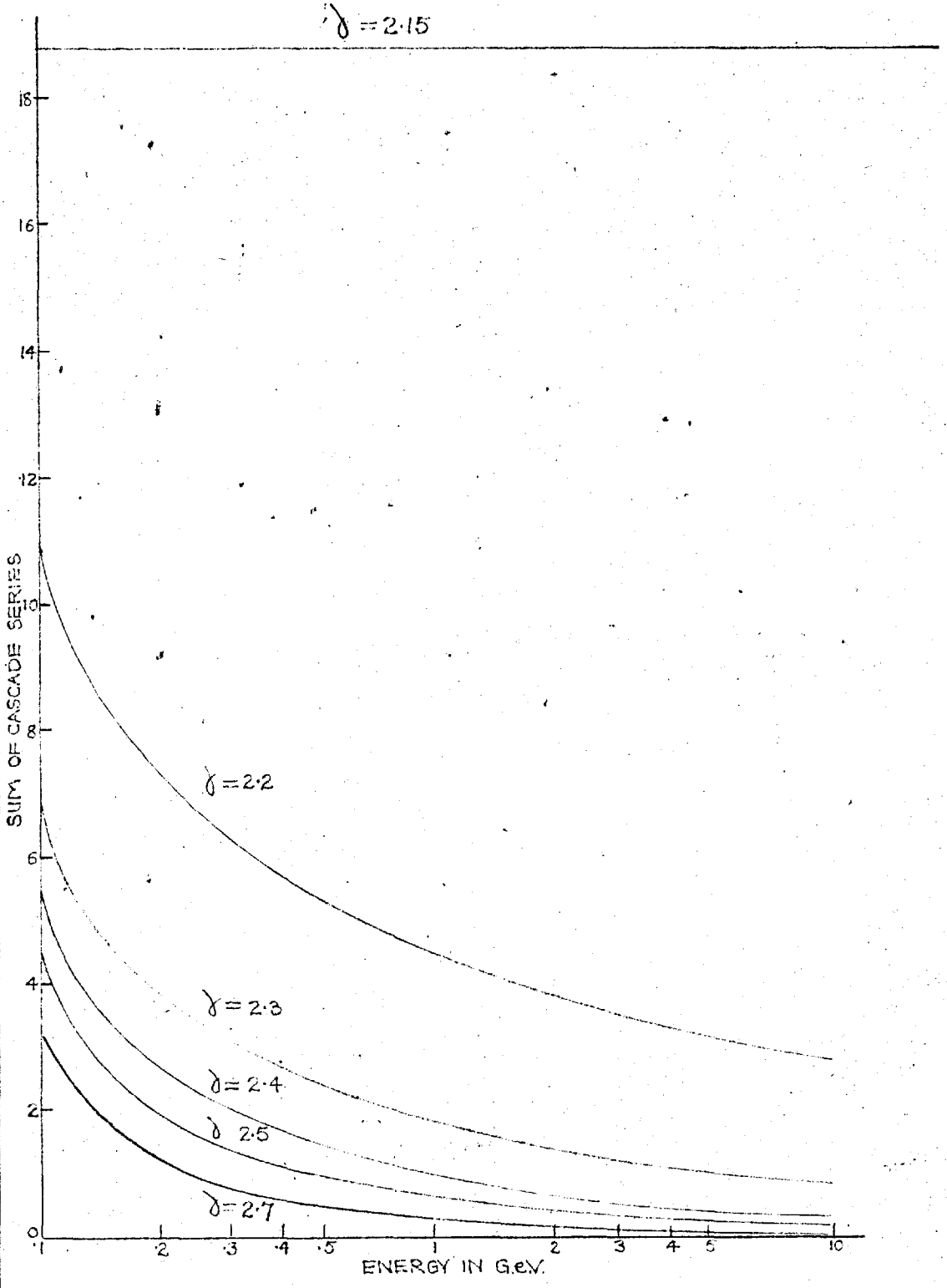
However, this agreement between the cascade theory and the experimental results does not prove the existence of the variation of attenuation with energy. In fact, the very good agreement could be regarded as fortuitous, because very slight changes in the parameters γ, ψ and β can completely change the nature of the cascade process.

This can be clearly shown if we consider the effect of varying the exponent γ, keeping the other parameters constant.

If $\gamma = 2.15$, then K, given by IV(13), is equal to 0, and the series terms in equation IV(12) become independent of energy. For $\gamma < 2.15$ these series terms actually diverge and one obtains an infinite number of nucleons under the absorber. However, for nucleons above 15 BeV γ is probably more than 2.5 and tends to increase with energy.

The series terms of equation IV(12) corresponding to various values of γ are shown below in Table IV.1.

FIG. IV. 2. VARIATION OF CASCADE SERIES TERMS WITH γ



As γ increases the effect of higher order cascade terms decreases. The sum of the series terms is shown in Figure IV.2. The value of these series terms gives the increase in the number of nucleons over that expected on a geometric attenuation, and it can be seen that quite small variations of γ would cause large changes in the energy distribution.

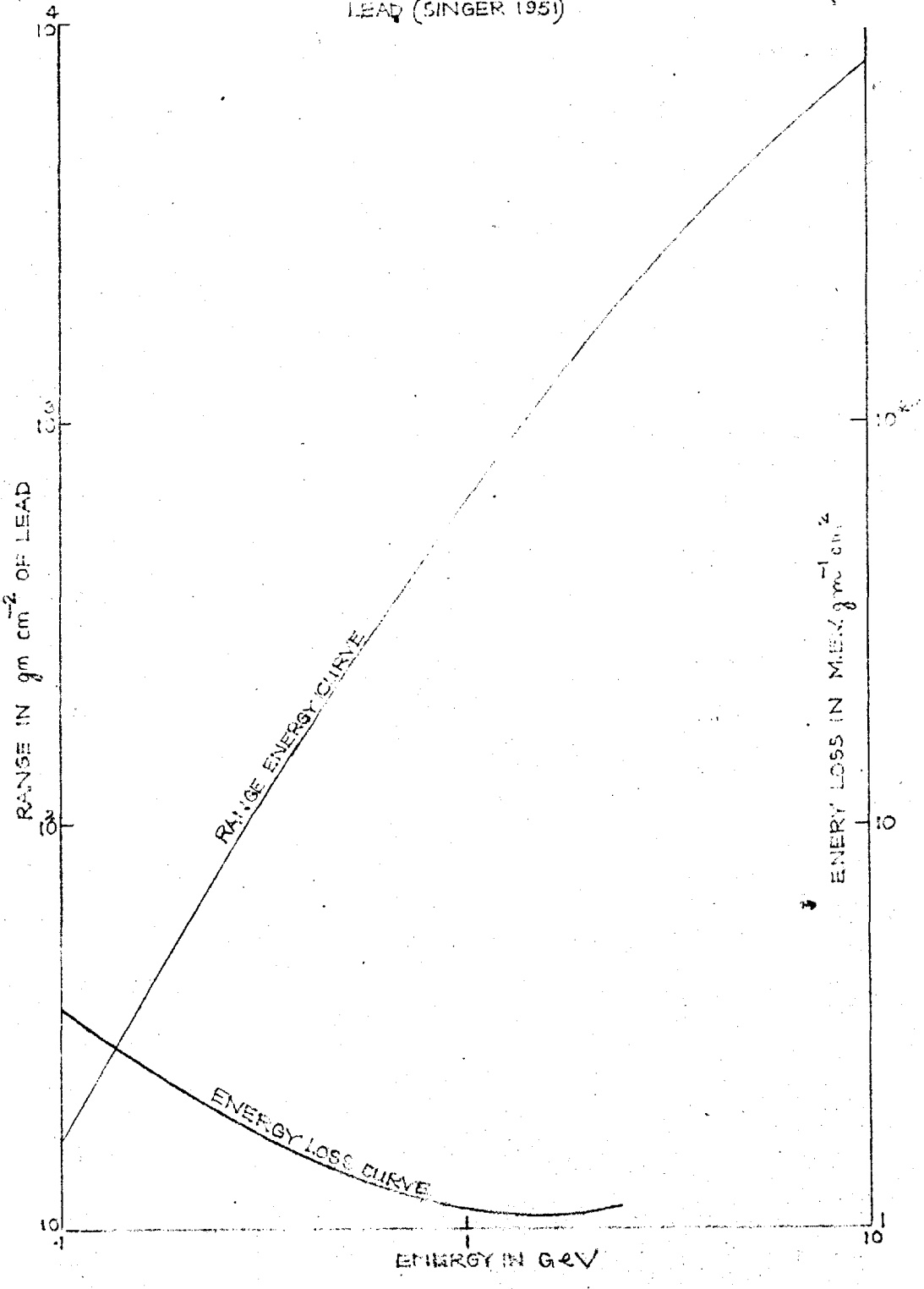
At first sight this would seem to be a very good method for determining γ, if the energy distributions above and below the absorber were known. However, the effect of varying γ, described above, applies equally well to variations of ψ and β, which are unknown factors for interactions in lead.

The neutron cascade can explain the observed increase in low energy nucleons if the values discussed in Section 3 are used. The effects of ionisation, discussed in the next section, will apply to a cascade with these initial constants.

5. Effect of Ionisation Loss on the Nucleon Cascade

At high energies the mesons and protons in the cascade suffer the same ionisation loss. For lower energies the protons predominate and so in the following calculations the charged component of the cascade will be treated as protons as regards ionisation loss, and the term protons will be understood to include charged mesons.

FIG. IV 3 RANGE ENERGY AND RATE OF ENERGY LOSS OF PROTONS IN LEAD (SINGER 1951)

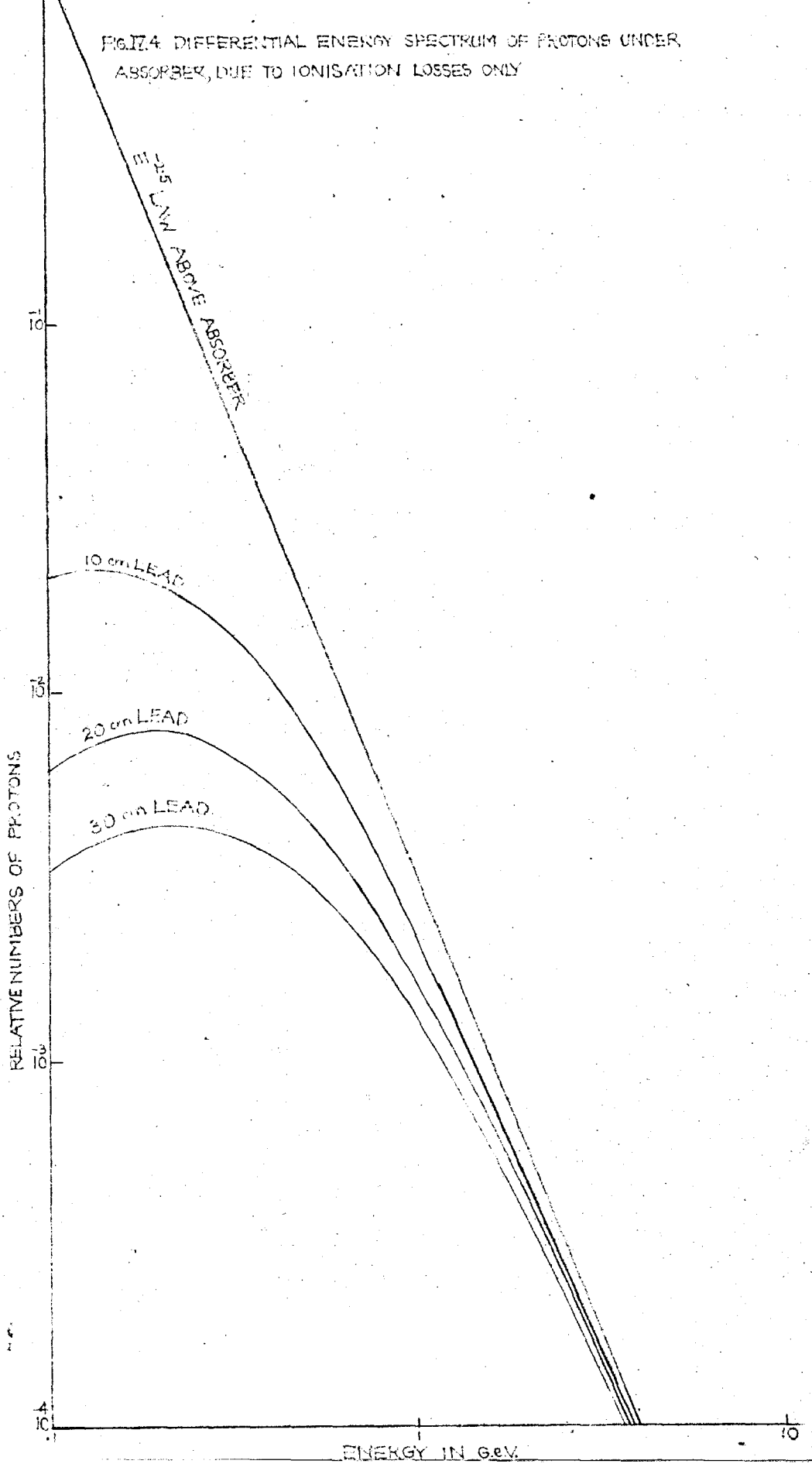


In correcting for ionisation losses, other authors (Thomson and Hodgson 1951, Messel 1950) have assumed constant ionisation loss for the charged component of the nucleon cascade. This is quite reasonable for energies greater than 1 GeV where a constant energy loss in lead of 1.15 MeV cm^2 gm^{-1} has been assumed. However, protons with an energy of 200 MeV have an ionisation loss of four times minimum, and hence for protons of energy less than 1 GeV range-energy curves in lead, calculated by Dr. S.F. Singer (1952), have been used.

The range-energy curves and energy loss curves are shown in Figure IV.3. It can be seen that only protons incident with energy greater than 650 MeV will emerge from an absorber 30 cm. (340 gm cm^{-2}) thick.

If the protons have a differential energy spectrum above the lead given by a power law with negative exponent $\gamma = 2.5$, than this spectrum is considerably modified by ionisation losses in the lead. The energy distributions of protons after penetrating 10 cm., 20 cm. and 30 cm. of lead are shown in Figure IV.4. The effect of the 30 cm. absorber is to give a maximum number of protons with energy of the order of 200 MeV. While the number of protons of this energy is effectively reduced by a factor of 40, this factor will only be 2 for protons of 1 GeV. It is clear that the ionisation causes a strong reduction in the low energy component of the protons, but this

FIG.17.4 DIFFERENTIAL ENERGY SPECTRUM OF PROTONS UNDER ABSORBER, DUE TO IONISATION LOSSES ONLY



effect decreases with increasing energy. The curve for 30 cm. lead shown in Figure IV.4 will apply to those protons passing through the lead without nuclear interaction.

It has been shown in Section 4 that only the first two stages of the cascade are effective for a cascade in 30 cm. lead. Ionisation corrections have been applied to each stage of the two-stage cascade, assuming firstly that equal numbers of neutrons and protons above 1 GeV in energy are incident on the absorber, and secondly that in each nuclear disintegration equal numbers of ionising and non-ionising particles are emitted. As a result of ionisation loss in the cascade, an emergent nucleon of energy E will be associated with an incident nucleon of higher energy than that given by the non-ionising cascade. Hence, for nucleons taking part in the cascade, ionisation loss tends to reduce the low energy component, but this is counteracted by the increase in low energy nucleons in the cascade process itself.

In applying ionisation corrections, the following cases are examined:

i. One-stage process

(a) neutrons produced by protons $(p, n)_i$

(b) protons produced by neutrons $(n, p)_i$

(c) protons produced by protons $(p, p)_i$

ii. Two-stage process

(a) neutrons produced by protons $(p,n)_{ii}$ } produced by higher energy nucleons

(b) protons produced by neutrons $(n,p)_{ii}$ } produced by higher energy nucleons

(c) protons produced by protons $(p,p)_{ii}$

(i) One-stage process

The term corresponding to a one-stage process, neglecting ionisation, can be obtained from equation IV(12), and it is equal to

$$N_o \, e^{-\alpha \frac{\alpha}{\beta} m} \, E^{-\gamma} \left(E/E_1\right)^{\gamma} \frac{E_1}{E} \, E_1^{\psi} \, dE \qquad \text{IV(14)}$$

where E_1 is equal to $(E/x)^{\frac{1}{\beta}}$

Relation IV(14) still stands for a one-stage process of neutrons produced by neutrons, but m is replaced by m', representing that portion of secondaries emitted as neutrons.

(a) neutrons produced by protons $(p,n)_i$

A proton interacting in a lead absorber and producing a neutron will lose energy by ionisation in traversing the distance (y cm.) from the top of the absorber to the interaction. If E_1 is the energy of the proton at the interaction, $E_1(y)$ will represent the initial energy at the top of the absorber. $E_1(y)$ can be obtained as a function of E_1 and y from the range-energy relations in Figure IV.3. For energies of E_1 above 1 GeV, $E_1(y) = E_1 + by$, where b is the minimum ionisation per unit distance. For an

absorber a cm. thick the term in the cascade corresponding to a (p,n) interaction is therefore equal to

$$N_o\, e^{-\alpha}\, \frac{\alpha m'}{\beta}\; E^{-\gamma}\; \frac{1}{a} \int_{y=0}^{a} \left\{E/E_1(y)\right\}^{\gamma}\; \frac{E_1}{E}\; E_1^{\psi}\, dE\; dy \qquad \text{IV(15)}$$

If E_1 is greater than 1 GeV, $E_1(y)$ can be replaced by $E_1 + by$, and IV(15) becomes

$$N_o\, e^{-\alpha}\, \frac{\alpha m'}{\beta}\; E^{-\gamma}\; \left(\frac{E}{(E_1 + ba/2)}\right)^{\gamma}\; \frac{E_1}{E}\; E_1^{\psi}\, dE \qquad \text{IV(16)}$$

neglecting terms of the order of $(\frac{ab}{E_1})^2$ compared with unity. For a 30 cm. lead thickness ab = 400 MeV.

(b) protons produced by neutrons $(n,p)_i$

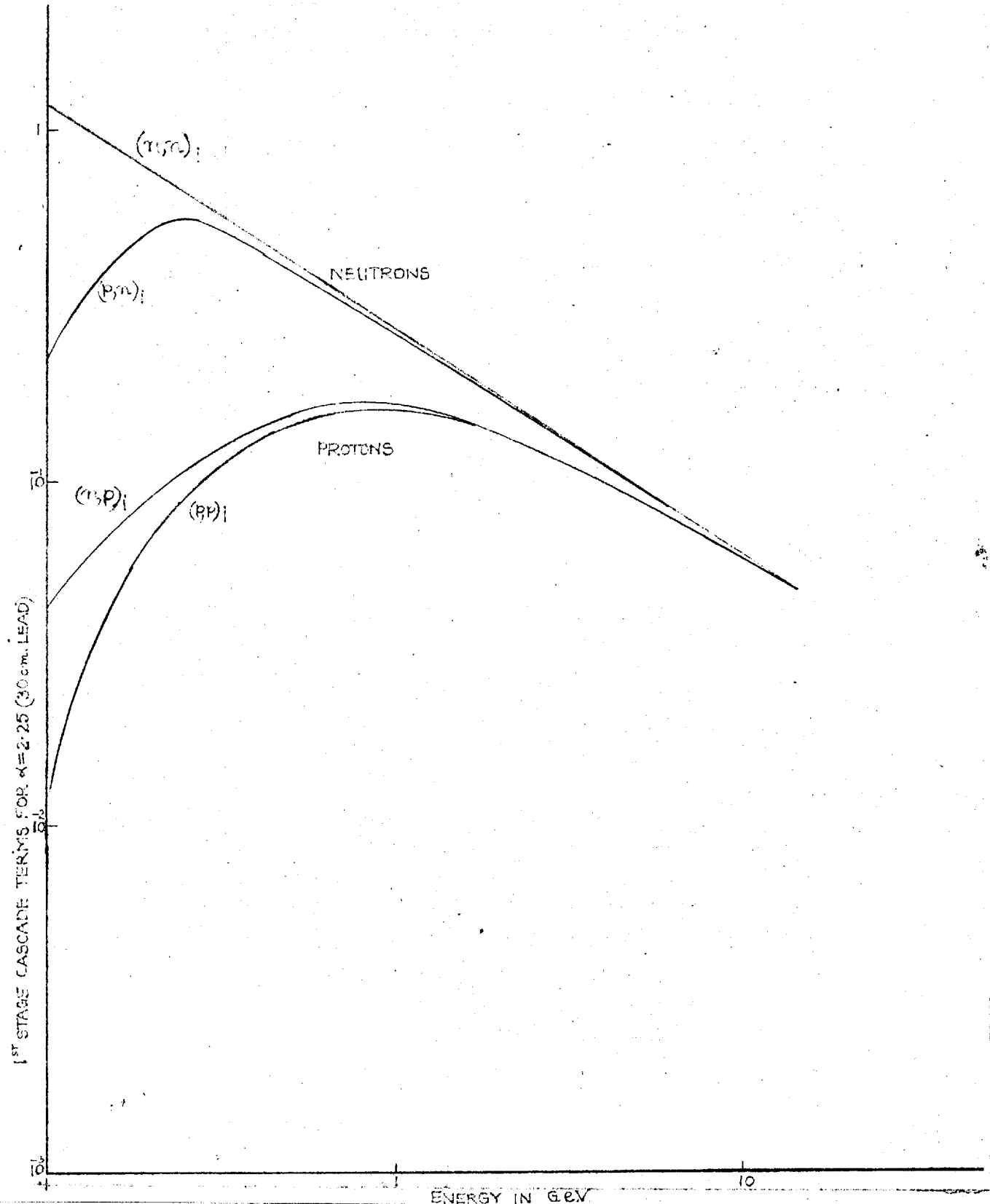
Protons produced by neutrons, and emerging from the absorber with energy E, will have been produced with energy E(z), where z is the distance from the bottom of the absorber. Owing to the varying ionisation loss for protons under 1 GeV, the term dE is replaced by $\frac{dE(z)}{dE}\, dE$, and the term in the cascade corresponding to a $(n,p)_i$ interaction is equal to

$$N_o\, e^{-\alpha}\, \frac{\alpha m'}{\beta}\; E^{-\gamma}\; \frac{1}{a} \int_{z=0}^{a} \left(\frac{E}{E(z)_1}\right)^{\gamma}\; \frac{E(z)_1}{E(z)}\; E(z)_1^{\psi}$$

$$\frac{dE(z)}{dE}\, dE\, dz \qquad \text{IV(17)}$$

For proton energies greater than 1 GeV (E > 1 GeV),

FIG. IV 5 1ST STAGE CASCADE TERMS, WITH IONISATION LOSS



expression IV(17) can be written as

$$N_o\, e^{-\alpha}\, \frac{\alpha m'}{\beta}\; E^{-\gamma} \left\{\frac{E}{\left((E+\frac{ab}{2})_1\right)}\right\}^{\gamma} \frac{(E+\frac{ab}{2})_1}{E+\frac{ab}{2}}\; (E+\tfrac{ab}{2})_1^{\psi} \qquad \text{IV(18)}$$

neglecting terms of the order of $(\frac{ab}{E})^2$ compared with unity.

(c) protons produced by protons $(p,p)_i$

This is a very similar process to (b), but in addition a parent proton suffers ionisation loss before the interaction. The term in the cascade corresponding to a (p,p) interaction is equal to

$$N_o\, e^{-\alpha}\, \frac{\alpha m'}{\beta}\; E^{-\gamma}\; \frac{1}{a} \int_{z=0}^{a} \left\{\frac{E}{E(z)_1 + b(a-z)}\right\}^{\gamma}$$

$$\frac{E(z)_1}{E(z)}\; E(z)_1^{\psi}\; \frac{dE(z)}{dE}\; dE\, dz \qquad \text{IV(19)}$$

For proton energies greater than 1 GeV, expression IV(19) can be written as

$$N_o\, e^{-\alpha}\, \frac{\alpha m'}{\beta}\; E^{-\gamma} \left\{\frac{E}{(E+\frac{ab}{2})_1 + \frac{ab}{2}}\right\}^{\gamma} \frac{(E+\frac{ab}{2})_1}{E+\frac{ab}{2}}\; (E+\tfrac{ab}{2})_1^{\psi} \qquad \text{IV(20)}$$

The expressions IV(14) to IV(20) were evaluated up to nucleon energies of 10 GeV and the results are shown in Figure IV.5. The reduction in low energy nucleons caused by ionisation is clearly shown.

(ii) Two-stage process

In a similar manner as described in (i) ionisation corrections have been applied to a two-stage cascade process. For the simplest case of neutrons produced by neutrons the term corresponding to a two-stage cascade is equal to

$$N_o\, E^{-\gamma}\, \exp(-\alpha)\, dE\, \left(\frac{E}{E_2}\right)^{\gamma}\, \frac{m^2\alpha^2}{\beta^2\, 2}\, \frac{E_2}{E}\, E_1^{\psi}\, E_2^{\psi} \qquad \text{IV(21)}$$

where $E_1 = \left(\frac{E}{x}\right)^{\frac{1}{\beta}}$ $\qquad$ $E_2 = \left(\frac{E_1}{x}\right)^{\frac{1}{\beta}}$

(a) neutrons produced by protons $(p,n)_{ii}$ produced by "primary" nucleons. The term corresponding to a $(p,n)_{ii}$ interaction is equal to

$$N_o\, E^{-\gamma}\, \exp(-\alpha)\, \frac{m^2\alpha^2}{2\beta^2}\, \left(\frac{E}{E_2}\right)^{\gamma}\, \frac{E_2}{E(y)}\, \frac{E_1}{E}\, E_1^{\psi}(y)\, E_2^{\psi}\, dE \qquad \text{IV(22)}$$

where $E_1(y) = \left(\frac{E}{x}\right)^{\frac{1}{\beta}} * \frac{ba}{2}$ $\qquad$ $E_2 = \left(\frac{E_1}{x}\right)^{\frac{1}{\beta}}$

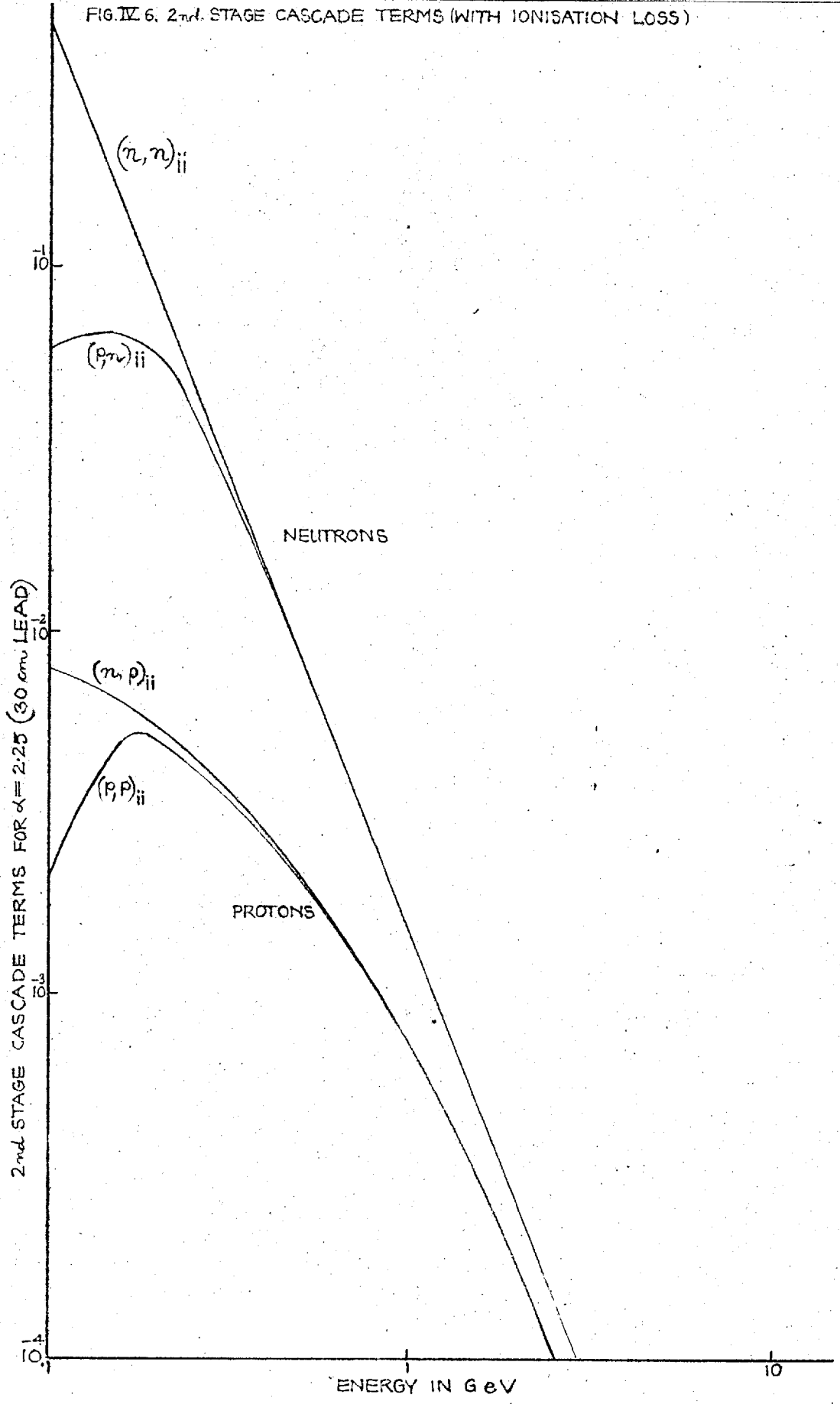
(b) protons produced by neutrons $(n,p)_{ii}$ produced by "primary" nucleons. The term corresponding to a $(n,p)_{ii}$ interaction is equal to

$$N_o\, E^{-\gamma}\, \exp(-\alpha)\, \frac{m^2\alpha^2}{2\beta^2}\, \frac{1}{a} \int_o^a \left(\frac{E}{E_2(y)}\right)^{\gamma} E_1^{\psi}(y)\, \frac{E_2}{E(y)}$$

$$E_2^{\psi}(y)\, \frac{dE(y)}{dE}\, dE\, dy \qquad \text{IV(23)}$$

where $E(y)$ is the energy corresponding to E due to

FIG. IV. 6. 2nd. STAGE CASCADE TERMS (WITH IONISATION LOSS)



ionisation loss in y g cm.$^{-2}$

where $E_1(y) = (\frac{E(y)}{x})^{\frac{1}{\beta}}$ $E_2(y) = (\frac{E_1(y)}{x})^{\frac{1}{\beta}}$

(c) protons produced by protons $(p,p)_{ii}$ produced by "primary" nucleons. The term corresponding to a $(p,p)_{ii}$ interaction is equal to

$$N_o E^{-\gamma} \exp(-\alpha) \frac{m^2\alpha^2}{2\beta^2} \frac{1}{a} \int_o^a \left(\frac{E}{E_2(y) + by}\right)^{\gamma} \frac{dE(y)}{dE}$$

$$\frac{E_2(y)}{E_1(y)+\frac{ab}{2}} \frac{E_1(y)}{E(y)} E_1^{\psi}(y) E_2^{\psi}(y) \, dE \, dy \qquad \text{IV(24)}$$

For higher energies relations (b) and (c) both become

$$N_o E^{-\gamma} \exp(-\alpha) \frac{m^2\alpha^2}{2\beta^2} \left(\frac{E}{E_2}\right)^{\gamma} \frac{E_2}{E + \frac{ab}{2}} E_1^{\psi} E_2^{\psi} \qquad \text{IV(25)}$$

where $E_1 = (\frac{E + \frac{ab}{2}}{x})^{\frac{1}{\beta}}$ $E_2 = (\frac{E_1}{x})^{\frac{1}{\beta}}$

The expressions IV(21) to IV(25) were evaluated for values of E up to 10 GeV and the results are shown in Figure IV.6. The effect of ionisation is very similar to that for the 1st stage cascade.

The energy distributions of the neutrons under the absorber is simply obtained by adding the total cascade terms to the constant factor 1 and multiplying by the geometric attenuation:

FIG. IV.7 TOTAL CASCADE TERMS FOR 30 cm OF LEAD
(WITH IONISATION LOSS)

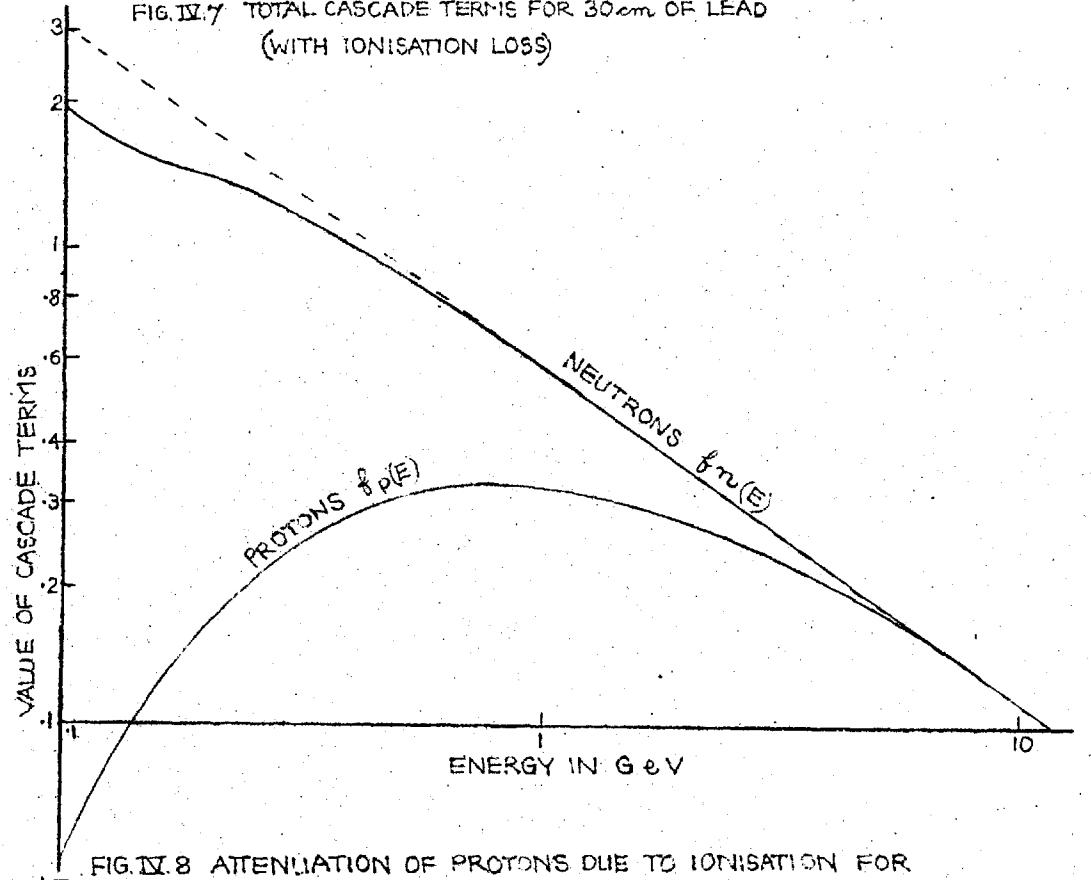


FIG. IV.8 ATTENUATION OF PROTONS DUE TO IONISATION FOR DIFFERENT THICKNESSES OF LEAD

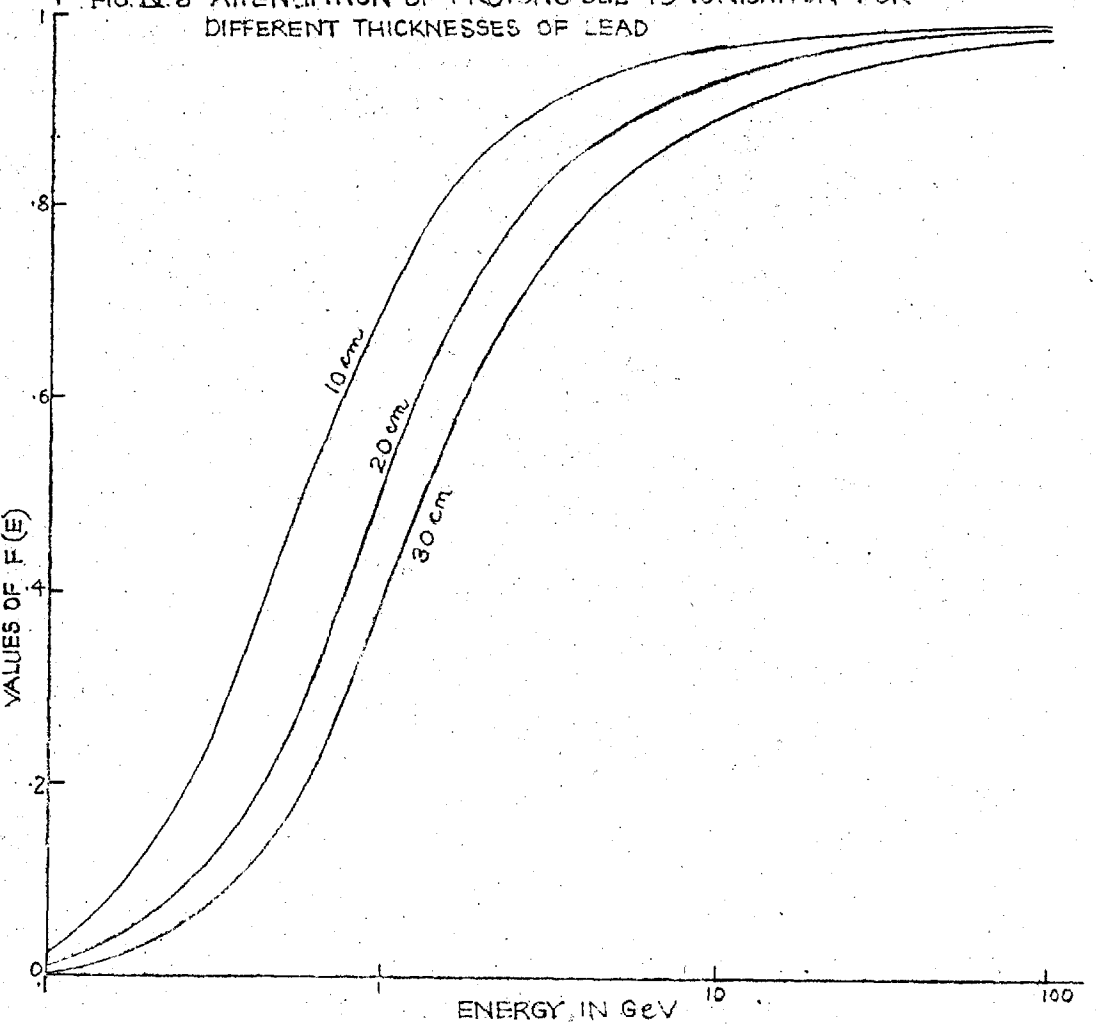
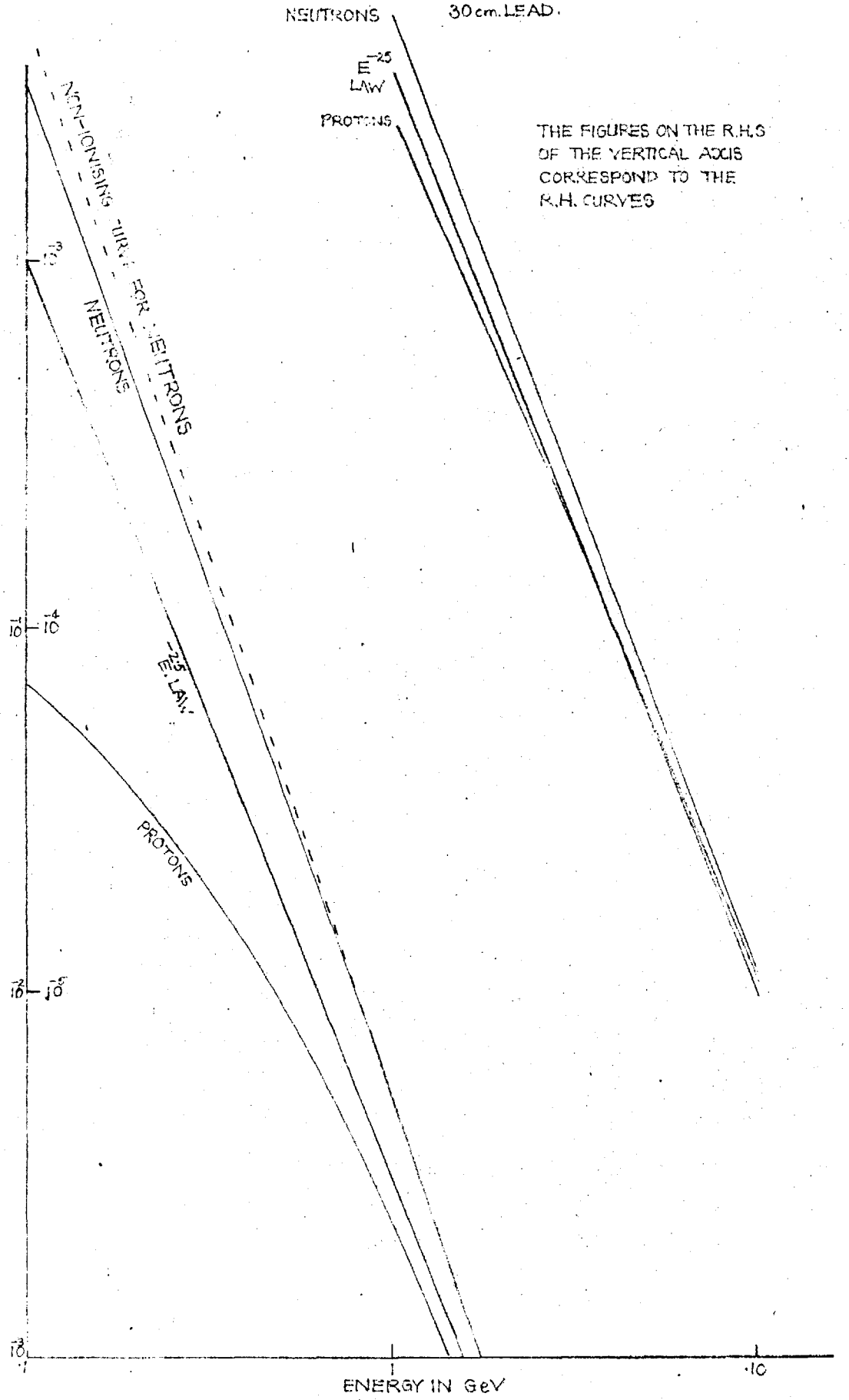


FIG. IV 9 ENERGY DISTRIBUTION OF NEUTRONS AND PROTONS UNDER 30 cm. LEAD.



that is

$$N_n(E)\,dE = N_o\,E^{-\gamma}\,\exp(-\alpha)\,dE\{1 + f_n(E)\} \qquad \text{IV(26)}$$

where $f_n(E)$ is the sum of the 1st and 2nd stage cascade terms for neutrons. This total cascade term is shown in figure IV.7, together with the corresponding term $f_p(E)$ for protons.

However, the energy distribution of the protons is not quite analogous to that of the neutrons. It is actually given by

$$N_p(E)\,dE = N_o\,E^{-\gamma}\,\exp(-\alpha)\,dE\{F(E) + f_p(E)\} \qquad \text{IV(27)}$$

where the F(E) term represents the additional attenuation of the original protons due to ionisation loss only. This F(E) term is shown in Figure IV.8, and reduces the proton component for energies less than 10 GeV.

Using relations IV(26) and IV(27) the energy distributions can be determined.

The resulting energy distributions of neutrons and protons under 30 cm. of lead are shown in Figure IV.9 and can be compared with that obtained from the simple cascade developed in Section 2. It can be seen that the number of low energy neutrons is still always greater than that given by an $E^{-2.5}$ law, while the converse is true for protons below 3 GeV.

As the neutrons above the absorber have an E-2.5 law

distribution of energy above the absorber, it is evident that there is a relative increase in the number of low energy neutrons. However, ionisation loss in the atmosphere will cause a similar reduction in low energy protons as that effected in the lead absorber, and it is not obvious whether there is an increase or decrease in low energy protons. In the next section the cascade results are interpreted in terms of star-size distributions in nuclear emulsions, and a direct comparison with the observed star-size distributions is possible.

6. Size Distribution of Stars caused by Nucleons formed in the Cascade

The size of stars formed in nuclear emulsions is defined by the number of "heavy tracks", that is, by the number of tracks with a grain density greater than 1.5 minimum. In general, the more energetic the incident particle, the greater is the size of the star. However, investigation of disintegrations produced by monoenergetic beams of particles of known energy from cyclotrons (Bernadini, Booth and Lindenbaum 1952; Germain 1951; and Titterton 1951) showed that particles of the same energy produce stars with a distribution of sizes. Messel (1951) and Barford (1951) have developed cascade theories within the nucleus which lead to a distribution in the number of nucleons emitted. Hence a star of a given size can have

been formed by nucleons in a wide energy range. For a given energy distribution of primaries, however, the resulting size distribution of stars can be calculated, if the following functions are known:

(a) The variation of the cross-section for star production with energy.

(b) The relation between the incident particle energy E and the mean size m of the resulting stars.

(c) The distribution in size of stars formed by primaries of energy E about the mean size m.

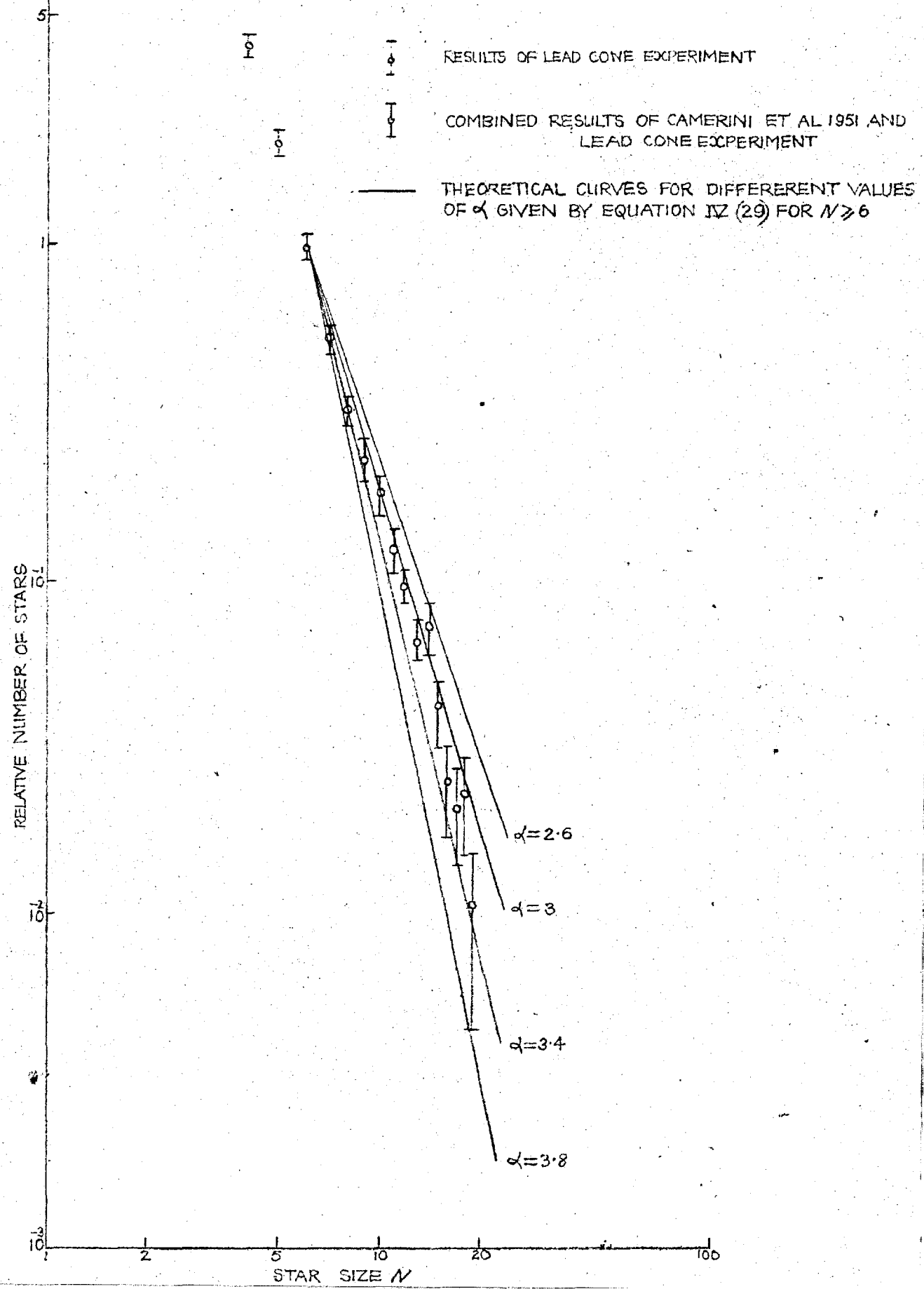
All these functions are averaged over all the elements in the photographic emulsion, and it is assumed that they are independent of the nature of the primary particle, depending only on its energy.

In the following analysis the rather drastic assumption of constant cross-section for star production is made. This will overestimate the numbers of stars produced by particles in the energy region 400 MeV, as the cross-section passes through a minimum in this region (De Juren 1951). As discussed in Section 3, this will tend to compensate for the overestimated attenuation of these low energy nucleons in the lead absorber. Over the whole energy range considered, the cross-section does not vary by more than a factor of 2.

Hodgson (1952) has considered this problem of

star-size distribution in detail, and he found that the distribution in size of stars formed by primaries of a given energy could be represented by a Poisson distribution. This has also been used by other investigators (Clementel and Puppi 1949; Yamaguchi 1949). The size distributions observed by Germain (1951) and Titterton (1951) for stars produced by monoenergetic beams of particles agree quite well with a Poisson distribution. Using the results of Barton et al. (1951), Hodgson assumed that the differential distribution of energies released in stars (excluding particles of "shower" particle energy) can be expressed as an inverse power law, with exponent 2.5. Using this, he derived the best relationship between star-energy and mean star-size, which gives the experimental star-size distribution at the Jungfraujoch (Barford and Davis 1952). This relationship can be expressed as $E = 1.4\ (37\ m + 4\ m^2)$, where the term in brackets is the result obtained by Brown et al. (1949) for the mean energy of stars of size m. In obtaining agreement with experiment, he found it necessary to assume a lower cut off energy of about 50 MeV in the primary spectrum, corresponding to a mean star-size of m = 1. This cut off, however, only affects stars of 3 or 4 tracks.

If the energy distribution of primaries is equal to $f(E)\ dE$, and the primary-energy mean star-size relation is given by $E = \varphi\ (m)$, then the relative size distributions


RESULTS OF LEAD CONE EXPERIMENT
COMBINED RESULTS OF CAMERINI ET AL 1951 AND LEAD CONE EXPERIMENT
THEORETICAL CURVES FOR DIFFERERENT VALUES OF α GIVEN BY EQUATION IV (29) FOR N ≥ 6
RELATIVE NUMBER OF STARS
STAR SIZE N
α=2·6
α=3
α=3·4
α=3·8
5
1
1/10
1/10²
1/10³
1
2
5
10
20
100

of the stars formed in photographic emulsions is given by

$$S(N) = \int_{m_o}^{\infty} \frac{m^N}{N!} e^{-m} f\{\varphi(m)\} \frac{dE}{dm} dm \qquad \text{IV(28)}$$

The first factor on the R.H.S. of the above equation represents the probability that a primary, producing stars with a mean star-size m, will produce a star with actual size N. The middle factor in brackets gives the number of primaries in the energy range E to E+dE, corresponding to mean size m to m+dm. If both the functions f(E) and φ (m) can be represented by power laws, where f(E) equals $E^{-\gamma}$, and φ (m) equals cm^a, then substituting these values, equation IV(28) becomes

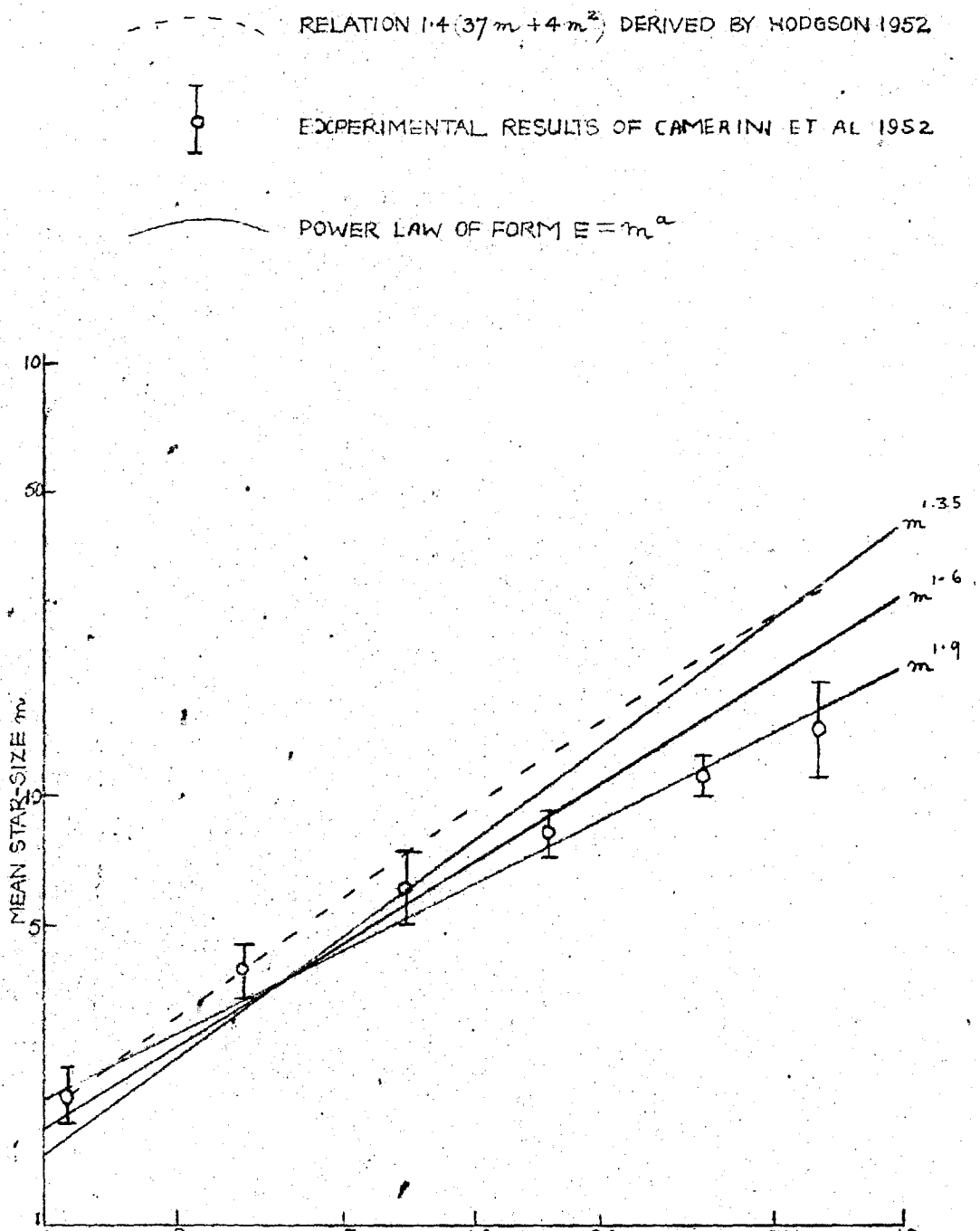
$$S(N) = c^{1-\gamma} a \frac{1}{N!} \int_{m_o}^{\infty} e^{-m} m^{N-\alpha} dm \qquad \text{IV(29)}$$

where $\alpha = (\gamma - 1) a + 1$ IV(30)

The cut off m_o does not affect the integral for values of N greater than 5, if α is not greater than 3. The integral in equation IV(29) is now equal to the complete gamma function $\Gamma (N - \alpha + 1)$ for $N > 5$.

The relative star-size distribution for stars with more than 6 tracks is thus proportional to $\frac{1}{N!} \Gamma (N - \alpha + 1)$. These distributions are shown for various values of α in Figure IV.10, and may be compared with the observed star-size distribution at the Jungfraujoch. The latter curve

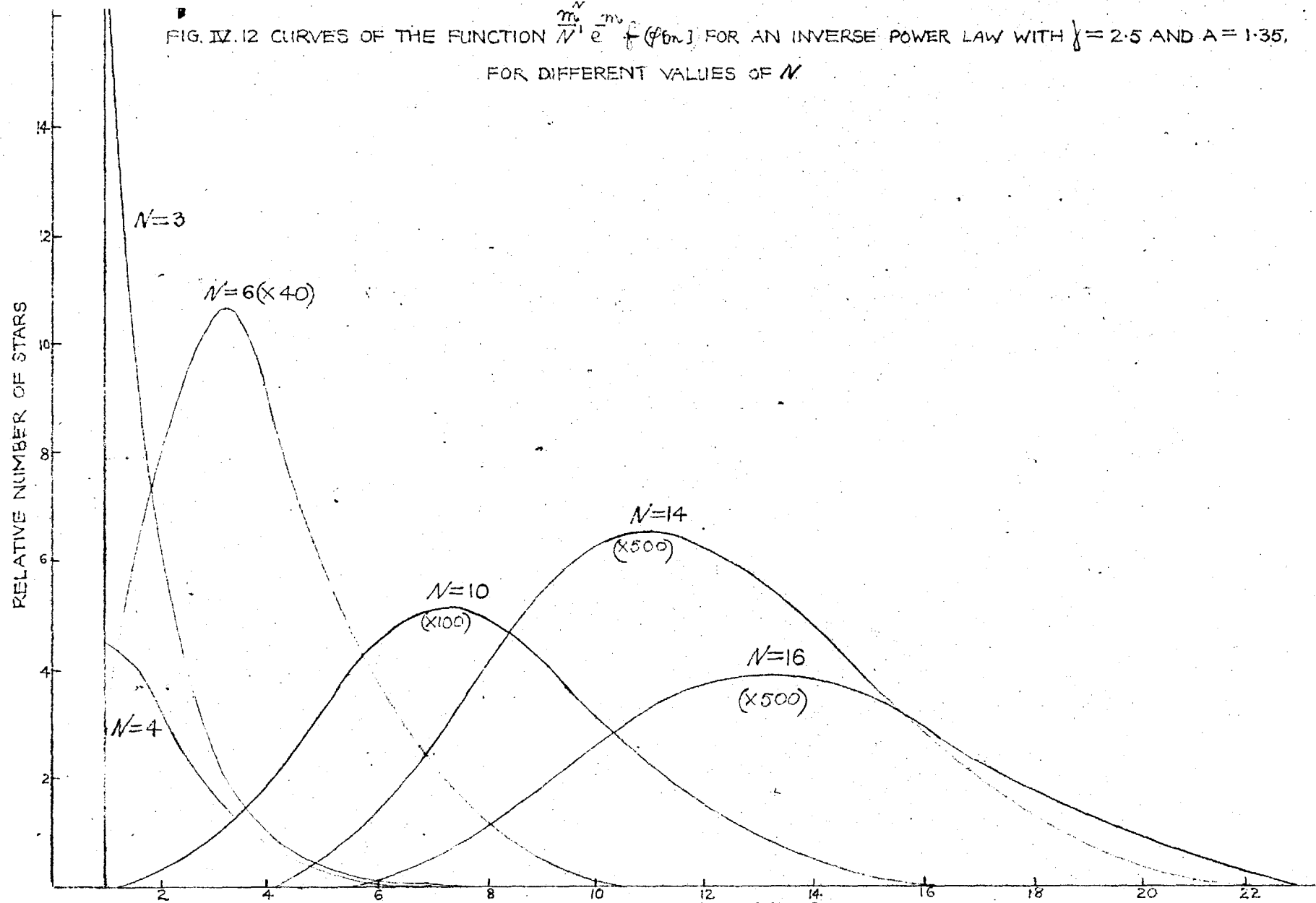
FIG IV. 11. MEAN STAR-SIZE AS A FUNCTION OF PRIMARY ENERGY



was obtained using the results of Part II for stars with 5 or less tracks, and the combined results of Brown et al. (1949) and Part II are used for stars with more than 5 tracks. The values of α giving best agreement with experiment are given by $\alpha = 3 \pm 0.4$. If the exponent of the inverse power law equals 2.5, this means that the best value of the exponent a, in the mean star-size against primary energy relation, is equal to 1.35 ± 0.2.

However, this relation has been derived experimentally by Camerini et al. (1951). Their results are shown in Figure IV.11, and the relation between mean star-size and primary energy can be expressed as $E \propto m^{1.9}$ for the energy region between 0.1 and 5 GeV. It can be seen that the curve given by $a = 1.35$ is not in agreement with the experiment results for large stars. However, if the value of a is increased to 1.9, to conform with the experimental results, then in order to obtain the observed star distribution above the absorber, γ has to be changed to 2.1 ± 2. This is in contrast with the value of 2.5 assumed in setting up the nucleon cascade. It is interesting to note that Messel (1951) also found indications that the power law should have an exponent 2.1 instead of 2.7, the value which he had assumed. As explained in Section 4, if this change is made in γ, the whole cascade will be altered, as long as the values for the other constants are left unchanged.

FIG. IV. 12 CURVES OF THE FUNCTION $\frac{m_1^N}{N!} e^{-m_1} f(\varphi_{0n})$ FOR AN INVERSE POWER LAW WITH $\gamma = 2.5$ AND $A = 1.35$, FOR DIFFERENT VALUES OF N



However, by slightly varying the other parameters ψ and β, the values of which are quite unknown for interactions in lead, a good fit with the experimental results could be obtained, with the new value of γ of 2.1.

Since in the cascade process γ was taken as 2.5, in order to obtain the observed size distribution of "n" stars above the absorber, a star-size relation of the form $E = 0.3\ m^{1.35}$ was taken. This was then used in determining the size distribution under the absorber.

In calculating the star-size distributions under 30 cm. of lead, the integral in equation IV(28) has been evaluated for neutrons and protons at each stage of the cascade. A cut off energy corresponding to m = 1 was taken. Typical curves for this integral are shown in Figure IV.12 for incident nucleons with an $E^{-2.5}$ differential energy spectrum. It is apparent that the cut off is effective only for stars with less than 6 tracks. Each of the curves in Figure IV.12 shows the contributions of nucleons of various energies (corresponding to mean star-size m) to a star of size N. It can be seen that the maximum on a curve N corresponds to a mean star-size less than N. This means that the average energy of nucleons producing stars of a given size N is less than the nucleon energy corresponding to a mean size N, as was pointed out by Hodgson.

FIG IV. 13. STAR SIZE DISTRIBUTIONS UNDER 30 cm LEAD

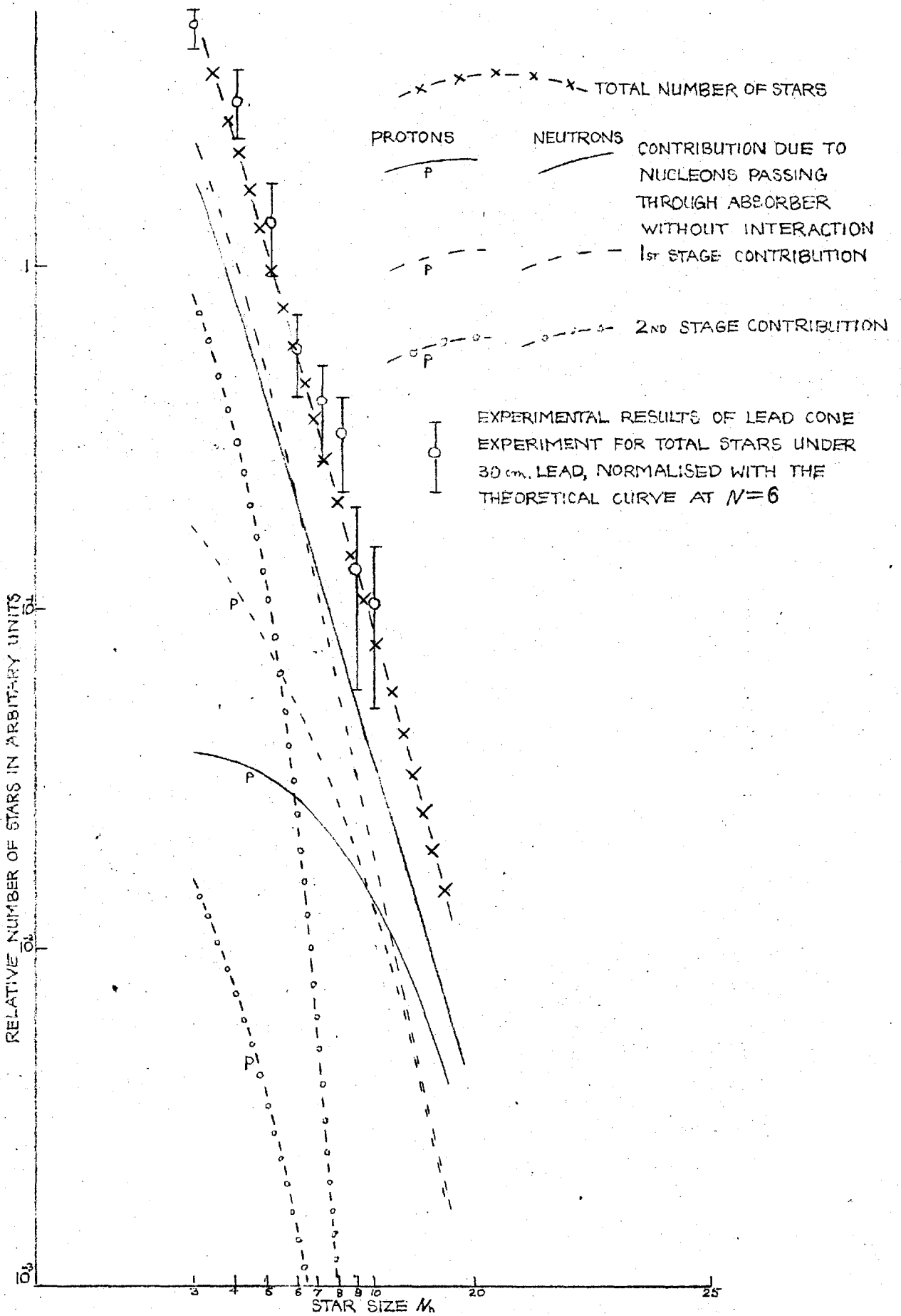
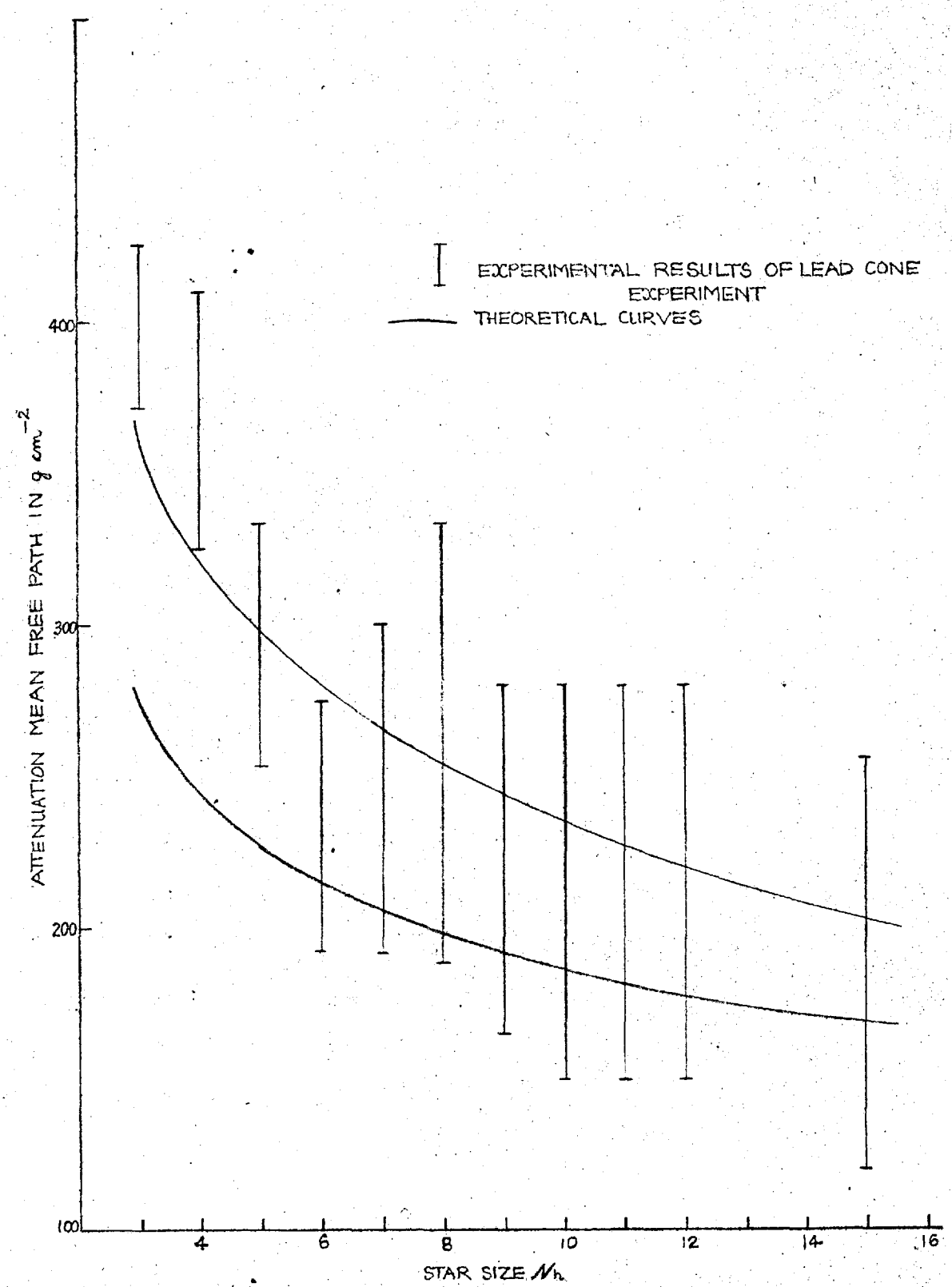


FIG. IV. 14. ATTENUATION MEAN FREE PATH GIVEN BY CASCADE THEORY

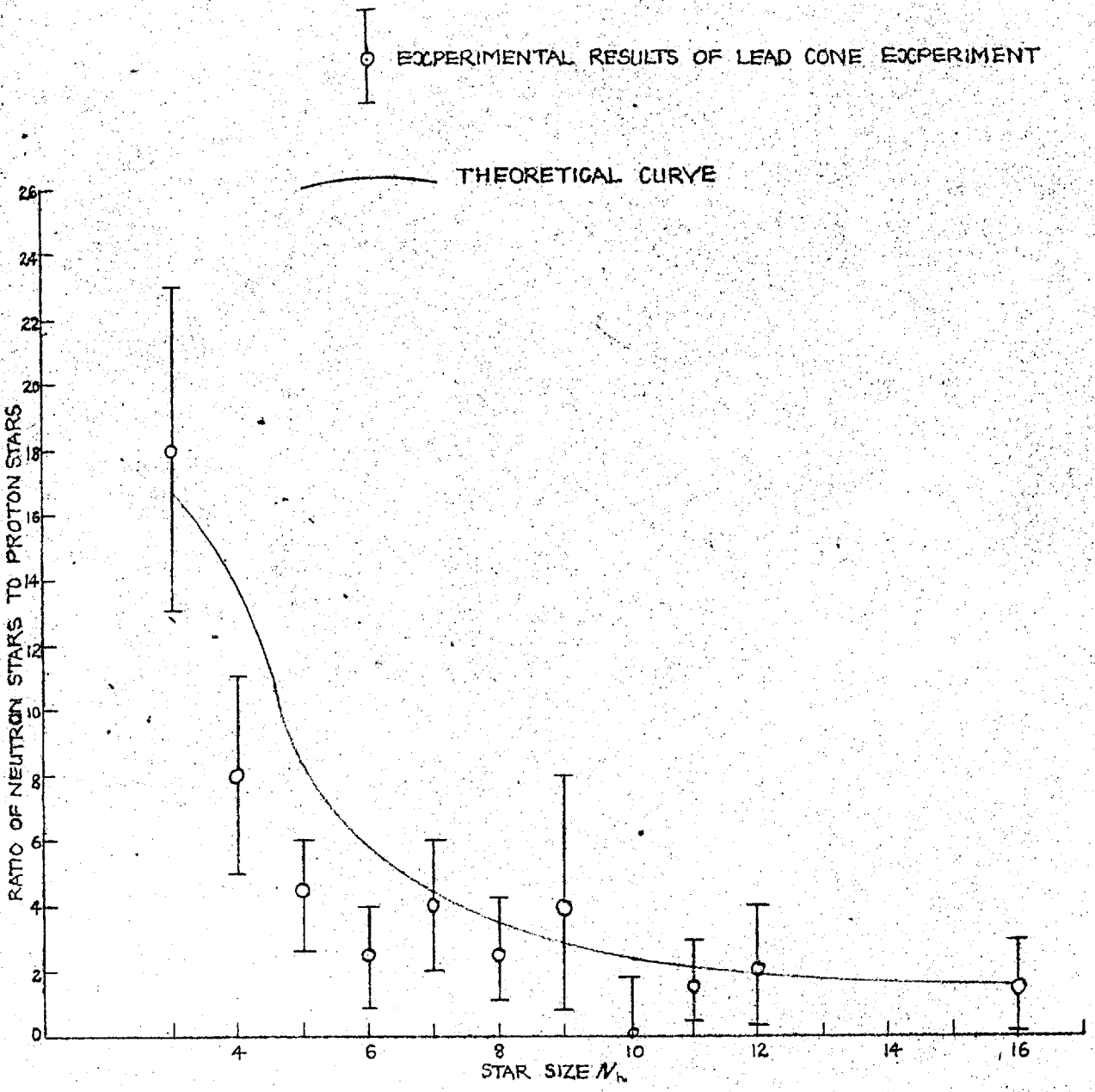


7. Comparison of the Results of the Theory with Experiment

The star-size distributions under absorber are shown in Figure IV.13, and the separate contributions due to neutrons and protons at each stage of the cascade are given. The relative size distribution for all the stars agrees quite well with the results of Part II of this thesis and the results are normalised to fit the theoretical curve at N = 6.

It is possible to calculate the attenuation mean free path for radiation producing stars of different sizes. This is shown in Figure IV.14 for neutron stars, and can be compared with the corresponding results of the lead cone experiment. The theoretical curve shows the same qualitative features as the experimental results but does seem to be rather low. This suggests that the assumed geometrical mean free path for interaction of 150 gm cm.$^{-2}$ may be too low. In calculating the geometric cross-section of the lead nucleus the nuclear radius was taken as $r_A = 1.45\ A^{1/3}\ 10^{-13}$ cm. However, the uncertainty in the value of the constant 1.45 is about 10%, and this leads to an uncertainty of some 20% in the mean free path. To explain the discrepancy between the theoretical curve and the experimental results, one could take the interaction mean free path as 180 gm cm.$^{-2}$. This reduces the cascade component, but at the same time increases the

FIG. IV 15. RATIO OF NEUTRON STARS TO PROTON STARS UNDER 30 cm LEAD



number of nucleons penetrating the absorber. The resulting attenuation length of neutron stars is also shown in Figure IV.14, and it is clear that this is a better fit for the experimental results.

The ratio of neutron to proton stars under lead has been calculated and is shown in Figure IV.15. Owing to the criterion for minimum tracks (being less than 1.5 minimum grain density) only protons having more than 330 MeV energy will be recognised as causing p stars. Hence, many p stars with less than 5 tracks will be regarded as n stars in the lead cone analysis. The comparison between neutron and proton stars can therefore only apply to stars with more than 6 tracks.

8. Discussion of Cascade Theory

It is not claimed that the cascade model developed in this thesis gives more than an approximate description of the nucleon cascade in lead. Indeed, the mathematical methods applied here were necessarily simple to permit rather general assumptions as to the average numbers and energies of secondary particles in the basic nucleon-nucleus interaction. It was assumed in the non-ionising model that all the secondary particles had the same energy. However, the statistical fluctuations in energies and numbers of these secondary particles will undoubtedly have a considerable effect on the properties of the cascade in

lead and could lead to different quantitative results from the simple picture developed in Section 2 of Part IV.

The highly efficient mathematical techniques of Messel and his collaborators are more suitable for tackling the cascade problem, not only as regards fluctuations in numbers and energies of the emergent nucleons, but also in the three dimensional properties of the cascade.

However, it must be pointed out that the refined cascade treatment developed by Messel can only be applied to problems which assume a homogeneous form of the basic nucleon-nucleon cross-section. That is where the cross-section for production of 2 nucleon energies E_1 and E_2 by a primary of energy E is given by a function of the form $f(\frac{E_1}{E}\ \frac{E_2}{E})\ \frac{dE_1 dE_2}{E^2}$. For a non-homogeneous form of the cross-section the general differential equations for the cascade would be extremely difficult to solve. It was shown in Part IV, Section 4 that given such a homogeneous cross-section, a power law spectrum of nucleons will remain as a power law with the same exponent at all thicknesses of the absorber. If the continuous change in attenuation length with star size, reported in Part III, is a real effect, it could indicate a departure from the homogeneous cross-section.

Although this decrease in attenuation mean free path could have been due to statistical fluctuations, the cascade model developed here can give a qualitative

description of this increase for certain values of the basic parameters. The fact that the original values assumed for these parameters actually showed a general decrease in attenuation mean free path with increasing energy cannot be taken to prove its existence, as very slight changes in any of the basic parameters can cause the entire aspect of the cascade to change.

With the original values of the parameters the theory shows that the attenuation mean free path of the nucleons should decrease with increasing energy, tending towards the collision mean free path. If one accepts the theory quantitatively, then the experimental results for the attenuation mean free path could indicate an interaction mean free path in lead some 1.25 times the accepted geometric value of 150 gm cm^{-2}. In view of the many simplifying assumptions in the theory no attempt has been made to find the set of parameters giving the best fit with experiment.

The analysis of star-size distribution, shown in Section 6, does seem to show that the different energy spectra of the star-producing radiation at the Jungfraujoch is represented by an $E^{-2.1\pm0.2}$ law instead of the previously reported $E^{-2.5}$ law.

SUMMARY OF CONCLUSIONS

Part I

The general features of the expected spatial distribution of stars have been discussed in some detail. It was shown that the main contribution to an excess of close star pairs would be by a regenerative nucleon or cascade process which produces an excess of the order of 10^{-3} star pairs per star for separations up to 1500μ. This compares with the value of 2.10^{-2} reported by Li (1950). The data used by Li have been carefully examined and it was found that the excess was mainly due to small stars, which were subject to rather inefficient searching. On re-searching a portion of these plates rather more efficiently, the excess tended to disappear, and it is concluded that no real evidence exists for an excess as large as that reported by Li.

In tackling statistical problems of this nature using the nuclear emulsion technique, very great care must be taken to achieve really efficient scanning of the emulsions. Anomalous results introduced by inefficient scanning could certainly be of the same order as the expected excess of star-pairs.

Parts II, III and IV

The angular distribution of the ionising component of the star-producing radiation is found to follow a

$\cos^{5+1}\theta$ zenith angle distribution law. The corresponding distribution for the total star-producing radiation depends on the nature of the cascade process in the lead absorbers. However, it is certainly more collimated than a $\cos^2\theta$ steradian^{-1} distribution and may be of the form $\cos^4\theta$ steradian^{-1} for the high energy component.

The efficiency for finding small stars is higher than that achieved by earlier observers. The rate of production of all stars with 3 or more heavy prongs is 17.0 ± 0.4 cm^{-3} day^{-1} for emulsions exposed at the Jungfraujooh.

The attenuation mean free path in lead for the total star-producing component is equal to 330 ± 15 g cm^{-2}, in reasonable agreement with the results of other observers. There is a definite increase in the proportion of small stars under lead, the attenuation length of the radiation producing 3- and 4-track stars being 370 ± 30 g cm^{-2}. In addition, there are some indications that the attenuation mean free path continues to decrease with increasing star size to a value of 210 ± 70 g cm^{-2} for stars with 13 or more tracks. However, the statistics are rather poor and the continued decrease could be due to statistical fluctuations in the small numbers of stars involved. The cascade model developed in this thesis can show this effect of an increase of the attenuation mean free path with increasing energy for certain values of the basic parameters. Under these conditions the attenuation length

actually tends to the interaction length at high energies. The energy distribution of star-producing nucleons has been expressed in terms of an equivalent star-size distribution and it is shown that the differential energy distribution of the star-producing component at the Jungfraujoch is represented by an $E^{-2.1\pm0.2}$ law.

REFERENCES

Addario, M. and Tamburino, S. 1949 Phys. Rev. 76, 983.
.. .. 1950 Phys. Rev. 80, 749.
Alfvén, H. 1949 Phys. Rev. 75, 1732.
.. 1950 Phys. Rev. 77, 375.
Barbanti, Silva, L., Bonacini, C., Depietri, C., Lovero, G., Fedeli, and Perilli, E. 1952 Nuovo Cimento 9, 630.
Barbour. 1951 Phys. Rev. 82, 280.
Barford, N.C. 1951 Private communication.
Barford, N.C. and Davis, G. 1952 Proc. Roy. Soc. A, 214, 225.
Barton, J.C., George, E.P. and Jason, A.C. 1951 Proc. Phys. Soc. A, 64, 175.
Bernardini, G., Booth, E.T. and Lindenbaum, S.J. 1950 Phys. Rev. 80, 905.
.. .. .. 1952 Phys. Rev. 85, 826.
Bernardini, G., Cortini, G. and Manfredini, A. 1949 Nuovo Cimento 6, 431.
Bierens de Haan, D. 1858 Tables D'Intégrales Définies.
Bierman, L. and Schlüter, A. 1951 Phys. Rev. 82, 863.
Boehmer, H.W. and Bridge, H.S. 1952 Phys. Rev. 85, 863.
Bridge, H.S., Hazen, W.E., Rossi, B. and Williams, R.W. 1948 Phys. Rev. 74, 1083.
Brown, H. 1949 Phys. Rev. 21, 625.
Brown, R.H., Camerini, U., Fowler, P.H., Heitler, H., King, D.T. and Powell, C.F. 1949 Phil. Mag. 40, 862.
Camerini, U., Davies, Fowler, P.H., Franzinetti, C., Muirhead, H., Lock, W.D., Perkins, D.H. and Yekulieli, G. 1951 Phil. Mag. 42, 1241.
Carlson, A.G., Hooper, J.E. and King, D.T. 1950 Phil. Mag. 41, 701.

Chang-Yun Fan. 1951 Phys. Rev. 82, 211.
Clementel, E. and Puppi, G. 1949 Nuovo Cimento 6, 494.
Coates, A.C. and Herz, R.H. 1949 Phil. Mag. 40, 1088.
Cook, L.J., McMillan, E.M., Peterson, J.M. and Sewell, D.C. 1949 Phys. Rev. 75, 7.
Danysz, M. and Yekutieli, G. 1951 Phil. Mag. 42, 1185.
Davis, G. 1952 Phil. Mag. 43, 472.
De Juren, J. 1950 Phys. Rev. 80, 23.
.. .. 1951 Phys. Rev. 81, 919.
Fahy, E.F. 1951 Phys. Rev. 83, 413.
Fahy, E.F. and Schein, M. 1949 Phys. Rev. 75, 207.
Fermi, E. 1949 Phys. Rev. 75, 1169.
Fox, Leith, Wouters and MacKenzie. 1950 Phys. Rev. 80, 23.
George, E.P. and Jason, A.C. 1949 Proc. Phys. Soc. A, 62, 243.
Germain, L.S. 1951 Phys. Rev. 82, 596.
Gregory, B.P. and Tinlot, J.H. 1951 Phys. Rev. 81, 667.
Harding, J.B. 1950 Phil. Mag. 41, 405.
.. 1951 Phil. Mag. 42, 63.
.. 1952 Nature 169, 747.
Herz, A.J., Hodgson, P.E. and Tennent, R.M. 1952 Phil. Mag. (in press).
Hilberry. 1941 Phys. Rev. 60, 7.
Hoang, T.F. 1951 Thesis (Paris).
Hodgson, P.E. 1951 Phil. Mag. 42, 82.
.. 1952 Private communication.
Kaplon, M.F., Peters, B., Reynolds, H.L. and Ritson, D.M. 1952 Phys. Rev. 85, 295.
Kikuchi, S. 1951 Phys. Rev. 83, 2355.
Leprince-Ringuet, L. and Heidman, J. 1948 Nature, 169, 747.
Li, T.T. 1950 Phil. Mag. 41, 1152.
Li, T.T. and Perkins. 1948 Nature 161, 846.
Lock, W.O. and Yekutieli, G. 1952 Phil. Mag. 43, 231.
Lord, J.J. 1951 Phys. Rev. 81, 901.
Messel, H. 1951 Comm. Dublin Inst. for Advanced Studies A, No.17.

Messel, H. 1952 Proc. Phys. Soc. A, 65, 465.
Messel, H. and Ritson, D.M. 1950 Proc. Phys. Soc. A, 63, 1359.
Michaelis, E. 1952 Private communication.
Page, N. 1950 Proc. Phys. Soc. A, 63, 250.
Peters. 1952 Progress in Cosmic Ray Physics.
Regener, V.H. 1951 Phys. Rev. 84, 161.
Richtmyer, R.D. and Teller, E. 1949 Phys. Rev. 75, 1729.
Rosser, W.G.V. and Swift, M.W. 1951 Phil. Mag. 42, 856.
Rossi, B. 1948 Rev. Mod. Phys. 20, 537.
Schopper, E., Höcher, K.H. and Rössle, E. 1951 Z. Naturforsch 6 a, 603.
Shapiro, M.M., Stiller, B., Birnbaum, M. and O'Dell, F.W. 1951 Phys. Rev. 83, 455.
Singer, F. 1952 Private communication.
Stinchcomb, T.G. 1950 (a) Phys. Rev. 78, 321.
.. 1950 (b) Phys. Rev. 80, 479.
.. 1951 Phys. Rev. 83, 422.
Tennent, R.M. 1952 Private communication.
Thomson, G.P. and Hodgson, P.E. 1951 Phil. Mag. 42, 978.
Tidman, D.A. and Hodgson, P.E. 1952 Phil. Mag. 43, 992.
Titterton, E.W. 1951 Phil. Mag. 42, 109.
Unsöld, A. 1951 Phys. Rev. 82, 857.
Walker, W.D. 1950 Phys. Rev. 77, 686.
Walker, W.D., Walker, S.P. and Greisen, K. 1950 Phys. Rev. 80, 546.
Winchler, J.R., Stix, T., Dwight, K. and Sabin, R. 1950 Phys. Rev. 79, 656.
Yamaguchi, Y. 1949 Prog. Theor. Phys. 4, 569.

PUBLICATIONS

"The Double Star Effect in Nuclear Emulsion Plates Exposed to the Cosmic Rays". Phil. Mag. 7, xliii, 472 (1952).

"The Angular Distribution and Attenuation of the Star-Producing Component of Cosmic Rays", with N.C. Barford. Proc. Roy. Soc. A, 214, 225 (1952).

From the PHILOSOPHICAL MAGAZINE, Ser. 7, vol. xliii, p. 472,
April 1952.

The Double Star Effect in Nuclear Emulsion Plates Exposed to the Cosmic Rays

By G. DAVIS
Imperial College, London*

LI (1950) reported an excess of close star pairs over that expected on a random distribution, in plates exposed at the Jungfraujoch. The excess was of magnitude 2×10^{-2} close pairs per star, the effect extending up to a star-pair separation of $1500\,\mu$ (for $100\,\mu$ plates). This 'Li effect' was more pronounced for plates exposed under absorbing materials. Li included 2-track stars in his analysis.

The excess is difficult to explain by any known regenerative or shower process, since rather high cross-sections for star production are required. Moreover, examination of 351 stars found in 16 cm^2 of recently searched $400\,\mu$ G.5 plates (exposed under lead) does not show the Li effect. It was therefore decided to re-analyse the two sets of plates for which Li found the maximum close-pair excess, referred to as 'ice' and 'Pb' plates in his paper.

The distribution of close pairs was found to be identical with Li's results. However, on subtracting 2-track stars from the analysis, the excess completely disappeared for the 'Pb' plates (374 stars), while remaining for the 'ice' plates (1126 stars). Both these sets of plates were searched in the early days of this laboratory, and the inexperienced searchers were very likely to miss 2-track stars. But 2-track stars may have a greater probability of being found in the neighbourhood of other stars, due to the increased alertness of the searcher in the short period following the discovery of a star (for plates with a star density of the order of 5 per cm^2). Furthermore, the difficulty of identifying 2-track stars makes their inclusion unsuitable in an analysis of high accuracy. Li was aware of this effect but thought that the searching was so efficient that it did not matter. It is unlikely that the Li effect, if it existed, should be found only if 2-track stars are included in the analysis. The 351 stars analysed by the author showed no Li effect, either when 2-track stars were included, or when they were excluded from the analysis.

It seemed very probable that the remaining excess of close star-pairs in the ice plates (2-track stars excluded) could also be due to preferential inefficient searching. One tenth of the ice plates were carefully researched

*Communicated by Sir G. P. Thomson, F.R.S.

and the original efficiency was found to be slightly under 80%, contrasting markedly with the estimate of 98% reported by Li. The excess observed could then be explained by preferential inefficient searching. The areas researched did, in fact, show a decrease in the total number of excess star-pairs. If this trend were uniform among all the ice plates, it would be sufficient to explain the remaining excess of close star-pairs.

It is concluded that the experimental data used by Li do not show that there is a double star effect.

Reference

Li, 1950, *Phil. Mag.*, **41**, 1152.

Reprinted without change of pagination from the
Proceedings of the Royal Society, A, *volume* 214, p. 225, 1952

The angular distribution and attenuation of the star-producing component of cosmic rays

By N. C. Barford and G. Davis
Imperial College of Science and Technology, London

(*Communicated by Sir George Thomson, F.R.S.—Received* 28 *February* 1952)

Some properties of cosmic rays at 3570 m have been studied by observing nuclear disintegrations in G 5 emulsion under lead absorbers. Good geometrical definition was ensured by making these absorbers in the form of inverted lead cones of various half-angles. The nuclear cascade process is such that the overall attenuation in lead of the star-producing component increases with energy, the attenuation length varying from 370 ± 30 to 210 ± 70 g cm^{-2} over the range of energy responsible for the stars examined. Interpretation of the results to give the angular distribution of the star-producing radiation depends upon the nature of the cascade process. However, it is certainly more collimated than a $\cos^2 \Theta$ steradian^{-1} distribution, where Θ is the zenith angle, and may be of the form $\cos^4 \Theta$ steradian^{-1} for the high-energy component. For the charged component alone a direct measurement gave $\cos^{5 \pm 1} \Theta$ steradian^{-1}.

The rate of production in emulsion under no absorber of all stars with three or more heavy prongs is $17{\cdot}0 \pm 0{\cdot}4$ cm^{-3} day^{-1}.

1. Introduction

In analyzing the properties of that part of cosmic radiation which causes nuclear disintegrations ('stars') it is necessary to investigate the types of stars produced, the effect of absorbers upon the radiation and the angular distribution of this

radiation. Experiments dealing with the first two aspects have been described (e.g. Brown, Camerini, Fowler, Heitler, King & Powell 1949; Rosser & Swift 1951), but the experimental conditions have been geometrically unsuitable for giving information about the third. The experiment described here was designed particularly for the latter purpose, although in the course of the work interesting results have been obtained for the other two.

2. Experimental procedure

(i) *General*

Ilford G 5 nuclear emulsion plates (double-sided 200 μ and single-sided 400 μ) were exposed at the Jungfraujoch (3570 m, 47° geomagnetic N) during 1950 and 1951 under inverted lead cones of various half-angles.

Each cone was split into three shells of 10 cm thickness so that absorption under 10, 20 and 30 cm of lead could be investigated. The plates were stacked vertically below the cones, and only those parts of the emulsions were searched which lay within a vertical circular cylinder of diameter 2 cm and height 2 cm at the apex of each cone. The essential features of the experimental arrangement are shown in figure 1. For a cone of half-angle Θ we can define angles δ_1 and δ_2 such that any undeviated ray reaching the searched volume of emulsion with declination less than $\Theta - \delta_1$ must pass through the total thickness of lead, while if it is greater than $\Theta + \delta_2$ it can pass through no lead. δ_1 and δ_2 are given in table 1 for the various values of Θ using 30 cm lead (shells 1, 2 and 3). For 20 cm (shells 1 and 2) and 10 cm (shell 2) they are less. The probable error in the Θ co-ordinate of our measurements is clearly less than δ_1 or δ_2, and we may certainly say that the angular measurements have a precision within 10 %.

Each set of plates was sealed at approximately 15° C in an atmosphere of 30 to 40 % relative humidity and maintained at 10 to 20° C throughout the experiment to obviate risks of fading. The emulsion was developed by the temperature cycle method to a minimum grain density of 30 to 40 grains per 100 μ of track. We rejected plates which were so distorted as to impair searching efficiency or the classification of stars.

The emulsion thickness of one-third of all plates was measured before and after development. From this a shrinkage factor $2{\cdot}5 \pm 0{\cdot}05$ was calculated and used to determine the initial thickness of the emulsion in the remaining plates which were measured only after development. Variations of 10 % or more from the nominal emulsion and glass thicknesses were common.

The boxes containing the plates and scaffolding supporting the cones contributed approximately 1 g cm^{-2} of absorber extra, but this has been neglected throughout.

(ii) *Searching*

The plates were searched at 250 × magnification, and all the events recorded were checked at 800 × magnification. Any event showing three or more tracks of grain density greater than 1·5 × minimum and length greater than 4 μ were used in the analysis unless

(*a*) all such tracks were less than 70 μ long in which case the event was assumed to be a radioactive disintegration,

(*b*) one track could have been caused by a slow meson travelling towards the centre of the event—a σ-star, and

(*c*) it could be interpreted as a proton-proton scatter.

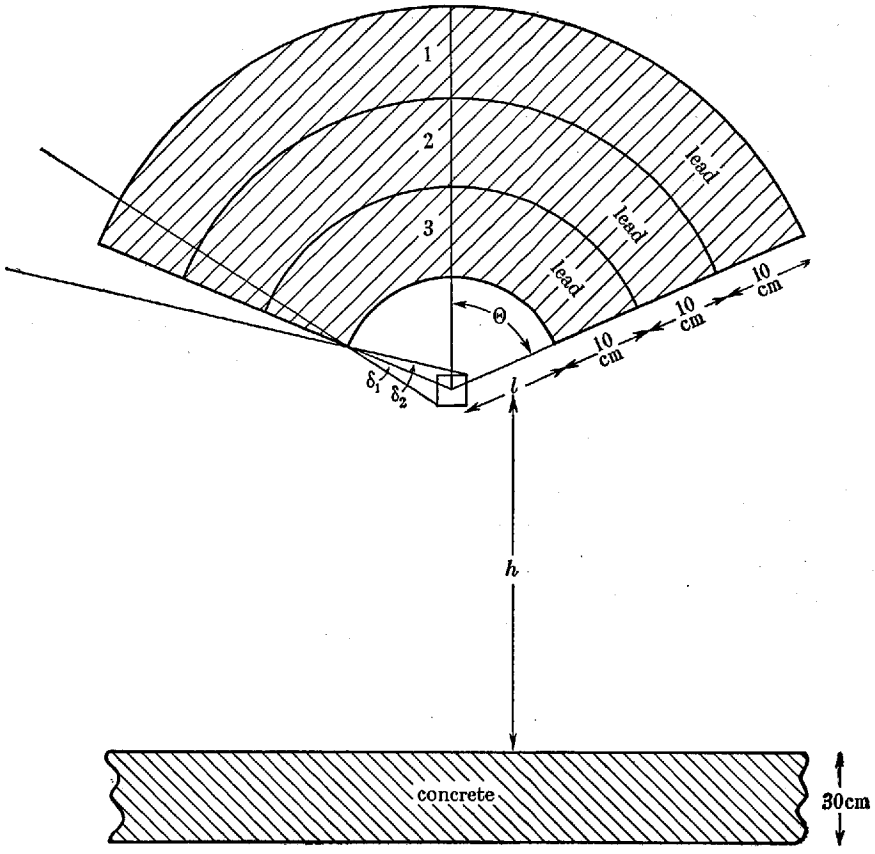


FIGURE 1. Geometrical details.

TABLE 1. GEOMETRICAL DETAILS

Θ (°)	0	10	20	40	60	90
δ_1 (°)	—	2·2	2·8	5·2	7·9	0
δ_2 (°)	—	2·0	3·0	5·4	7·4	15·0
l (cm)	—	30	25	15	10	1·5
h (cm)	27·7	26·3	26·9	26·7	28·5	28·0

Our minimum-grain-density standard neglected the difference between the true minimum and 'plateau' grain densities reported by Voyvodic (1951). However, the similarity between our results and previous ones (Brown *et al.* 1949; Rosser & Swift 1951) for large stars shows that the grain-density standards are in good agreement.

Inefficient searching soon showed up as irregularities in the plots of star density against cone angle and led us to consider this problem in detail. Some of the emulsion was carefully searched twice and, assuming the overall efficiency of this to be 100 %, it was found possible to divide the six searchers who took part into two groups. The four experienced searchers were 95 to 100 % efficient and the two inexperienced ones were 80 to 90 % efficient in finding three- and four-pronged stars. In the analysis of such stars a correction factor of 1·1 was therefore applied to those found by the latter. As this applied only to a small fraction of the results the overall correction factor is in most cases nearly 1·0 (see tables 2, 3, 4, 5 and 6), and none of our conclusions is invalidated if no such correction is made.

Very few stars of five or more prongs were missed by any searcher and no corrections have been applied to them.

3. Results

These are summarized for all cone angles in tables 2 and 3, while those of particular importance—the star intensities under no absorber and under the hemispherical lead shells—are given in greater detail in tables 4, 5 and 6. Plates under no absorber were exposed during the experiment with 20 cm of lead and that with 30 cm, and the stars observed in them are given separately in tables 2 and 3. The latter give a rate of star production somewhat greater than the former, but the difference is not statistically significant. We have therefore combined both results together with some obtained during the experiment with 10 cm of lead to give the star intensities under no absorber in table 4.

(i) *Classification*

The usual classification of tracks in terms of their grain density, g, relative to minimum grain density, g_m, was employed. The numbers of 'minimum' tracks ($g \leqslant 1{\cdot}5g_m$), 'grey' tracks ($1{\cdot}5g_m \leqslant g \leqslant 7g_m$) and 'black' tracks ($7g_m \leqslant g$) were recorded for each star. If at least one of the minimum tracks lay in the upper hemisphere it was assumed that the disintegration was caused by a charged particle (a p-star) and the number of shower particles (n_s) was taken as one less than the number of minimum tracks. If not it was assumed that the primary particle was neutral (producing an n-star), and n_s was taken equal to the number of minimum tracks. The number of 'heavy' prongs, N_h, is the sum of the grey and black tracks.

(ii) *Errors and corrections*

The correction factor for searching inefficiency has already been discussed. We must allow also for sea-level exposure before and after the experiments. To do this we have assumed an absorption length in air for all types of stars of 135 g cm^{-2} (Bernardini, Cortini & Manfredini 1949) and have expressed the correction in terms of a total equivalent exposure time at the Jungfraujoch.

It must be emphasized that all the numbers given in the tables are of stars found and checked—corrections are applied only in the subsequent analysis.

TABLE 2. NUCLEAR DISINTEGRATIONS UNDER 20 CM LEAD AT 3570 M

cone half-angle	emulsion volume (cm^3)	exposure time (days)	corrected exposure time (days)	$3 \leqslant N_h \leqslant 4$, $n_s = 0$		$5 \leqslant N_h \leqslant 9$, $n_s = 0$		$10 \leqslant N_h$, $n_s = 0$		$3 \leqslant N_h$, $n_s \geqslant 1$		searching factor $3 \leqslant N_h \leqslant 4$
				n	p	n	p	n	p	n	p	
0°	0·60	51	51·8	265	26	105	28	12	5	32	23	1·00
10°	0·66	51	51·9	298	19	92	32	13	3	31	39	1·00
20°	0·15	51	52·1	60	9	22	3	4	2	8	5	1·00
40°	0·88	51	52·6	310	23	95	26	7	10	25	17	1·04
60°	0·15	51	52·7	48	3	15	2	1	0	4	1	1·00
90°	1·06	51	53·8	271	31	110	21	7	4	21	18	1·05

TABLE 3. NUCLEAR DISINTEGRATIONS UNDER 30 CM LEAD AT 3570 M

cone half-angle	emulsion volume (cm^3)	exposure time (days)	corrected exposure time (days)	$3 \leqslant N_h \leqslant 4$, $n_s = 0$		$5 \leqslant N_h \leqslant 9$, $n_s = 0$		$10 \leqslant N_h$, $n_s = 0$		$3 \leqslant N_h$, $n_s \geqslant 1$		searching factor $3 \leqslant N_h \leqslant 4$
				n	p	n	p	n	p	n	p	
0°	0·86	46	46·4	380	38	144	32	24	5	58	36	1·0
10°	1·01	46	46·5	429	35	157	32	22	9	31	20	1·0
20°	0·34	46	47·2	118	14	51	11	3	3	19	11	1·0
40°	1·12	46	47·9	324	24	117	17	9	6	18	22	1·0
60°	0·34	46	50·3	74	8	18	7	0	0	5	2	1·0
90°	1·50	46	50·8	288	24	79	16	9	1	21	17	1·0

N_h = number of heavily ionizing particles; n_s = number of shower particles; n = neutral primary; p = charged primary.

TABLE 4. NUCLEAR DISINTEGRATIONS UNDER NO LEAD AT 3570 M

n_s \ N_h	3	4	5	6	7	8	9	10	11	12	13	14	15	16	17	18	19	20	$3 \leqslant N_h \leqslant 6$	$7 \leqslant N_h$	Bristol $3 \leqslant N_h \leqslant 6$	Bristol $7 \leqslant N_h$	Manchester $3 \leqslant N_h \leqslant 6$	Manchester $7 \leqslant N_h$
$0(n)$	488	291	146	70	33	23	14	13	9	4	5	4	3	2	2	1	0	0	995 ± 32	113 ± 11	600 ± 11	101 ± 4	835 ± 25	116 ± 9
$0(p)$	35	34	31	14	14	6	6	5	3	2	1	0	1	0	0	0	0	0	114 ± 11	38 ± 6	54 ± 3	45 ± 3	70 ± 7	46 ± 6
$\geqslant 1(n)$	31	22	11	7	5	5	4	0	2	6	0	1	1	0	1	0	1	1	71 ± 8	27 ± 5	31 ± 2	32 ± 2	72 ± 7	37 ± 5
$\geqslant 1(p)$	9	14	6	7	4	2	4	1	5	3	2	3	0	1	1	1	0	1	36 ± 6	29 ± 5	29 ± 2	33 ± 2	45 ± 6	18 ± 4
total	563	361	194	98	56	36	24	19	19	15	8	8	5	3	4	2	1	2	1216	207	714	211	1022	217

Corrected exposure 84·3 cm³ days. Searching factor 1·01 ($3 \leqslant N_h \leqslant 4$).

TABLE 5. NUCLEAR DISINTEGRATIONS UNDER 20 CM LEAD HEMISPHERE AT 3570 M

n_s \ N_h	3	4	5	6	7	8	9	10	11	12	$\geqslant 13$	$3 \leqslant N_h \leqslant 6$	$7 \leqslant N_h$
$0(n)$	188	83	62	18	15	9	6	1	0	3	3	351	37
$0(p)$	12	19	5	7	8	1	0	1	0	1	2	43	13
$\geqslant 1(n)$	4	3	2	1	2	1	3	1	1	0	3	10	11
$\geqslant 1(p)$	6	2	2	1	2	1	2	1	1	0	0	11	7
total	210	107	71	27	27	12	11	4	2	4	8	415	68

Corrected exposure 57·0 cm³ days. Searching factor 1·05 ($3 \leqslant N_h \leqslant 4$).

TABLE 6. NUCLEAR DISINTEGRATIONS UNDER 30 CM LEAD HEMISPHERE AT 3570 M

n_s \ N_h	3	4	5	6	7	8	9	10	11	12	$\geqslant 13$	$3 \leqslant N_h \leqslant 6$	$7 \leqslant N_h$	Manchester $3 \leqslant N_h \leqslant 6$	Manchester $7 \leqslant N_h$
$0(n)$	190	98	42	13	11	9	4	3	3	2	1	343 ± 19	33 ± 6	256 ± 8	24 ± 2
$0(p)$	9	15	6	5	2	3	0	0	1	0	0	35 ± 6	6 ± 2	26 ± 2	11 ± 2
$\geqslant 1(n)$	6	4	2	3	1	0	0	1	0	2	2	15 ± 4	6 ± 2	16 ± 2	10 ± 2
$\geqslant 1(p)$	2	0	4	2	1	1	1	0	1	2	3	8 ± 3	9 ± 3	16 ± 2	10 ± 2
total	207	117	54	23	15	13	5	4	5	6	6	401	54	314	55

Corrected exposure 76·2 cm³ days. Searching factor 1·00 ($3 \leqslant N_h \leqslant 4$).

N_h = number of heavily ionizing particles; n_s = number of shower particles; n = neutral primary; p = charged primary.

If N events were observed the errors assumed in obtaining the final results were $\pm\sqrt{N}$ if $N \geqslant 40$, while for smaller values of N the fiducial limits discussed by Regener (1951) were used.

4. Analysis

The simplest analysis of the results is obtained by making the following assumptions: star-producing radiation travels in straight lines; if a primary particle in this radiation gives rise to a secondary particle, itself capable of produeing a star, the latter continues in the same direction as the former (we shall call this a collimated secondary); radiation at any angle traversing a distance d in the absorber suffers an overall reduction to a fraction $\alpha(d)$ of its original value. Then if the angular distribution of the radiation is proportional to $\cos^m\Theta$ steradian^{-1} in the upper hemisphere and zero in the lower hemisphere, where Θ is the zenith angle, we shall expect the rate of star production in the emulsion at the apex of a cone of half-angle Θ and thickness d to be of the form

$$N(\Theta) = N(0)\,\alpha(d)\,[1+\cos^{m+1}\Theta(1/\alpha(d)-1)]. \tag{1}$$

Whatever the value of m, $\alpha(d)$ is given by

$$N(\tfrac{1}{2}\pi) = N(0)\,\alpha(d). \tag{2}$$

If, for various values of d, the experimental results satisfy a variation of type (1) for the same value of m, the zenith angle law of distribution will be verified (subject to the assumptions already mentioned). If, in addition, for variations of d there is a constant λ satisfying

$$\alpha(d) = \mathrm{e}^{-d/\lambda}, \tag{3}$$

we shall be justified in talking of effective exponential attenuation and in defining λ as the attenuation path length.

We have examined various classes of stars to see how well laws (1) and (3) are obeyed and to determine the relevant values of m and λ. Examples are given in figures 2 and 3. In order to obtain the 'best' values of m and λ we adopted the following procedure. $N(0)$ was taken as the experimental value at $\Theta = 0$. For the two thicknesses of lead—20 and 30 cm—two values of the attenuation length were then obtained from the formula

$$d/\lambda = \log[N(0)/N(\tfrac{1}{2}\pi)],$$

derived from (2) and (3). If they were consistent their weighted mean was taken as λ. With these values of $N(0)$ and λ curves of type (1) were constructed for various values of m to see if such a description was adequate. In general, this was so, and the values of m were such that the greatest precision in its determination was given by the experimental results at $\Theta = 40°$. Searching was therefore concentrated at this value. The final value of m was taken as the weighted mean of the values best fitting the results for 20 and 30 cm absorber.

The alternative method of obtaining m from the formula

$$\log[N(\Theta)-N(\tfrac{1}{2}\pi)] = (m+1)\log\cos\Theta + \log[N(0)-N(\tfrac{1}{2}\pi)]$$

gave the same result in all cases.

While our determination of the best values for N and m is not very refined, the labour of a complete least-square analysis seemed hardly to be warranted.

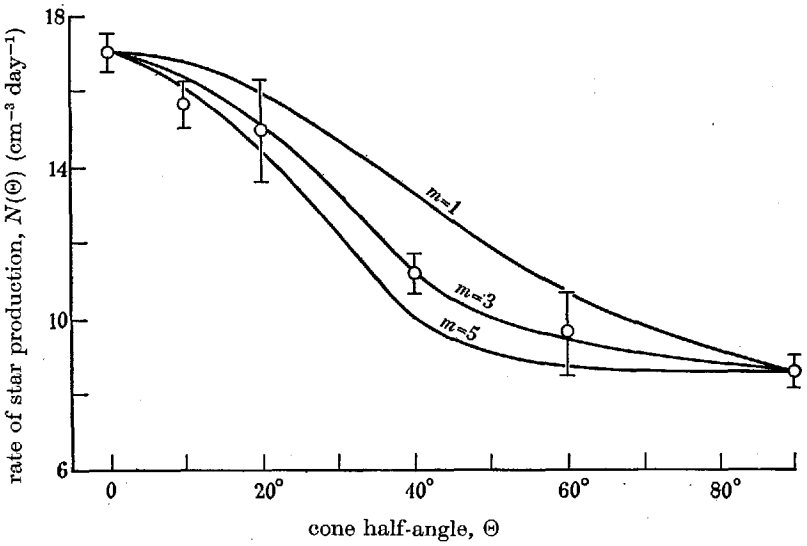


FIGURE 2. Rate of production of all stars with $N_h \geqslant 3$ under 20 cm of lead. —, $N(\Theta) = 8{\cdot}6(1 + 0{\cdot}98 \cos^{m+1} \Theta)$.

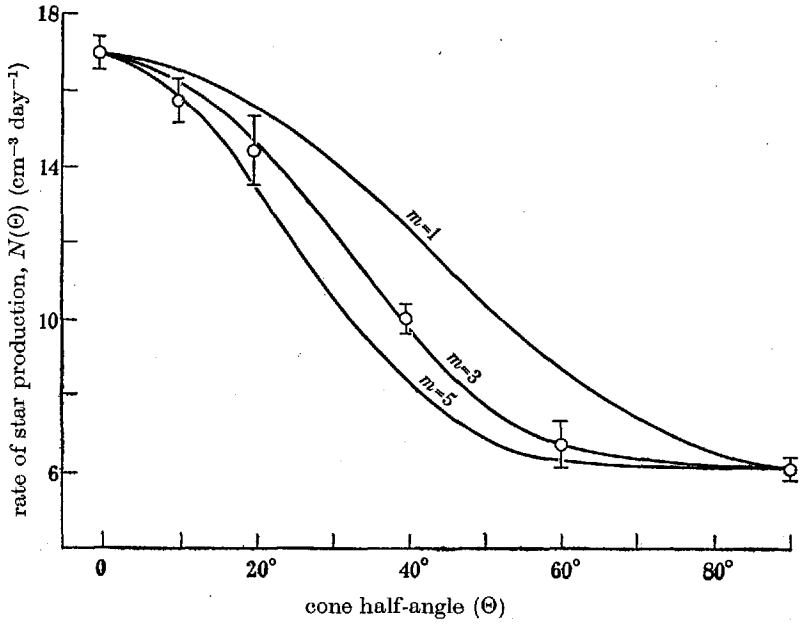


FIGURE 3. Rate of production of all stars with $N_h \geqslant 3$ under 30 cm of lead. —, $N(\Theta) = 6(1 + 1{\cdot}83 \cos^{m+1} \Theta)$.

5. DISCUSSION

(i) *Absolute rate of star production*

The rate of production of all stars with $N_h \geqslant 3$ in nuclear emulsion of $17{\cdot}0 \pm 0{\cdot}4$ cm^{-3} day^{-1} is greater than previously reported. For comparison the stars recorded by the Bristol and Manchester groups (Brown *et al.* 1949; Rosser & Swift 1951) are

shown in tables 4 and 6. These are corrected to the same exposure time, and in the latter case for the difference in altitude also. It can be seen that the differences involve small stars only. It may be noted, that we observe more than twice as many three-pronged stars as the Bristol group. It has been shown (Tidman & Hodgson 1952, private communication) that this significantly alters the energy versus star size law, $E = 37N_h + 4N_h^2$, given by Brown *et al.* (1949).

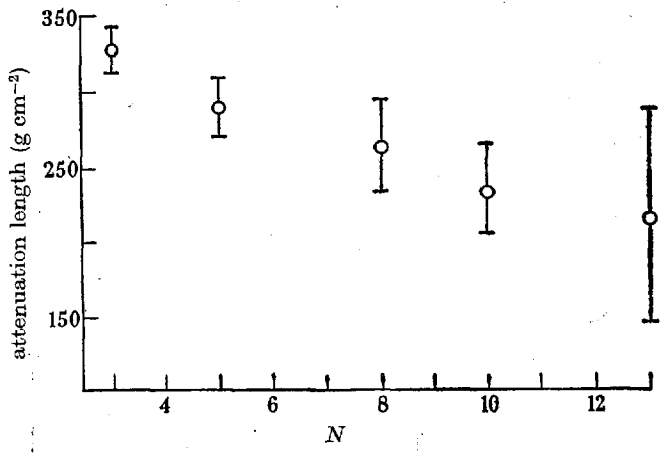


FIGURE 4. Attenuation length for stars with $N_h \geqslant N$.

(ii) *Attenuation*

Figure 4 shows an attenuation length in lead for all stars with $N_h \geqslant 3$ of $330 \pm 15\,\mathrm{g\,cm^{-2}}$ which agrees with the earlier values of $310 \pm 20\,\mathrm{g\,cm^{-2}}$ (George & Jason 1949) and $305 \pm 7\,\mathrm{g\,cm^{-2}}$ (Rosser & Swift 1951). For small stars only ($3 \leqslant N_h \leqslant 4$) produced by neutral radiation it is rather greater at $370 \pm 30\,\mathrm{g\,cm^{-2}}$. However, we find a smaller proportion of large stars under lead similar to that found with air as absorber by Addario & Tamburino (1949), but not observed at a slightly lower altitude by Rosser & Swift (1951). This gives a definite trend towards smaller attenuation lengths for large stars. The smallest length, $210\,\mathrm{g\,cm^{-2}}$, may be compared with the 'geometrical' mean free path of $150\,\mathrm{g\,cm^{-2}}$ based on a nuclear radius $r = 1{\cdot}45 \times 10^{-13} A^{\frac{1}{3}}$ cm.

Since the average primary particle energy must be greater for large than for small stars, this appears to give clear evidence that the effective attenuation of an absorber is less for the low-energy component of the star-producing radiation than for the high-energy component. This has an important bearing on any theory of the nucleon cascades in the star-producing radiation. For if we assume that this radiation has a differential energy distribution of the form

$$\mathrm{d}N = KE^{-\gamma}\,\mathrm{d}E,$$

even the fairly general law that a nuclear collision of a primary of energy E yields n_1 secondaries of energy $\alpha_1 E$, n_2 of energy $\alpha_2 E$, etc., themselves capable of producing further stars, where $n_1, n_2, \ldots, a_1, \alpha_2, \ldots$ are constants, would merely reproduce the same power distribution law at all thicknesses of absorber and therefore give the same effective attenuation for radiation of all energies.

To obtain the effect we have observed we could assume that in a nuclear disintegration initiated by a high-energy particle a greater proportion of the primary energy is lost (as far as subsequent star production is concerned) than in those initiated by low-energy primaries. This is reasonable in view of the possibility of creating meson rest mass at great energies.

We could also assume that there is a low-energy cut-off to the primary spectrum at the Jungfraujoch which is greater than the minimum energy required for a three-pronged star. Both assumptions lead to an energy degradation process in the absorber which increases the proportion of low-energy star-producing radiation.

For all classes of stars examined our results were consistent with exponential attenuation. We should not have expected in any case to observe the transition effect for small thicknesses of lead (Shapiro, Stiller, Birnbaum & O'Dell 1951; Schopper, Höcker & Rössle 1951), but the measurements under 20 cm of lead showed no effect of the type reported by the latter authors for stars with two or more prongs.

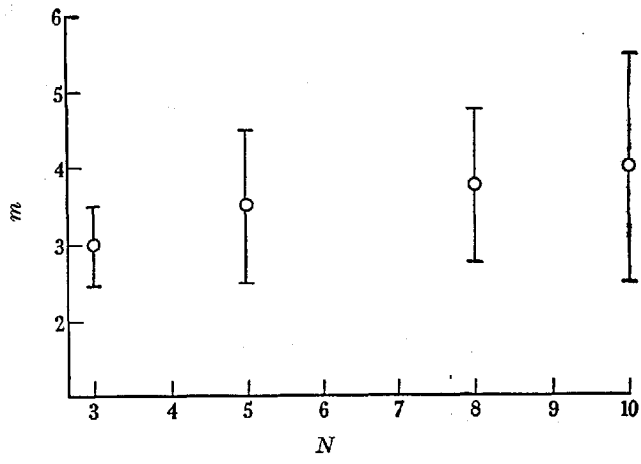


FIGURE 5. Angular distribution exponent, m, for stars with $N_h \geqslant N$.

(iii) *Angular distribution*

For the lowest energy stars (n-stars with $3 \leqslant N_h \leqslant 4$) we find $m = 2{\cdot}5 \pm 0{\cdot}5$. Although this and all the values of m given in figure 5 are consistent with the value $3{\cdot}0 \pm 0{\cdot}5$, there is some indication that the high-energy radiation is more collimated than the low-energy component. We might expect this from the fact that the large stars have a greater proportion of charged primaries than do the small stars; since they suffer ionization as well as nuclear collision losses, passage through the air absorber above 3570 m will tend to collimate them more than the neutral primaries.

It has been assumed that $m = 2$ (e.g. Harding 1951; Schopper *et al.* 1951) on the basis of measurements by Coates & Herz (1949) and Page (1950). The former were, however, of 'straight-line tracks' at sea-level and were presumably mostly caused by μ-mesons. The latter measurements were of charged primaries only, so that in neither case is there a direct measure of the angular distribution of the total radiation, most of which is neutral at 3570 m.

However, we have also investigated the distribution of charged primaries by two methods and find them considerably more collimated. First, p-stars only were analyzed by the method described above and this gave the value $m = 4{\cdot}0 \pm 1{\cdot}0$. This is still not a direct measure of the angular distribution because of the secondary processes in the lead absorber. To obtain this the zenith angles of the primaries of 200 p-stars found under no absorber were measured. These are shown in figure 6 and give the value $m = 5{\cdot}0 \pm 1{\cdot}0$. This may be compared with the angular distribution of the charged particles producing showers determined by Walker (1950) at a similar altitude. From the nature of his apparatus the counts $A^1B^1C^3$ will include large stars of great energy. This angular distribution has $m = 7{\cdot}3 \pm 1{\cdot}0$. It is also of interest to consider the corresponding distribution at great altitude. Lord (1951) has given the angular distribution of charged star primaries at 28700 m, 54° N (magnetic). Taking a Gross transformation of this to give the air attenuation we find that at 3570 m the distribution up to 60° zenith angle is best fitted by the law $\cos^{4{\cdot}5}\theta$.

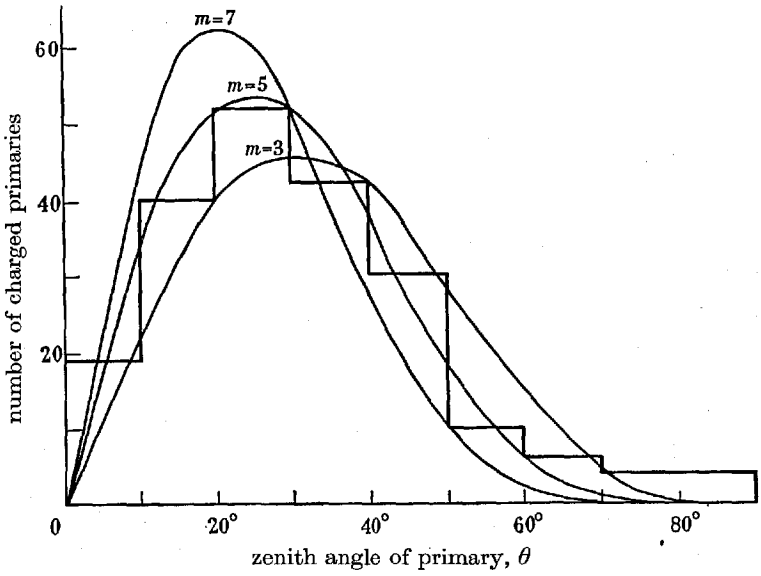


FIGURE 6. Angular distribution of charged primaries of stars under no absorber at 3570 m. —, $K \sin\theta \cos^m\theta$ normalized to 200 primaries.

It is important to realize that the effective angular distribution determined by absorption in the lead cones is the true angular distribution of the primaries above the lead only if our assumption of collimated secondaries is true. We must now consider to what extent our results are affected by varying this assumption.

The flux of star-producing radiation measured by the number of stars observed in the emulsion below a lead cone consists of two parts. There is first that fraction of the primary radiation which reaches the emulsion without any nuclear collisions. The second part consists of secondary radiation produced in the lead. The difference between the true and effective angular distribution increases as

(*a*) the proportion of non-collimated secondaries to primaries entering the emulsion is increased (by decreasing the attenuation length for the primaries),

(*b*) the angular distribution of secondaries changes from collimated towards isotropic.

We have investigated these effects on the basis of a single-stage generation of secondaries, neglecting ionization losses. In general, the true values of m are smaller than those obtained by the method of § 4. The extreme possibilities for (*a*) and (*b*) —that the attenuation length is geometrical and that the emission of secondaries is completely isotropic—give a value, $m = 2{\cdot}2$. This is the least true value that could give an apparent value, $m = 3{\cdot}0$. An attenuation length of $210\,\mathrm{g\,cm^{-2}}$ with the secondary distribution still isotropic would increase this to $m = 2{\cdot}5$, and with some degree of secondary collimation it would rise still further.

A more detailed knowledge of the production of secondaries is required before the angular distribution of the primaries can be established with certainty. However, there is evidence that the true value of m cannot be much less than the effective value, $m = 3$, from the fact that the experiments under 20 and 30 cm of lead both gave this result. Since the proportion of secondaries is very different in the two cases their effect in determining the effective distribution cannot be very great.

For the larger stars only, the problem is much more complicated, for charged primaries here play a much greater part and we are no longer justified in neglecting ionization losses. The general effect of these is to sharpen the overall collimation and thus counteract the effect of non-collimated secondary production. To judge from the effective and true angular distributions obtained above for p-stars the former effect may be slightly the greater.

6. Conclusion

A rate of production of $17{\cdot}0 \pm 0{\cdot}4\,\mathrm{cm^{-3}\,day^{-1}}$ of all stars with $N_h \geqslant 3$ in nuclear emulsion has been determined at 3570 m above sea-level. The radiation producing these stars is absorbed in lead at a rate equivalent to an attenuation length of $330 \pm 15\,\mathrm{g\,cm^{-2}}$ and to an angular distribution proportional to $\cos^{3\pm0{\cdot}5}\Theta$ steradian^{-1}, where Θ is the zenith angle. The true distribution is probably nearer to $\cos^{2{\cdot}5\pm0{\cdot}5}\Theta$, but the collimation appears to increase slightly with increasing energy and may reach the value $\cos^4\Theta$ for the radiation producing the largest stars. For charged primary radiation alone the distribution is proportional to $\cos^{5\pm1}\Theta$ steradian^{-1}.

There is a considerable increase in the effective attenuation of the radiation as its energy increases, the attenuation length varying from 370 ± 30 to $210 \pm 70\,\mathrm{g\,cm^{-2}}$ over the range considered (~ 200 to ~ 2000 MeV).

We should like to thank Sir George Thomson, F.R.S., for the interest he has shown in our work. We are indebted to Mr S. Lattimore for help in preparing the apparatus and to Mr A. J. Herz and Miss M. Edgar for developing the plates. The experiment was only made possible by the facilities available at the Jungfraujoch, and for these we are grateful to Professor von Muralt, Dr R. Stämpfli and Herrn H. Wiederkehr.

References

Addario, M. M. & Tamburino, S. 1949 *Phys. Rev.* **76**, 983.
Bernardini, G., Cortini, G. & Manfredini, A. 1949 *Phys. Rev.* **76**, 1792.
Brown, R. H., Camerini, U., Fowler, P. H., Heitler, H., King, D. T. & Powell, C. F. 1949 *Phil. Mag.* **40**, 862.
Coates, A. C. & Herz, R. H. 1949 *Phil. Mag.* **40**, 1088.
George, E. P. & Jason, A. C. 1949 *Proc. Phys. Soc.* A, **62**, 243.
Harding, J. B. 1951 *Phil. Mag.* **42**, 63.
Lord, J. J. 1951 *Phys. Rev.* **81**, 901.
Page, N. 1950 *Proc. Phys. Soc.* A, **63**, 250.
Regener, V. H. 1951 *Phys. Rev.* **84**, 161.
Rosser, W. G. V. & Swift, M. W. 1951 *Phil. Mag.* **42**, 856.
Schopper, E., Höcker, K. H. & Rössle, E. 1951 *Z. Naturforsch.* 6*a*, 603.
Shapiro, M. M., Stiller, B., Birnbaum, M. & O'Dell, F. W. 1951 *Phys. Rev.* **83**, 455.
Voyvodic, L. 1951 *Proc. Bristol Conf. V. Particles and heavy mesons*, p. 16.
Walker, W. D. 1950 *Phys. Rev.* **77**, 686.

PRINTED IN GREAT BRITAIN AT THE UNIVERSITY PRESS, CAMBRIDGE
(BROOKE CRUTCHLEY, UNIVERSITY PRINTER)